IS-T--1054

DE83 016131

Synthesis and characterization of several molybdenum chloride cluster compounds

by

William Winder Beers

Phd. Thesis submitted to Iowa State University

Ames Laboratory, DOE

Iowa State University

Ames, Iowa 50011

Date Transmitted: June 1983

PREPARED FOR THE U.S. DEPARTMENT OF ENERGY
UNDER CONTRACT NO. W-7405-eng-82

DISCLAIMER

DISCLAIMER

Printed in the United States of America

Available from
National Technical Information Service
U.S. Department of Commerce
5265 Port Royal Road
Springfield, VA 22161

TABLE OF CONTENTS

Synthesis and characterization of several molybdenum chloride cluster compounds[1]

William Winder Beers

Under the supervision of Robert E. McCarley
From the Department of Chemistry
Iowa State University

Investigation into the direct synthesis of $Mo_4Cl_8[P(C_2H_5)_3]_4$ from $Mo_2[OAc]_4$ led to a synthetic procedure that produces yields greater than 80%. The single-crystal structure disclosed a planar rectangular cluster of molybdenum atoms. Metal–metal bond distances suggest that the long edges of the rectangular cluster should be considered to be single bonds and the short metal-metal bonds to be triple bonds. This view is reinforced by an extended Hückel calculation.

Attempts to add a metal atom to $Mo_4Cl_8[PR_3]_4$ to form $Mo_5Cl_{10}[PR_3]_3$ led instead to a compound with the composition $Mo_8Cl_{16}[PR_3]_4$. Solution and reflectance uv-visible spectra and x-ray photoelectron spectra suggest that tetranuclear molybdenum units are present. The facile reaction between $Mo_8Cl_{16}[PR_3]_4$ and PR_3 imply that the linkage between tetrameric units is weak.

---

[1]DOE Report IS-T-1054. This work was performed under Contract W-7405-eng-82 with the Department of Energy.

Spectroscopic measurements of $Mo_8Cl_{16}[PR_3]_4$ revealed similarities to β-$MoCl_2$. This observation led to the low temperature synthesis of β-$MoCl_2$ from $Mo_2[OAc]_4$ and $AlCl_3$. β-$MoCl_2$ formed by this route is much more reactive than that produced by previous methods. Isolation of $Mo_4Cl_8[PEt_3]_4$ from a room temperature reaction of β-$MoCl_2$ with PEt_3 suggests that β-$MoCl_2$ contains tetrameric units.

Cyclic voltammetric measurements and chemical redox reactions in acetonitrile have established that the $[Mo_5Cl_{13}]^{n-}$ cluster anion may be obtained with n = 1, 2, or 3. The $[Mo_5Cl_{13}]^{3-}$ cluster is stable for greater than 1 day in the absence of air, but the $[Mo_5Cl_{13}]^{1-}$ anion quickly reverts to $[Mo_5Cl_{13}]^{2-}$. Electronic spectra of solutions in acetonitrile show related bands at 725-790, 550-580, and 455-490 nm for the three anions. Magnetic susceptibility measurements over the range 100-295°K for $[Bu_4N]_2Mo_5Cl_{13}$ yield μ = 1.67. The presence of a dynamic Jahn-Teller effect in the ESR spectrum of $[Bu_4N]_2Mo_5Cl_{13}$ indicates that the HOMO is doubly degenerate. The crystal structure of $[C_6H_5CH_2N(CH_3)_3]_2Mo_5Cl_{13}$ illustrates a static distortion of the cluster. Susceptibility measurements of $[Bu_4N]_3Mo_5Cl_{13}$ indicate that it is diamagnetic, from which a singlet HOMO is deduced. The Cl 2p photoelectron spectrum for $[Bu_4N]_2Mo_5Cl_{13}$ was resolved into components giving binding energies for the terminal, edge-bridging, and face-bridging chlorine atoms in the cluster unit.

GENERAL INTRODUCTION

Metal-atom cluster compounds have been defined as those compounds containing a group of metal atoms with bonds directly between the metal atoms (1). The examination of metal atom cluster compounds has grown rapidly in the last 15 years, but the first compounds of this type were synthesized many years ago. The initial correct formulation of a metal cluster was that of $Ta_6Cl_{14}\cdot 7H_2O$ in 1913 (2). Confirmation of this formulation by structure determination occurred in 1950 (3), and the presence of metal-metal bonds was deduced from the short metal-metal distances in the octahedron of metal atoms. Crystal structures of other compounds containing metal-metal bonds had been previously determined. For example, in 1935 the tungsten-tungsten distance in $K_3W_2Cl_9$ was found to be about 2.5 A (4), and the octahedral cluster of molybdenum atoms was found in $[Mo_6Cl_8][Cl_4(H_2O)_2]\cdot 6H_2O$ in 1946 (5). However, in-depth investigations of metal atom cluster compounds were not begun until after the 1963 crystal structure of $Cs_3Re_3Cl_{12}$ (6). This was the first recognized instance of multiple metal-metal bonds and emphasized the importance and strength of metal-metal bonds. The breadth and depth that the field has attained is reflected in the many review articles and books that have been recently published (7-9).

A considerable stimulus for the current interest in transition-metal clusters has arisen from the search for new catalysts and a better understanding of those catalysts presently employed. The structure and active sites of heterogeneous catalysts are frequently unknown, and the use of transition-metal clusters to model transition-metal surfaces has been

suggested, by Muetterties in particular (10). The question then arises as to what size of cluster is needed for satisfactory imitation of the metal surface. Theoretical calculations suggest that the cluster compound must be very large (11,12). For example, a cluster of nickel atoms must contain 15 atoms for the cluster to exhibit metal-like properties and a cluster of silver atoms must contain over 30 atoms (13). Some small metal cluster compounds, for example $Ni_4[CN(t\text{-}Bu)]_7$ (14), have demonstrated catalytic activity. This cluster contains three bridging isocyanide ligands (15) which is similar to the multicenter bonding of isocyanides on nickel metal surfaces (16). However, the current belief is that additional metal clusters must be synthesized and studied before any definite trends between metal clusters and metal surfaces can be established (17).

The systematic designed synthesis of polynuclear transition-metal clusters is not yet generally possible. The formation of dinuclear compounds from mononuclear compounds and the reaction of metal-metal multiple bonds provide some guidance for future work. Mononuclear compounds will sometimes couple and form a metal-metal bond if ligand dissociation can be induced. This is demonstrated by the loss of PPh_3 from $Pt[PPh_3]_4$ in refluxing benzene to form dinuclear $Pt_2[\mu_2\text{-}PPh_2]_2[PPh_3]_2$ (18). Therefore, one might predict that two clusters could be fused if some of their ligands were forced to dissociate. This was demonstrated by the loss of methanol from $Mo_2Cl_4[PPh_3]_2[MeOH]_2$ to form $\{MoCl_2[PPh_3]_2\}_n$ which, when reacted with PEt_3, yielded $Mo_4Cl_8[PEt_3]_4$ (19).

Metal complexes can be added across metal carbenes or metal carbynes to form compounds with metal-metal bonds bridged by carbon (20) (Eqn. 1). Cluster size can also be increased by the addition of a metal complex across a bridging alkylidyne (Eqn. 2) (21). A similar reaction also occurs between $O{=}Mo(OR)_4$ and $[OR]_3Mo{\equiv}Mo[OR]_3$. This reaction yields a capping oxygen atom and alkoxy group in the product, $Mo_3[\mu_3\text{-}O][\mu_3\text{-}OR][\mu_2\text{-}OR]_3[OR]_6$ (R = neopentyl) (22).

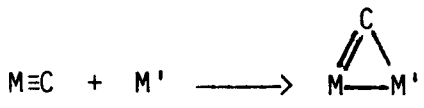

(1)

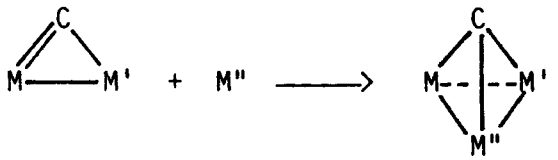

(2)

The high electron density found at a metal-metal multiple bond is similar to that found in metal carbenes or metal carbynes. Attack of a molecule on the metal-metal multiple bond frequently severs the bond completely; however, it is possible to retain a portion of the bond. A compound that exhibits the latter property is $Cp_2Mo_2[CO]_4$ (23). For example, Curtis and co-workers have shown that acetylenes react readily to form dimetallatetrahedrane derivatives. Transition-metal compounds also add across a metal-metal multiple bond. The reaction of $Cp_2Mo_2[CO]_4$ with $Pt[PPh_3]_4$ yields $\{Cp[CO]_2Mo\}_2Pt[PPh_3]_2$ which is suggested to contain a Mo_2Pt trimeric cluster (23). The addition of the metal atom of a transition-metal compound to a multiple bond in a trimeric cluster to form

a tetranuclear cluster has also been demonstrated in the reaction between $Os_3[\mu\text{-}H]_2[CO]_{10}$ and $Pt[C_2H_4]_2[PR_3]$ or $Pt[C_2H_4][PR_3]_2$ (Eqn. 3) (24).

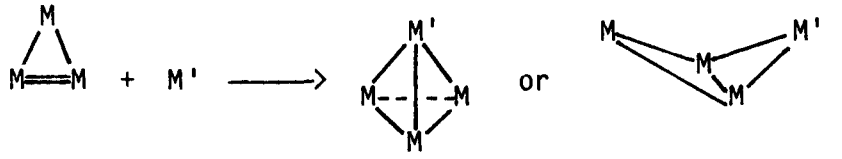

(3)

Considering the above reactions as additions to metal-metal multiple bonds, one should not be too surprised that dimers containing multiple metal bonds react to form larger clusters. One example, $Mo_4Cl_8[PR_3]_4$, has already been mentioned. The reaction between $Mo_2[O(i\text{-}Pr)]_6$ and CH_3COCl also couples two molecules of the dimeric compound to produce $Mo_4Cl_4[O(i\text{-}Pr)]_8$ which contains a square array of molybdenum atoms. However, if CH_3COBr is used instead of CH_3COCl, the resulting structure has a "butterfly" arrangement of metal atoms (25). This metal framework is also found in $[Bu_4N]_2Mo_4I_{11}$ which was first prepared by the thermal decomposition of $Bu_4NMo[CO]_4I_3$ (26) but later was synthesized by coupling dimeric $Mo_2[OAc]_4$ in methanol by reaction with HI and adding Bu_4NI (27). A fourth structure that arises from the coupling of two dimers is that of $W_4[OEt]_{16}$ (28). This compound is synthesized by heating $W_2[NMe_2]_6$ with ethanol in a hydrocarbon solvent (Eqn. 4). Dinuclear compounds do not always couple, however. The reaction of HX with $Re_2[OAc]_4X_2$ (X = Cl, Br, I) at 300°C yields trinuclear Re_3X_9 rather than a tetranuclear product (29,30).

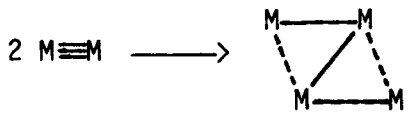

(4)

The possibility of adding a metal atom from a transition-metal compound to a metal cluster containing excess electron density led to the investigation reported in this dissertation. Two molybdenum chloride cluster compounds, $Mo_4Cl_8[PEt_3]_4$ and $[Bu_4N]_2Mo_5Cl_{13}$, seemed particularly suitable for this work. The bonding in the rectangular Mo_4 unit of $Mo_4Cl_8[PEt_3]_4$ was assessed as consisting of two triple bonds and two single bonds (19). Therefore, it was reasoned that a metal atom might capture the extra electrons available by addition across the multiple metal bonds and thus form a larger cluster. The square pyramidal $Mo_5Cl_{13}^{2-}$ cluster (31) has been shown to be susceptible to the addition of metal atoms (32). Our goal was to understand the addition better and hopefully exploit it.

The field of metal cluster chemistry has been growing rapidly, but there is still much to learn. With continued synthetic endeavors, guided by theoretical insight into cluster bonding (33,34), the designed synthesis of a specified, desired cluster will become a reality.

Explanation of Dissertation Format

The dissertation contains four sections, each of which is written in a form suitable for publication in a technical journal. Although references cited in the general introduction are found at the end of the dissertation, each section contains a listing of reference and notes which are cited in that section. The author has conducted all the research presented in each section.

SECTION I. STRUCTURE AND BONDING OF $Mo_4Cl_8(PEt_3)_4$

INTRODUCTION

Several compounds have recently been reported that are synthesized by the self-addition of dimers across a metal-metal bond (1,2). The first report of this type of reaction involved the synthesis of $Mo_4Cl_8[PEt_3]_4$ (3). Further investigations into the synthesis of this tetranuclear cluster led to its direct synthesis from $Mo_2[OAc]_4$ (4). With additional refinement of the synthetic procedure, we have now found that yields of greater than 80% are attainable. A preliminary report of the structure of $Mo_4Cl_8[PEt_3]_4$ was previously communicated (3). The major structural features of the cluster were clearly discerned; however, refinement of the atom parameters did not proceed satisfactorily. Consequently, in the present work new crystals were grown, and a new single crystal x-ray diffraction data set was obtained. Results of the redetermined structure are presented here in addition to an extended Hückel molecular orbital calculation on the molecule $Mo_4Cl_8[PH_3]_4$ which exhibits C_{2h} point group symmetry.

EXPERIMENTAL

Materials

Because $Mo_4Cl_8[PEt_3]_4$ is slightly air and moisture sensitive, materials used in the synthesis were dried and handled with Schlenk techniques. Tetrahydrofuran (THF) was dried and peroxides removed by stirring with sodium and benzophenone. After this treatment, the THF was vacuum distilled onto molecular sieves for storage. Purification of $AlCl_3$ by sublimation was necessary before use. The sublimer consisted of two compartments separated by a coarse frit. A Teflon sleeve in the compartment for the sublimed material and a large, greaseless O-ring joint on the end of this compartment facilitated the recovery of the $AlCl_3$. Commercial $AlCl_3$ was purchased from several sources; however, only the material obtained from Fisher Scientific Company was satisfactory. Other sources supplied $AlCl_3$ that contained a yellow impurity which concurrently sublimed with the $AlCl_3$. Addition of aluminum metal strips to the crude material chamber of the sublimer, a procedure that should eliminate $FeCl_3$, did not diminish the contamination of the sublimed material. After sublimation, the $AlCl_3$ was stored in a nitrogen filled drybox. Chlorobenzene was refluxed over CaH_2, then distilled and stored under nitrogen. Other solvents and triethylphosphine were used as received. The starting material for the preparation of the tetranuclear cluster, $Mo_2[OAc]_4$, was synthesized according to literature procedure (5). $Mo_4Cl_8[PEt_3]_4$ was stored under either vacuum or nitrogen to prolong shelf life.

Synthesis

For a typical preparation of the tetramer, 3.0 g $Mo_2[OAc]_4$ (7.0 mmol), 3.73 g $AlCl_3$ (28 mmol) and 2.1 mL PEt_3 (14.2 mmol) were utilized. The $AlCl_3$ and $Mo_2[OAc]_4$ were placed in a reaction flask in the drybox. About 20 mL of THF were vacuum distilled into the flask, then phosphine was added under a nitrogen flow. After refluxing for 4 hours, the solution was cooled and filtered. An aluminum chloride-acetate species, possibly $AlCl_2[OAc]$, and $Mo_2Cl_4[PEt_3]_4$ were removed from the product by washing the product several times with methanol. A brief wash with a minimal amount of diethyl ether was followed by vacuum drying. This procedure gave an 84% yield (3.37 g) of $Mo_4Cl_8[PEt_3]_4$.

X-ray Structure Determination

Crystals of $Mo_4Cl_8[PEt_3]_4$ were grown from chlorobenzene by placing the solvent and powdered product in a small glass tube which was then sealed. The tube was placed vertically in a sand bath which was gently heated on the bottom. After several days, crystals of suitable size were observed in the tube. A crystal was selected and glued in a capillary with Canada Balsam, then indexed on the Ames Laboratory diffractometer (6) using the automatic indexing program ALICE (7). The unit cell was indicated to be primitive monoclinic. Standard reflections were checked every 75 reflections and found not to vary significantly. Two full octants of data (h,k,l and -h,-k,l) and a portion of a third (-h,k,-l) were collected for a total of 5340 reflections. These data

were corrected for Lorentz and polarization effects. An empirical absorption correction was carried out using diffractometer ϕ-scan data and the program ABSN (8). Other important crystallographic data are given in Table I-1.

Table I-1. Crystal data for $Mo_4Cl_8[PEt_3]_4$

mol. wt.	1140 g/mol
color	yellow-brown
cryst. dimens. mm	0.25X0.20X0.10
space group	$P2_1/a$
cell dimens.[a]	
a Å	14.44(1)
b Å	12.593(2)
c Å	13.75(1)
β deg.	119.10(7)
cell volume, $Å^3$	2184(2)
molecules/cell	2
wavelength Å	0.71034
linear abs. coeff. cm^{-1}	17.7
2θ limit, deg	50
unique no. data	4453
obs. data [$Fo>3\sigma(Fo)$]	2843
final residuals	
R_F	0.050
R_w	0.060
max. residual e^- density	0.9 $e^-/Å^3$

[a]At 25°C, least-squares fit of 16 reflections with $2\theta>20°$.

Structure Solution and Refinement

Systematic absences in the 0k0 and h0l reflections coupled with the information from the HPR plot (9), which indicated a centric cell, led to the selection of the space group $P2_1/a$. A Patterson map was used to

determine the position of the first molybdenum (10). The position of the second molybdenum atom was apparent in the electron density map obtained after the first calculation of structure factors. Subsequent electron density maps were used to locate the remaining atoms. There were six unique ethyl groups, but two of the groups on the P2 atom were disordered as illustrated in Figure I-1. Inclusion of isotropic thermal parameters

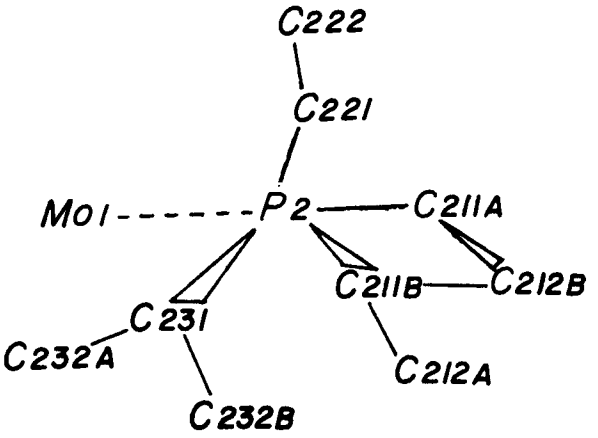

Figure I-1. Carbon atom disorder in $Mo_4Cl_8[P(C_2H_5)_3]_4$

for the disordered carbon atoms and anisotropic thermal parameters for the ordered carbons as well as the heavier atoms in the parameter refinement led to a R factor of 0.079. There were unexplained electron densities located above and below the Mo-Mo short bond. Inclusion of a disordering of the molybdenum atoms to these positions and varying the occupancy decreased the R value to 0.053. The resulting occupancy of the molybdenum

atoms was about 93% in the major position and 6% in the minor position. The data were inspected and found not to need secondary extinction correction. At this point, the data were reweighted based on the requirement that $\overline{\omega\Delta^2}$ should be a constant function of sin θ/λ (11). Methylene hydrogen positions were calculated for the ordered ethyl chains utilizing a C-H bond of 1.05 Å and H-C-H angle of 109.54°. The final hydrogen positions were determined by inserting the hydrogen atom positions, then refining on the carbon atom positions. The new carbon positions were then used to calculate new hydrogen positions. This procedure was repeated until the carbon atoms were shifting significantly less than 1 standard deviation. Tables I-2 and I-3 list final atom positional and thermal parameters for nonhydrogen atoms. Positional parameters for hydrogen atoms are listed in Table I-4. Table I-5 contains important bonding and nonbonding distances and angles. Figure I-2 is an ORTEP drawing of the tetranuclear unit while Figure I-3 shows the entire molecule with carbon and molybdenum disorder.

Extended Hückel Calculations

Extended Hückel calculations were performed with a program obtained from E. R. Davidson of the University of Washington. This program (12) allows iterative calculations to charge self-consistency and permits the use of three mirror planes in the molecule. Atomic coordinates (Table I-6) were obtained from the crystal structure of $Mo_4Cl_8[PEt_3]_4$; however, hydrogen atoms were substituted for the alkyl groups on the phosphine ligands. Hydrogen atom positions were calculated assuming a P-H bond

Table I-2. Positional parameters [x10^4] for $Mo_4Cl_8[PEt_3]_4$[a]

Atom	x	y	z	mult.[b]	U(ave)[c]
Mo(1)	6112.4(5)	4801.9(5)	1389.7(5)	0.932(3)	35
Mo(2)	4440.6(5)	5114.9(5)	941.1(5)	0.933(3)	36
Mo(3)	5305(8)	4073(9)	1131(9)	0.058(2)	38
Mo(4)	5299(8)	5821(9)	1226(9)	0.054(2)	41
Cl(1B)	5955(1)	3301(1)	198(1)	---	50
Cl(2B)	6462(1)	6203(2)	446(1)	---	47
Cl(1T)	4329(2)	6291(2)	2279(2)	---	63
Cl(2T)	6963(2)	3520(2)	2882(2)	---	53
P(1)	4034(2)	3763(2)	2077(2)	---	50
P(2)	7088(2)	6120(2)	2991(2)	---	60
C(111)	4889(7)	3780(8)	3588(7)	---	64
C(121)	3796(7)	2376(7)	1650(8)	---	66
C(131)	2718(7)	4145(8)	1911(8)	---	69
C(112)	4507(8)	3086(11)	4254(8)	---	99
C(122)	4724(8)	1770(8)	1686(9)	---	81
C(132)	1900(7)	4512(10)	746(9)	---	81
C(221)	7040(8)	5850(9)	4256(8)	---	69
C(222)	7963(9)	6196(13)	5344(10)	---	105
C(211A)	6500(20)	7580(20)	2600(20)	0.50	---
C(211B)	7160(30)	7480(20)	2780(20)	0.50	---
C(212A)	6250(30)	8160(40)	2340(40)	0.50	---
C(212B)	7080(20)	8370(20)	3500(20)	0.50	---
C(231)	8450(10)	6240(20)	3340(10)	1.00	---
C(232A)	8970(20)	5630(20)	2770(20)	0.50	---
C(232B)	8870(20)	5420(20)	3520(20)	0.50	---

[a]Estimated standard deviations are given in parentheses for the last significant digits.

[b]Unless noted otherwise, multiplicity is 1.00.

[c]U(ave) [x 10^3, $Å^2$] is the average of U_{11}, U_{22} and U_{33}.

Table I-3. Thermal parameters [x10^3] for $Mo_4Cl_8[PEt_3]_4$[a]

Atom	U_{11}	U_{22}	U_{33}	U_{12}	U_{13}	U_{23}
Mo(1)	30.6(4)	39.5(4)	34.4(4)	0.0(3)	14.2(3)	0.8(3)
Mo(2)	32.4(4)	39.9(4)	36.3(4)	0.9(3)	16.8(3)	0.6(3)
Mo(3)	30(5)	44(6)	41(5)	-3(4)	16(5)	-3(5)
Mo(4)	39(6)	41(6)	43(6)	-4(5)	27(5)	-8(5)
Cl(1B)	56(1)	46(1)	49(1)	9.9(9)	24.3(9)	1.5(9)
Cl(2B)	47.1(9)	51(1)	41.8(9)	-11.8(8)	20.3(8)	-2.3(8)
Cl(1T)	71(1)	62(1)	57(1)	5(1)	37(1)	-10(1)
Cl(2T)	51(1)	60(1)	47(1)	11.1(9)	20.9(9)	11.4(9)
P(1)	45(1)	60(1)	45(1)	-4.2(9)	23.1(9)	6.5(9)
P(2)	62(1)	69(1)	48(1)	-21(1)	27(1)	-15(1)
C(111)	58(5)	77(6)	57(5)	3(4)	32(4)	6(4)
C(121)	66(5)	66(5)	67(5)	-9(4)	35(5)	9(4)
C(131)	54(5)	77(6)	75(6)	-4(4)	37(5)	8(5)
C(112)	79(6)	147(10)	70(6)	9(6)	44(5)	39(6)
C(122)	79(6)	58(5)	105(8)	6(5)	49(6)	6(5)
C(132)	52(5)	111(8)	80(6)	15(5)	27(5)	27(6)
C(221)	73(6)	87(6)	48(5)	-18(5)	30(5)	-15(5)
C(222)	82(6)	166(14)	68(6)	-22(8)	24(5)	-16(8)
C(211A)	82(6)	---	---	---	---	---
C(211B)	101(8)	---	---	---	---	---
C(212A)	171(14)	---	---	---	---	---
C(212B)	98(6)	---	---	---	---	---
C(231)	136(5)	---	---	---	---	---
C(232A)	80(5)	---	---	---	---	---
C(232B)	103(6)	---	---	---	---	---

[a]Estimated standard deviations are given in parentheses for the last significant digits. The anisotropic thermal parameter expression used is $\exp[-2\pi^2(U_{11}h^2a^{*2} + U_{22}k^2b^{*2} + U_{33}l^2c^{*2} + 2U_{12}hka^*b^* + 2U_{13}hla^*c^* + 2U_{23}klb^*c^*)]$ with U's in $Å^2$. Isotropic thermal parameters are given as U_{11} and are in $Å^2$.

Table I-4. Hydrogen positional parameters[a]

Atom	x	y	z
H(111)	4941	4568	3872
H(112)	5643	3510	3780
H(121)	3183	2344	821
H(122)	3574	1974	2166
H(131)	2832	4777	2460
H(132)	2396	3494	2107
H(221)	6959	5025	4297
H(222)	6367	6233	4189

[a]All hydrogen atoms were assigned isotropic U values of 50.7 x 10^{-3} $Å^2$.

Table I-5. Distances (Å) and angles (deg) for $Mo_4Cl_8[PEt_3]_4$[a]

Distances

Mo(1)-Mo(2')	2.904(3)	P(2)-C(23B)	1.795(18)
Mo(1)-Mo(2)	2.217(2)	P(2)-C(21A)	1.981(28)
Mo(1)-Cl(1B)	2.439(2)	P(2)-C(21D)	1.749(29)
Mo(1)-Cl(2B)	2.385(2)	C(111)-C(112)	1.549(15)
Mo(1)-Cl(2T)	2.421(3)	C(121)-C(122)	1.522(13)
Mo(1)-P(2)	2.563(3)	C(131)-C(132)	1.528(14)
Mo(2)-Cl(1B)	2.427(2)	C(221)-C(222)	1.504(16)
Mo(2)-Cl(2B)	2.382(2)	C(211A)-C(212B)	1.487(36)
Mo(2)-Cl(1T)	2.427(3)	C(211A)-C(212A)	0.818(58)
Mo(2)-P(1)	2.564(2)	C(211A)-C(211B)	0.856(42)
P(1)-C(111)	1.829(9)	C(212B)-C(212A)	1.483(51)
P(1)-C(121)	1.821(10)	C(212B)-C(211B)	1.528(37)
P(1)-C(131)	1.864(9)	C(231)-C(232A)	1.521(27)
P(2)-C(221)	1.806(9)	C(231)-C(232B)	1.163(33)

Nonbonding distances

Cl(1B)-Cl(2B)	3.710(3)	Cl(2B)-P(2)	3.162(4)
Cl(1B)-Cl(2B')	3.217(3)	Cl(1T)-P(1)	3.206(4)
Cl(1B)-Cl(1T)	3.267(4)	Cl(1T)-P(2)	3.617(5)
Cl(1B)-Cl(2T)	3.259(4)	Cl(2T)-P(1)	3.790(5)
Cl(2B)-P(1)	3.183(4)	Cl(2T)-P(2)	3.280(4)

Distances from disordered Mo(4) unit to ligands

Mo(3)-Mo(4')	2.921(15)	Mo(3)-P(1)	2.744(10)
Mo(3)-Mo(4)	2.205(16)	Mo(4)-Cl(1B)	2.210(11)
Mo(3)-Cl(1B)	2.156(10)	Mo(4)-Cl(2B)	2.440(11)
Mo(3)-Cl(2B)	2.440(10)	Mo(4)-Cl(1T)	2.526(11)
Mo(3)-Cl(2T)	2.513(11)	Mo(4)-P(2)	2.570(12)

[a]Estimated standard deviations are given in parentheses for the last significant digits.

Table I-5. (Continued)

Angles			
Mo(2')-Mo(1)-Mo(2)	90.50(8)	Cl(1B)-Mo(1)-Mo(2)	102.57(7)
Mo(1')-Mo(2)-Mo(1)	89.50(8)	Cl(2B)-Mo(1)-Mo(2)	101.96(7)
Mo(1')-Cl(1B)-Mo(2)	73.27(7)	Cl(1B)-Mo(2)-Mo(1)	102.03(7)
Mo(1')-Cl(2B)-Mo(2)	75.04(8)	Cl(2B)-Mo(2)-Mo(1)	101.35(8)
Mo(2')-Mo(1)-Cl(2T)	135.89(6)	Cl(2B')-Mo(2)-P(1)	80.04(8)
Mo(1')-Mo(2)-Cl(1T)	136.91(6)	Cl(1B')-Mo(2)-Cl(1T)	84.58(8)
Mo(2')-Mo(1)-P(2)	131.75(7)	Cl(1B)-Mo(1)-Cl(2T)	84.25(9)
Mo(1')-Mo(2)-P(1)	132.44(6)	Cl(2B)-Mo(1)-P(2)	79.31(8)
Mo(2)-Mo(1)-Cl(2T)	111.95(8)	Cl(1B')-Mo(2)-P(1)	152.53(7)
Mo(1)-Mo(2)-Cl(1T)	111.23(9)	Cl(2B')-Mo(2)-Cl(1T)	145.08(8)
Mo(2)-Mo(1)-P(2)	101.12(8)	Cl(1B)-Mo(1)-P(2)	155.77(7)
Mo(1)-Mo(2)-P(1)	104.68(7)	Cl(2B)-Mo(1)-Cl(2T)	143.90(7)
P(2)-Mo(1)-Cl(2T)	82.28(10)	P(1)-Mo(2)-Cl(1T)	79.89(8)
Cl(2B)-Mo(1)-Cl(1B)	100.56(8)	Cl(2B')-Mo(2)-Cl(1B')	101.00(9)

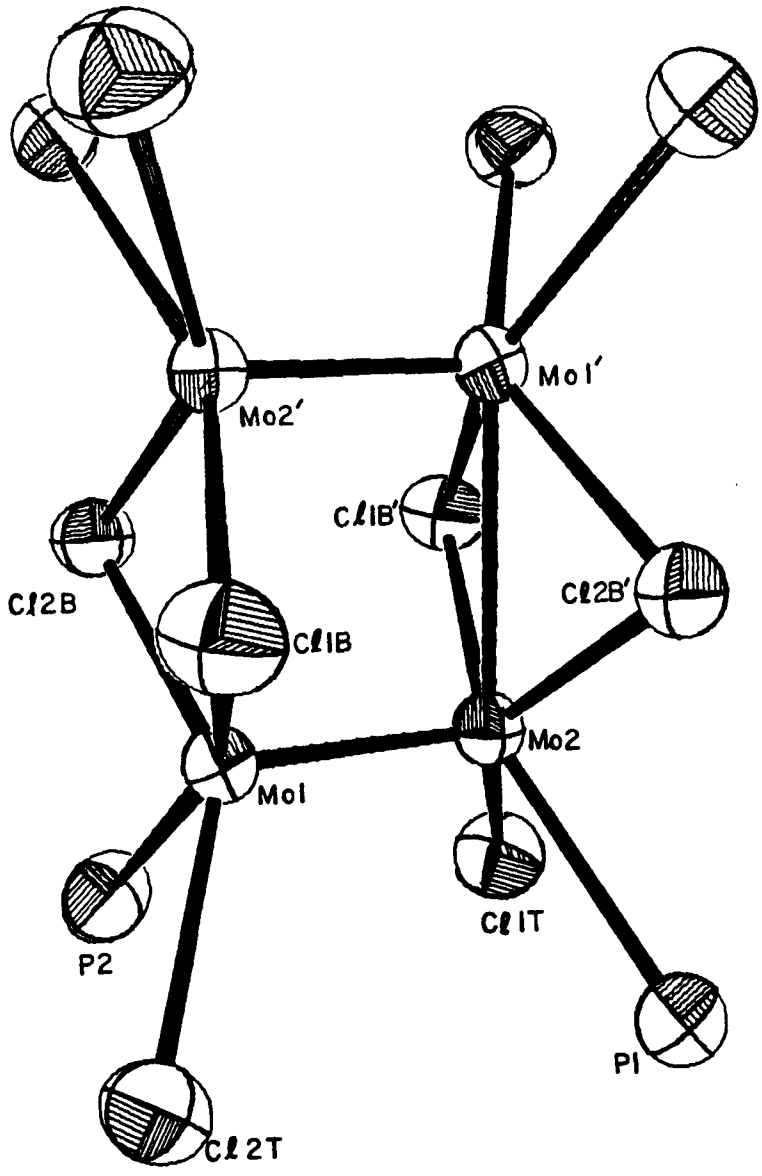

Figure I-2. Structure of $Mo_4Cl_8[P(C_2H_5)_3]_4$ with carbon atoms and disordered molybdenum atoms omitted

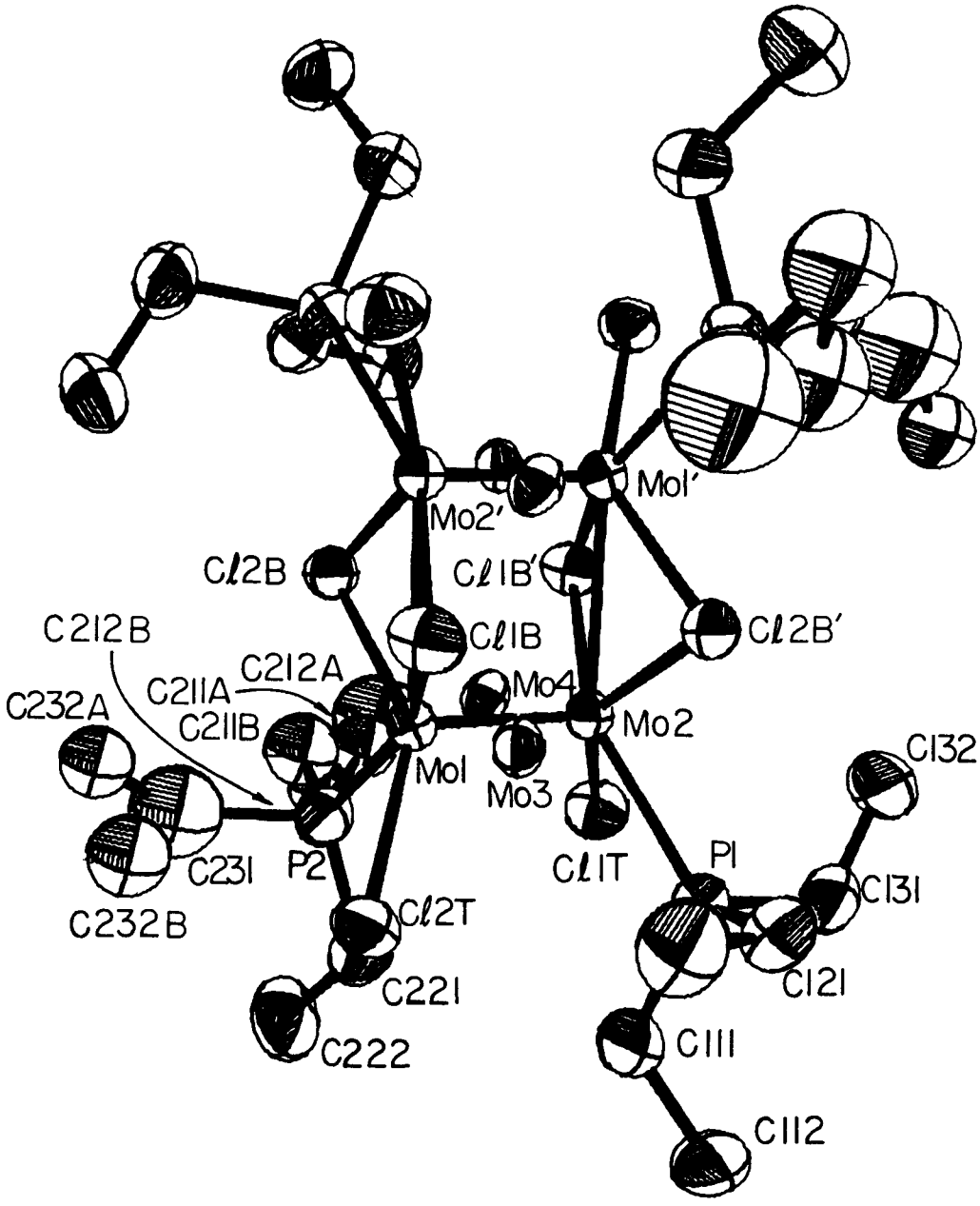

Figure I-3. Structure of $Mo_4Cl_8[P(C_2H_5)_3]_4$ showing disorder of molybdenum and carbon atoms

Table I-6. Parameters for $Mo_4Cl_8[PH_3]_4$ used in extended Hückel calculation[a]

Atom	x	y	z	final charge
Mo(1)	1.452	1.108	0.000	0.24
Mo(2)	1.452	-1.108	0.000	0.23
Cl(1T)	3.207	-2.000	1.413	-0.35
Cl(2T)	3.207	2.000	-1.413	-0.35
Cl(1B)	0.000	1.608	-1.855	-0.16
Cl(1B')	0.000	-1.608	1.855	-0.17
Cl(2B)	0.000	1.608	1.855	-0.14
Cl(2B')	0.000	-1.608	-1.855	-0.11
P(1)	3.171	-1.680	-1.813	0.13
P(2)	3.171	1.680	1.813	0.08
H	4.187	-0.717	-1.813	0.07
H	3.722	-2.940	-1.552	0.07
H	2.542	-1.695	-3.064	0.07
H	2.211	0.997	2.570	0.03
H	4.324	1.871	2.584	0.05
H	2.659	2.923	1.422	0.02

[a]A mirror in the yz plane generated the remainder of the molecule.

distance of 1.40 Å and a H-P-H angle of 109.5°. The valence orbital ionization energies for Mo, Cl and P were calculated (13) from atomic spectral data (14) and zeta exponents were determined from data compiled in Table 4 of the work by Cusachs and Corrington (15). These values are listed in Table I-7. The necessary parameters for hydrogen atoms are stored in the program. The extended Hückel calculation was iterated until the output atomic charges were within 0.0156 of the input charges for all atoms. The symmetry of the molecular orbitals was determined by examining the major contributing atomic orbitals.

Table I-7. Calculated parameters for extended Hückel calculation[a]

Atom	Orbital		VOIE (eV)	Zeta[b]
Mo	5s	neutral	-7.00	1.46
		(+1)	-12.4	
	5p	neutral	-4.26	1.46
		(+1)	-8.21	
	4d	neutral	-7.99	2.53
		(+1)	-13.35	
Cl	3s	neutral	-25.28	2.23
		(-1)	-17.0	
	3p	neutral	-13.72	1.86
		(-1)	-3.74	
P	3s	neutral	-19.32	1.79
		(+1)	-38.50	
	3p	neutral	-10.14	1.48
		(+1)	-29.27	

[a]The Wolfsberg-Helmholtz interaction constant, K, was assumed to be 1.89 for all orbitals.

[b]Calculated from data in Table 4 of reference 15.

RESULTS AND DISCUSSION

The differences between the structure that was initially reported (3) and the more accurate structure reported here are slight. The crystal quality was apparently significantly better in the current investigation as 20% more observed reflections were recorded for the correct unit cell which has 0.5% larger volume than previously reported. Although the current cell volume is essentially the same as the previously reported volume, the cell parameters are significantly different. The most obvious difference is the c axis which is about 0.5 Å shorter than the corresponding axis in the preliminary structure report. Both cells are monoclinic, but the β angle differs by 3 degrees. Bond distances and angles within the cluster unit, however, are essentially the same as those previously reported.

A feature that was not previously observed in the structure of $Mo_4Cl_8[PEt_3]_4$ is the 6% disordering of the molybdenum atoms. The plane containing those molybdenum atoms of lower occupancy is rotated about 79 degrees from the plane containing the molybdenum atoms of higher occupancy. This leads to considerably different distances from the minor molybdenum positions to the ligands (Table I-5) than from the major molybdenum positions to the ligands. The metal-metal distances within the plane of the rotated rectangular unit of molybdenum atoms are, within error, the same as those in the major plane. There was no obvious disorder of the chlorine and phosphorus atoms and no attempt was made to calculate the deviation from the true position of the ligands caused by the small amount of metal atom disorder.

Disorder of metal atoms within a ligand sphere has been previously observed for dinuclear compounds. The single crystal structure of $K_4Mo_2Cl_8 \cdot 2H_2O$ revealed that about 7% of the molybdenum-molybdenum dimers are perpendicular to the major orientation (16). The structure of $[Bu_4N]_2Re_2Cl_8$ disclosed the same type of disorder as in $K_4Mo_2Cl_8$, but the major position was occupied 74% and the minor position 26% (17). The crystal structure of $Re_2Cl_8[PEt_3]_4$ (18) also indicated disorder of the metal pair of atoms; however, the disorder was more severe. The Re-Re dimer equally occupied three mutually perpendicular orientations in this instance. In all of these examples, the ligand positions were only slightly affected by the metal atom disorder.

As has been previously discussed (3,19), the Mo-Mo bonding in $Mo_4Cl_8[PEt_3]_4$ is best described as triple bonds on the short edges of the rectangle and single bonds on the long edges. This seems very reasonable considering the bond distances (2.904(3) Å and 2.217(2) Å) and the acute angle at the bridging chlorine atoms (74.2° ave.).

The bridging chlorines are extremely crowded. Three of the four nonbonding bridging chlorine to ligand distances average about 3.2 Å which is considerably less than the sum of the van der Waals radii (20) of at least 3.4 Å. The nonbonding distances in the tetranuclear cluster are compared with the more reasonable values found in $K_4Mo_2Cl_8$ in Figure I-4 (21). Further evidence for the formation of a long Mo-Mo single bond is the displacement of the molybdenum atom pairs from the center of the box formed by the ligands towards the central plane of bridging chlorine atoms as shown in Figure I-5 (21).

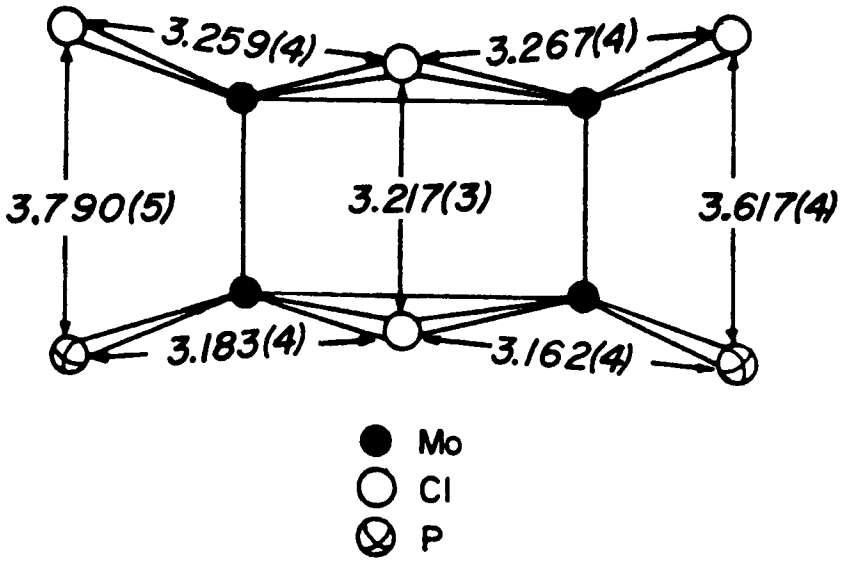

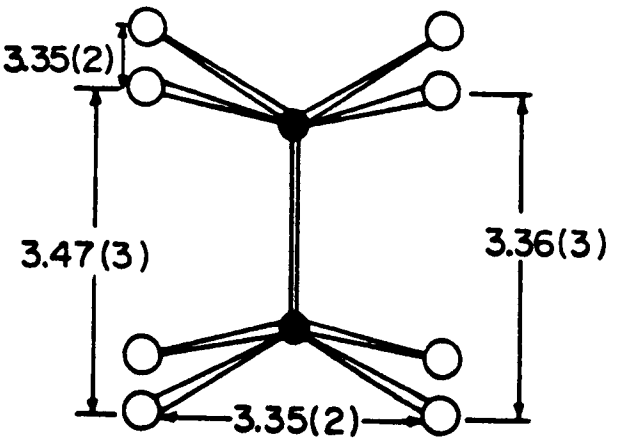

Figure I-4. Nonbonding contacts (Å) in $Mo_4Cl_8[P(C_2H_5)_3]_4$ and $K_4Mo_2Cl_8 \cdot 2H_2O$

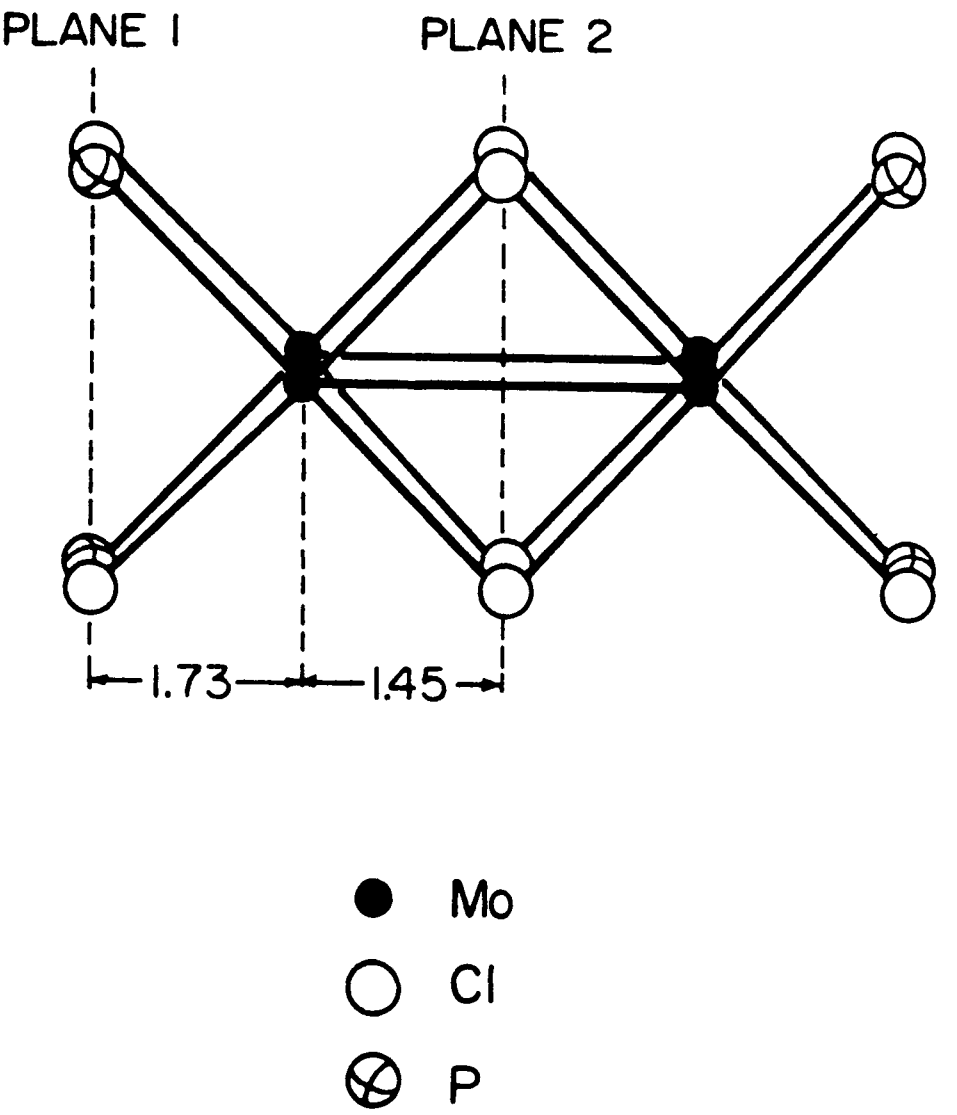

Figure I-5. Distances (Å) of molybdenum atoms from least-squares planes in $Mo_4Cl_8[P(C_2H_5)_3]_4$. Angle between Plane 1 and Plane 2 is 0.3°

The quadruple bond in dinuclear compounds such as $Mo_2Cl_4[PEt_3]_4$ consists of 1 σ, 2 π, and 1 δ bond. The electronic transition between the δ and δ^* energy levels occurs at about 560 nm and gives rise to the blue color of the compounds. The absence of the absorption in the tetranuclear compounds led to the conclusion that the δ-bond has been disrupted and that the electrons involved in the δ-bond are now forming the σ-bond on the long edge of the cluster (3,19). Although this rather simplistic view is consistent with the spectrum, we believed an extended Hückel molecular orbital calculation could be enlightening.

A portion of the energy level diagram resulting from the Hückel calculation is presented in Figure I-6. The symmetry labeled orbitals contain major contributions from the metal atoms. Unlabeled energy levels are primarily ligand based. As well as identifying the irreducible representation of each energy level, the symmetry with respect to the metal-metal bond was determined. For example, the highest occupied molecular orbital (HOMO) has a calculated energy of about -9.1 eV and has σ character on the long edge and δ^* overlap on the short edge of the rectangle. These types of overlaps are also illustrated in Figure I-6. The lowest unoccupied molecular orbital (LUMO) has, as expected, σ^* overlap on the long edge of the rectangle and the short edge has δ overlap. The transition of lowest energy ($b_u \rightarrow a_u$) appears to be a forbidden transiton which is $\delta^* \rightarrow \delta$ along the short edge rather than the $\delta \rightarrow \delta^*$ transition observed in quadruply bonded compounds. The remainder of the energy level diagram is as anticipated. The close approach of the molybdenum atoms on the short edge should make the orbital overlap along

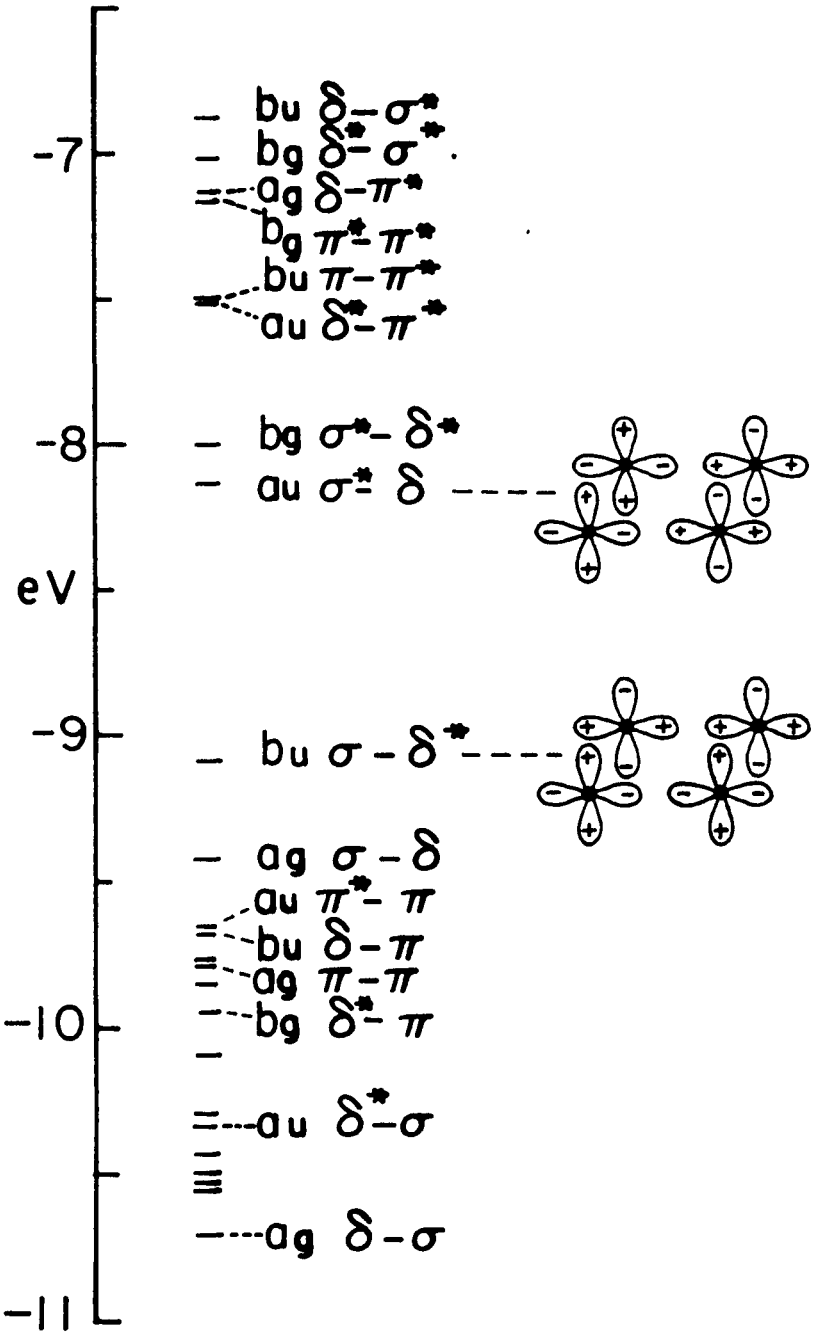

Figure I-6. Molecular orbitals for $Mo_4Cl_8(PH_3)_4$. Labeled orbitals are primarily metal based. Orbital overlap symmetry is given in the order long bond-short bond

that edge the major determining factor in arrangement of the molecular orbitals. Indeed, the two metal bonding orbitals lowest in energy have σ overlap along the short edge of the rectangle and the next four metal bonding orbitals have π overlap.

The extended Hückel calculation, therefore, substantiates the earlier interpretation that the Mo-Mo bonding in $Mo_4Cl_8[PEt_3]_4$ consists of alternating single and triple bonds in the rectangular Mo_4 unit.

REFERENCES AND NOTES

1. Chisholm, M. H.; Errington, R. J.; Folting, K.; Huffman, J. C. J. Am. Chem. Soc. 1982, 104, 2025.

2. Chisholm, M. H.; Leonelli, J.; Huffman, J. C. J. Chem. Soc., Chem. Commun. 1981, 270.

3. McGinnis, R. N.; Ryan, T. R.; McCarley, R. E. J. Am. Chem. Soc. 1978, 100, 7900.

4. Ryan, T. R.; McCarley, R. E. Inorg. Chem. 1982, 21, 2072.

5. McCarley, R. E.; Templeton, J. L.; Colburn, T. J.; Katovic, V.; Hoxmeier, R. J. Adv. Chem. Ser. 1976, 150, 319.

6. Rohrbaugh, W. J.; Jacobson, R. A. Inorg. Chem. 1974, 13, 2535.

7. Jacobson, R. A. J. Applied Crystallogr. 1976, 9, 115.

8. Karcher, B. A. Ph.D. Dissertation, Iowa State University, Ames, Iowa, 1981.

9. Howells, E. R.; Phillips, D. C.; Rodgers, D. Acta Cryst. 1950, 3, 210.

10. Structure factor calculations and least squares refinements were done using the block matrix/full matrix program ALLS (R. L. Lapp and R. A. Jacobson), Fourier series calculations were done using the program FOUR (D. R. Powell and R. A. Jacobson), and for molecular drawings the program ORTEP (C. K. Johnson) was used.

11. Cruickshank, D.W.J.; Pilling, D. E. In "Computing Methods and the Phase Problem in X-ray Crystal Analysis"; Pepsinsky, R.; Roberts, J. M.; Speakman, J. C.; Eds.; Pergamon Press: New York, 1961; pg 45.

12. Schaffer, A. M.; Gouterman, M.; Davidson, E. R. Theoret. chim. Acta (Berl.) 1973, 30, 9. This program was obtained and modified slightly for us by Dr. Stephen Elbert.

13. McGlynn, S. P.; Vanquickenborne, L. G.; Kinoshita, M.; Carroll, D. G. "Introduction to Applied Quantum Chemistry"; Holt, Rinehart and Winston, Inc.: New York, 1972.

14. Moore, C. E. "Atomic Energy Levels", Nat. Stand. Ref. Data Ser., Nat. Bur. Stand. (U.S.) 1971, No. 35.

15. Cusachs, L. C.; Corrington, J. H. In "Sigma Molecular Orbital Theory"; Sinanoglu, O.; Wiberg, K. B., Eds.; Yale University Press: New Haven, Conn., 1970; Chapter VI-4.

16. Brencic, J. V.; Cotton, F. A. Inorg. Chem. 1969, 8, 7.

17. Cotton, F. A.; Frenz, B. A.; Stults, B. R.; Webb, T. R. J. Am. Chem. Soc. 1976, 98, 2768.

18. Cotton, F. A.; Frenz, B. A.; Ebner, J. R.; Walton, R. A. J. Chem. Soc., Chem. Commun. 1974, 4.

19. Ryan, T. R. Ph.D. Dissertation, Iowa State University, Ames, Iowa, 1981, Section I.

20. Bondi, A. J. Phys. Chem. 1964, 68, 441.

21. This figure was taken from reference 19 and necessary corrections made.

SECTION II. PREPARATION AND CHARACTERIZATION OF $Mo_8Cl_{16}(PR_3)_4$

INTRODUCTION

Organic chemists have long been able to form, at will, large molecules containing primarily carbon atoms from small molecular building blocks, but this type of systematic chemistry has not been generally available to the inorganic chemist working with transition-metal compounds. The interest in modeling metal surfaces with metal clusters (1) has encouraged inorganic chemists to synthesize molecular metal clusters, and a number of very large clusters have been formed (2,3). Compounds containing metal-metal multiple bonds are a logical precursor for the synthesis of large clusters because of the potential for the addition of atoms or molecules to the multiple bond. The addition of transition-metal compounds to small cluster compounds to form larger clusters has been successful in some cases (4-6). The stepwise formation of small metal clusters is not satisfactorily understood and deserves further research. During a study of the addition of metal atoms to the $Mo_4Cl_8[PEt_3]_4$ cluster, we discovered the $Mo_8Cl_{16}[PR_3]_4$ compounds. Although a single crystal structure has not been completed, characterization by other instrumental techniques and chemical reactions leads us to believe that linkage of two of the rectangular $Mo_4Cl_8[PR_3]_4$ clusters has occurred.

EXPERIMENTAL

Materials

The air-sensitive nature of the compounds that were prepared required the use of Schlenk techniques and dry solvents. Tetrahydrofuran and chlorobenzene were dried and stored as previously described (7). Acetonitrile and dichloromethane were dried with CaH_2 then vacuum distilled onto molecular sieves for storage. Other solvents and phosphines were used as received. $AlCl_3$ was purified by sublimation as previously described (7). The $Mo[CO]_6$ was dried by storing in a desiccator containing $CaSO_4$ for several weeks before use. The starting material for the preparation of the tetranuclear clusters, $Mo_2[OAc]_4$, was synthesized according to literature procedure (8). The $Mo[CO]_4Cl_2$ was synthesized from $Mo[CO]_6$ and Cl_2 at -60°C (9). Chlorine was distilled from the cylinder into a trap where it was outgassed before distilling onto the molybdenum hexacarbonyl. After gas evolution had ceased, the excess Cl_2 was distilled from the product and the product was allowed to warm to room temperature. The $Mo[CO]_4Cl_2$ of highest purity was obtained when the $Mo[CO]_6$ had been dried and a fresh cylinder of Cl_2 was used.

Samples to be analyzed were decomposed in a $KOH-H_2O_2$ aqueous solution. In those instances where the sample resisted decomposition by this method, the sample was mixed with powdered NaOH and heated in a nickel crucible until decomposed. Molybdenum analyses were accomplished by precipitation of $MoO_2[C_9H_6ON]_2$ (10). The chloride content was obtained by potentiometric titration of the solution with standardized $AgNO_3$.

Carbon, nitrogen, hydrogen and phosphorus analyses were performed by the Ames Laboratory Analytical Services.

Physical Measurements

A Beckman IR4250 spectrometer was used to measure the infrared spectra. The solution uv-visible spectra were recorded with a Cary 14 spectrometer. A Beckman DU spectrophotometer was used for measuring the reflectance spectra. The reference compound for the reflectance spectra was $BaSO_4$.

X-ray photoelectron spectra were obtained by grinding the sample in a dry box, spreading the powder on a strip of Ag-Cd alloy, then transferring directly into the AEI ES200B spectrometer. Aluminum Kα radiation (1486.6 eV) was used to irradiate the sample. Nonmonochromatic radiation was used with a 4x4 slit setting. The electrostatic charge on the sample was kept constant by using an electron floodgun. Binding energies of resolved peaks were referenced to the C 1s signal which was assumed to be 285.0 eV. Data reduction and spectrum resolution computations were accomplished with APES (11), a computer program developed in this laboratory to resolve XPS spectra, using a previously described procedure (12).

Synthesis

$Mo_4Cl_8[PR_3]_4$

The tetrameric clusters were synthesized from $Mo_2[O_2CCH_3]_4$ using $AlCl_3$ in THF and the appropriate phosphine. The previously published

method, using a $Mo_2[OAc]_4$:$AlCl_3$:PR_3 mol ratio of 2:4:4, gave approximately a 50% yield (13), but by doubling the amount of $AlCl_3$ used (7), yields of close to 80% were achieved.

$$2\ Mo_2[OAc]_4 + 8\ AlCl_3 + 4\ PR_3 \longrightarrow Mo_4Cl_8[PR_3]_4 + 8\ AlCl_2(OAc)$$

Washing the product with methanol removes any $Mo_2Cl_8[PR_3]_4$ that is present for the tetrameric clusters formed with PEt_3, PPr_3, or $P[n\text{-}Bu]_3$. Apparently some $Mo_2Cl_4[PMe_2Ph]_2$ co-crystallizes with the tetranuclear compound in the synthesis of $Mo_4Cl_8[PMe_2Ph]_4$. A visible spectrum of the product indicated that about 2% of the dinuclear compound was present. Dissolving the tetrameric cluster in CH_2Cl_2 and reprecipitating it by adding hexane was necessary to remove the blue $Mo_2Cl_4[PMe_2Ph]_4$. The yield of pure material was about 75%. Anal. Calcd. for $Mo_4Cl_8[PMe_2Ph]_4$: Mo, 31.46; Cl, 23.25; C, 31.50; H, 3.64; Cl/Mo = 2.00, C/Mo = 8.00. Found: Mo, 31.19; Cl, 23.03; C, 31.10; H, 3.77; (Cl/Mo = 2.00, C/Mo = 7.96).

$Mo_8Cl_{16}[PR_3]_4$

The initial synthesis of $Mo_8Cl_{16}[PEt_3]_4$ resulted from the reaction between $Mo_4Cl_8[PEt_3]_4$ and $Mo[CO]_4Cl_2$ in a 1:1 mol ratio in refluxing chlorobenzene. After 24 hours, filtration of the mixture separated a yellow-brown solid from the brown solution. Vacuum distilling the solvent from the filtrate left dark-brown and yellow solids, which were separated by extracting with acetonitrile. The infrared spectrum of the yellow solid indicated that it was $Mo_4Cl_8[PEt_3]_4$. The infrared spectrum of the brown substance indicated the presence of carbonyl ligands. No further

characterization of the latter compound was undertaken, but it was presumed to be $Mo[CO]_3Cl_2[PEt_3]_2$ (9).

After the insoluble product from the above reaction was subjected to a chlorobenzene extraction to remove the tetranuclear cluster compound, an analysis was obtained. Found: Mo, 41.50; Cl, 30.14; C, 16.23; H, 3.37. Assuming all of the carbon present is from triethylphosphine, the calculation of 6.98% P was possible. This leads to a Cl/Mo ratio of 1.97 and a P/Mo ratio of 0.52. Calcd. for $Mo_8Cl_{16}[PEt_3]_4$: Mo, 42.47; Cl, 31.38; C, 15.95; H, 3.35; P, 6.85.

The analysis indicated that triethylphosphine had been lost from the tetrameric compound. The synthesis of pure $Mo[CO]_4Cl_2$ is difficult and time consuming; therefore, the use of other phosphine accepting compounds was investigated. The reaction of $Mo[CO]_6$ with $Mo_4Cl_8[PEt_3]_4$ in a 1:1 mol ratio in refluxing chlorobenzene was found to be the best synthetic route. After 2 hours, the product was filtered from the solution and extracted with the filtrate. A 78% yield of $Mo_8Cl_{16}[PEt_3]_4$ was obtained. The proposed octanuclear cluster compound was stable in air for short periods of time (<1 day) and should be stored under nitrogen or vacuum.

The synthesis of other phosphine derivatives of the proposed octanuclear cluster was possible. The tetranuclear compound, $Mo_4Cl_8[PR_3]_4$, was first synthesized with the desired phosphine ligand. The tetranuclear compound was then reacted with $Mo[CO]_6$ in a 1:1 mol ratio in refluxing chlorobenzene for several hours. The resulting precipitate was extracted with solvent distilled from the filtrate, dried, and analyzed. Anal. Calcd. for $Mo_8Cl_{16}[PPr_3]_4$: Mo, 38.85; Cl, 28.71; C,

21.88; H, 4.29. Found: Mo, 35.82; Cl, 26.10; C, 24.34; H, 4.40; (Cl/Mo = 1.97). Anal. Calcd. for $Mo_8Cl_{16}[PMe_2Ph]_4$: Mo, 40.67; Cl, 30.05; C, 20.36; H, 2.35; P, 6.56. Found: Mo, 37.30; Cl, 27.02; C, 24.54; H, 2.94; P, 6.36; (Cl/Mo = 1.96; P/Mo = 0.53).

RESULTS AND DISCUSSION

Chemical analysis of the product obtained from the reaction between $Mo_4Cl_8[PEt_3]_4$ and $Mo[CO]_4Cl_2$ in chlorobenzene, indicated the formulation to be $\{Mo_2Cl_4[PEt_3]\}_x$. The infrared spectrum was very similar to that of tetrameric clusters, but there were some obvious differences. The absorptions found at 1410 and 425 cm^{-1} in the spectra of $Mo_4Cl_8[PEt_3]_4$ were dramatically reduced in intensity, and the band at 970 cm^{-1} was absent. The region of the spectrum between 200-400 cm^{-1}, which contains mainly absorptions due to Mo-Cl stretching vibrations, also changed, as shown in Figure II-1. There were now three absorptions: 370 cm^{-1} sharp and strong, 335 cm^{-1} medium, and 275 cm^{-1} medium. The x-ray powder pattern indicated that the compound was crystalline and had a large unit cell. The largest observed d spacing was 14.53 Å, but strong diffraction lines also occurred at d values of 10.63 Å and 8.09 Å. The decreased phosphine content and also the apparent similarity to the tetrameric structure led to the deduction that $Mo[CO]_4Cl_2$ was acting as a phosphine acceptor and thereby promoting the linkage of two tetrameric clusters to form the proposed octanuclear cluster compound.

$$2\ Mo_4Cl_8[PEt_3]_4 + 2\ Mo[CO]_4Cl_2 \longrightarrow Mo_8Cl_{16}[PEt_3]_4 + 2\ Mo[CO]_3Cl_2[PEt_3]_2 + 2\ CO$$

The product is nearly insoluble in a variety of solvents ranging from hexane to acetonitrile. Because of the insolubility, reflectance spectroscopy was used to investigate the visible spectrum. For reference,

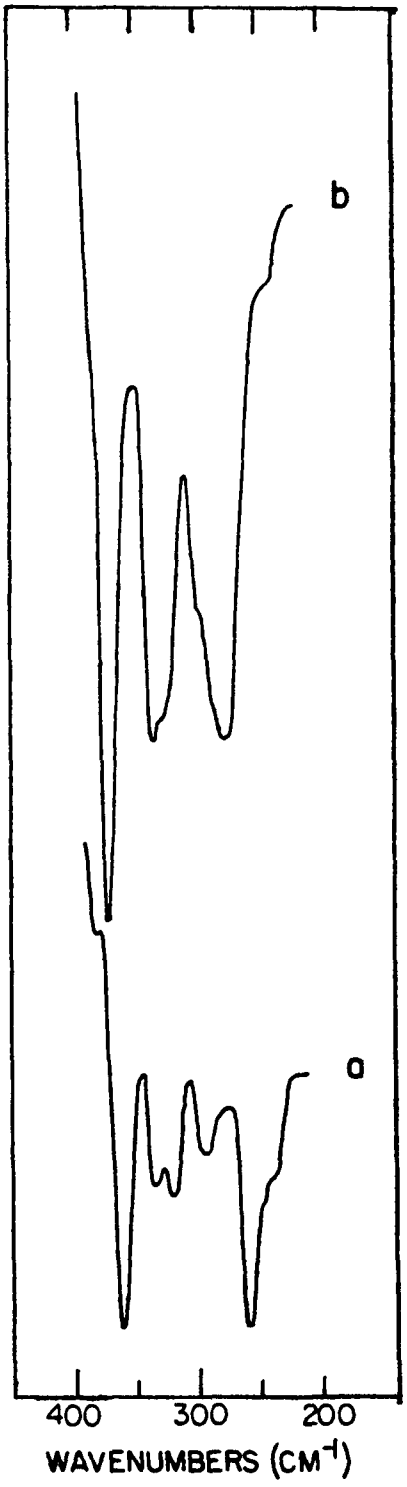

Figure II-1. Infrared spectra of a) $Mo_4Cl_8[PEt_3]_4$ and b) $Mo_8Cl_{16}[PEt_3]_4$

the reflectance spectrum of $Mo_4Cl_8[PEt_3]_4$ was also obtained in this investigation. Previous work (13) indicated that bands in the visible spectra of $Mo_4Cl_8L_4$ derivatives undergo a blue shift as L decreases in field strength according to the spectrochemical series. Since the formation of the proposed octanuclear cluster could be considered as resulting from the substitution of two of the trialkylphosphine ligands by two chlorine atoms, one might predict a blue shift of the absorptions when comparing the spectrum of the tetrameric compound to the spectrum of the proposed octameric compound. This blue shift does occur as can be seen in Figure II-2. The $Mo_8Cl_{16}[PEt_3]_4$ spectrum has an absorption at 520 nm which is not obvious in the $Mo_4Cl_8[PEt_3]_4$ spectrum. This band may have been accentuated by the blue shift of the tetranuclear absorption at 420 nm. The band at 305 nm in the spectrum of the tetranuclear cluster may be blue shifted when phosphine ligands are replaced by chlorine ligands causing it to coincide with the absorption at 270 nm. This would produce one broad band as is observed in the spectrum of $Mo_8Cl_{16}[PEt_3]_4$.

When the XPS spectrum of $Mo_4Cl_8[PBu_3]_4$ was obtained, the data indicated that the sample may be decomposing in the spectrometer (13). This experiment was performed with monochromatic radiation, which dictates extensive exposure time of the sample to radiation and high vaccum in the spectrometer. The XPS spectrum of $Mo_8Cl_{16}[PEt_3]_4$ was obtained using non-monochromatic radiation which allows the minimum data collection time. The data were collected and retained in three portions: scans 1-20, 21-50, and 51-70. The first and last sets of data were resolved using the APES computer program (11) and are shown in Figure II-3. The first

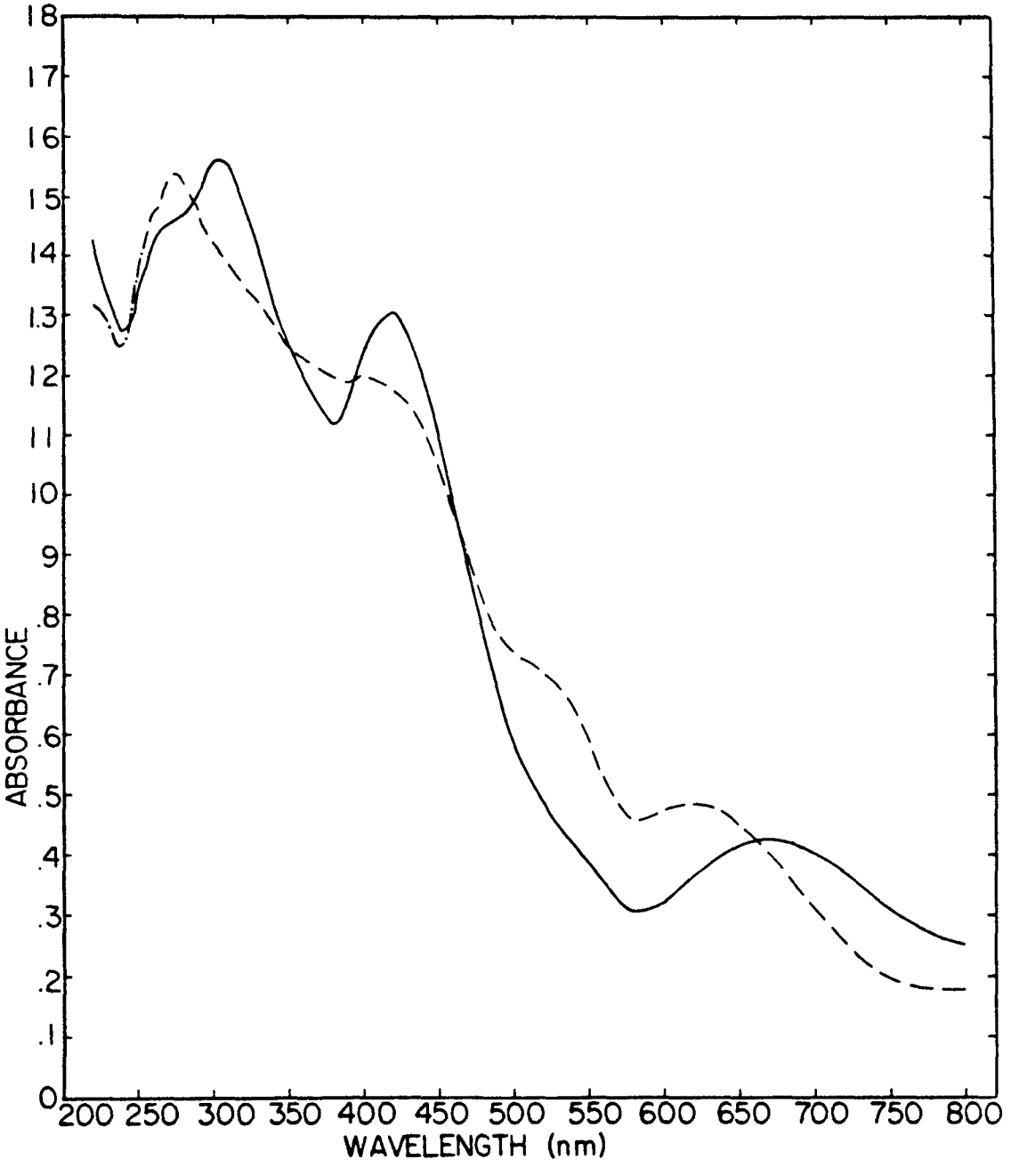

Figure II-2. Reflectance spectra of $Mo_4Cl_8[PEt_3]_4$ (——) and $Mo_8Cl_{16}[PEt_3]_4$ (-•-)

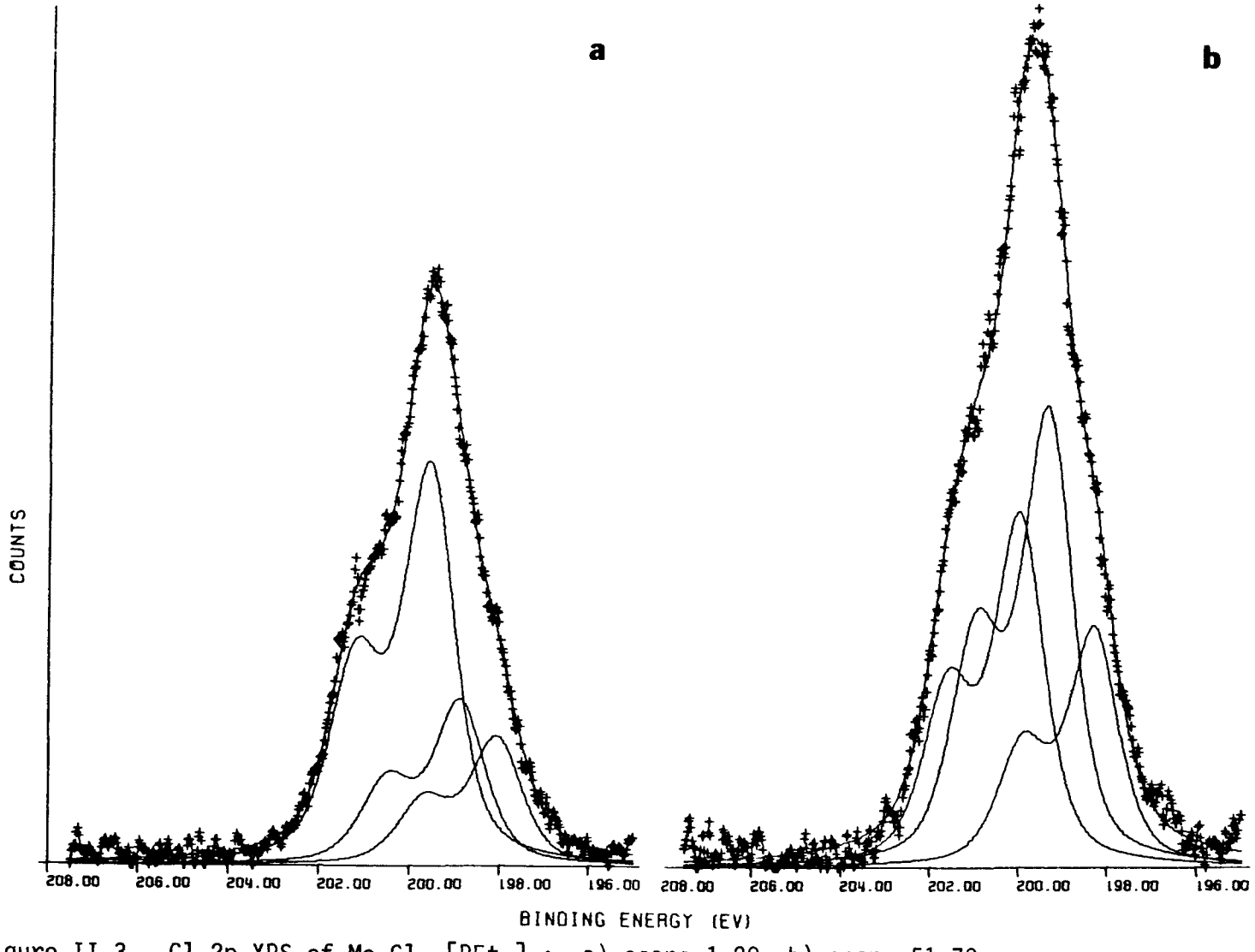

Figure II-3. Cl 2p XPS of $Mo_8Cl_{16}[PEt_3]_4$: a) scans 1-20; b) scans 51-70

resolutions were done with two types of chlorine atoms specified. Chlorine $2p_{3/2}$ binding energies of 199.5 eV and 198.4 eV were found for both sets of data, but the peak area ratios were 2.06/1.0 for the first 20 scans and 2.52/1.0 for scans 51-70. Because the band widths were too large, over 1.5 eV full-width at half-maximum (FWHM), three types of chlorine atoms were specified in the next resolutions. The Cl $2p_{3/2}$ binding energies determined from the data set consisting of the first 20 scans were 199.6, 198.9, and 198.1 eV; areas were in the ratio 2.72/1.51/1.0. Resolution of data for the last set of 20 scans was provided by chlorine $2p_{3/2}$ binding energies of 200.0, 199.3, and 198.3 eV. In this case, the area ratios were 1.32/1.99/1.0. In both sets of data, the FWHM was 1.3 eV for all three types of chlorine atoms. These spectra clearly indicate that decomposition is occurring under XPS conditions.

The highest chlorine binding energy found for $Mo_8Cl_{16}[PEt_3]_4$ is an appropriate value for a doubly bridging chlorine. In $Mo_5Cl_{13}^{2-}$, this type of chlorine has a binding energy of 199.8 eV (14); in $Mo_4Cl_8[PBu_3]_4$ it is 199.6 eV (13). The lowest binding energy in the proposed octameric cluster is typical for terminal chlorine (13,14). The binding energy of about 199 eV has been tentatively assigned to a "weakly doubly-bridging" chlorine. This is envisioned as a chlorine bridging two metal atoms that are not bound to each other. The peak area ratios are not very informative because the peak height is very sensitive to small changes in peak shape. This introduces a large error into the ratio of the peak areas. Therefore, one must be extremely careful in interpreting

information from the area ratios in cases where the spectrum has a broad, featureless shape.

Reactions of $Mo_8Cl_{16}[PEt_3]_4$ also indicate a weak linkage between tetrameric units. The octameric compound dissolved in hot chlorobenzene with excess PEt_3 yielded a yellow-brown solution. Further heating gave a blue solution which had absorptions at 588 and 330 nm, similar to the absorptions of $Mo_2Cl_4[PEt_3]_4$ (15). The addition of triethylphosphine to the presumed octameric cluster was later repeated at room temperature. A mixture containing a 4:1 mol ratio of PEt_3:$Mo_8Cl_{16}[PEt_3]_4$ in chlorobenzene was stirred for about 20 hours. After the solvent was stripped from the filtrate, the resulting residue was extracted with cyclohexane to remove any blue $Mo_2Cl_4[PEt_3]_4$. The yellow, cyclohexane insoluble product, recovered in a 55% yield, was identified as $Mo_4Cl_8[PEt_3]_4$ based upon its uv-visible spectrum and x-ray powder pattern.

The $Mo_2Cl_4[PEt_3]_4$ that was found in the reaction between the assumed octameric cluster and phosphine was presumed to arise from the tetrameric cluster reacting with excess triethylphosphine. In another experiment,

$$Mo_8Cl_{16}[PEt_3]_4 + 4\ PEt_3 \longrightarrow 2\ Mo_4Cl_8[PEt_3]_4$$

$$Mo_4Cl_8[PEt_3]_4 + 4\ PEt_3 \longrightarrow 2\ Mo_2Cl_4[PEt_3]_4$$

a solution of triethylphosphine in chlorobenzene was gradually added to the proposed octameric cluster compound in refluxing chlorobenzene. When a stoichiometric amount of triethylphosphine was added, most of the octameric cluster compound reacted. The uv-visible spectrum and x-ray powder pattern indicated the product was $Mo_4Cl_8[PEt_3]_4$. The yield was about 60%. $Mo_2Cl_4[PEt_3]_4$ was not detected in the uv-visible spectrum.

Needle-shaped crystals were produced in the reactions used for the synthesis of the triethylphosphine octameric compound, but they were too small for an x-ray structure determination. We speculated that a solvent with a higher boiling point might permit growth of larger crystals. When $Mo_8Cl_{16}[PEt_3]_4$ was refluxed in dichlorobenzene, the solution turned slightly brown, and after refluxing overnight, the solid appeared to be a darker brown. The infrared spectrum of the solid recovered from this treatment indicated that triethylphosphine was present, but the absorptions due to the triethylphosphine had lower intensity than in the spectrum of the starting material. The region of the infrared spectrum between 200-400 cm^{-1} now resembled that of β-$MoCl_2$. This region of the infrared spectrum of β-$MoCl_2$ (16) is shown in Figure II-4. A comparison of Figures II-1 and II-4 clarifies the changes that occur in the infrared spectrum and illustrates the usefulness of infrared spectroscopy in identifying which of the possible products is present. The x-ray powder pattern of the brown material had also changed to the broad, diffuse pattern characteristic of β-$MoCl_2$.

Confirmation of the octameric nature of $Mo_8Cl_{16}[PEt_3]_4$ could be obtained by a single crystal structure if a large crystal were available. Octameric cluster compounds were synthesized with other phosphine ligands in the search for a compound of which suitable crystals could be grown. Several reactions were executed using $Mo[CO]_6$ to remove phosphine from the tri-n-butylphosphine tetrameric compound. In the following reactions, $Mo[CO]_6$ and $Mo_4Cl_8[PBu_3]_4$ were added in a 1:1 mol ratio to chlorobenzene. In the first reaction attempt, the reaction

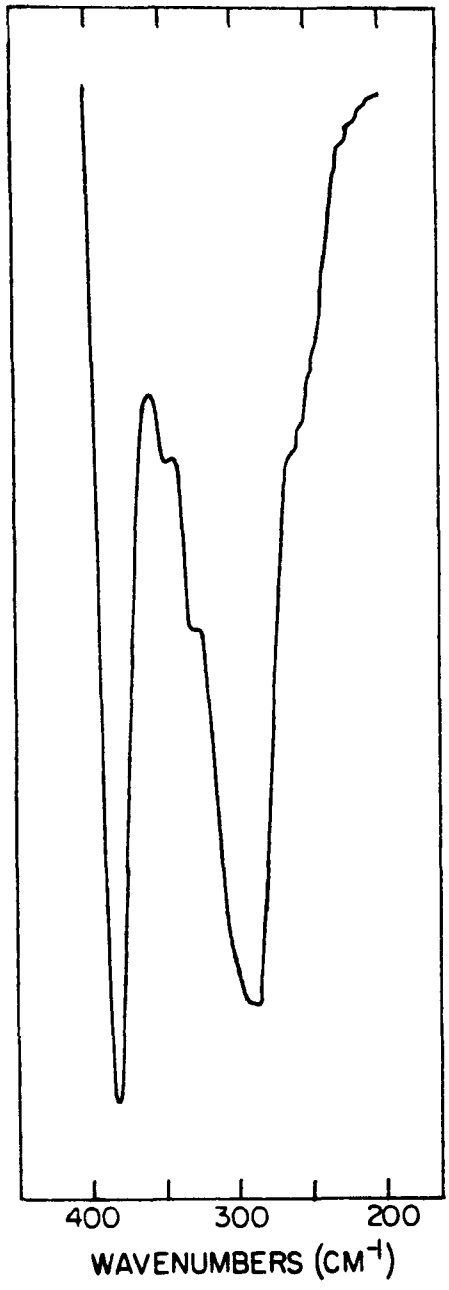

Figure II-4. Infrared spectrum of β-$MoCl_2$

mixture was held at reflux for 2 hours. A dark-brown precipitate was filtered from the solution. The infrared spectrum of this product contained the broad absorption at about 290 cm^{-1} typical of β-$MoCl_2$, but weak bands arising from bound phosphine were present. When the volume of the filtrate was doubled by adding hexane, a yellow-brown precipitate formed. The infrared spectrum contained bands originating from Mo-Cl stretching vibrations at 270, 330, and 375 cm^{-1}, very close to the frequencies found in $Mo_8Cl_{16}[PEt_3]_4$. A chlorobenzene solution of the yellow-brown material contained an absorption at 422 nm. This material is apparently not $Mo_4Cl_8[P(n\text{-}Bu)_3]_4$ because the latter has an absorption at 435 nm. The tetrameric cluster also absorbs at 310 nm. The corresponding absorption in the new compound must be below 300 nm, because it was obscured by the solvent absorption. Based upon the infrared and visible spectra, the yellow-brown material seemed to be $Mo_8Cl_{16}[P(n\text{-}Bu)_3]_4$. Warm cyclohexane dissolved the apparent octameric product, and a visible spectrum was obtained. The lowest energy absorption that was observed was at 420 nm. The other major absorption was a broad band at 285 nm, which could be resolved into absorptions at 282 and 288 nm. The spectrum of the cyclohexane solution also indicated a shoulder at about 360 nm.

When the above reaction was repeated, a precipitate was observed after refluxing for 30 minutes, but the reaction was continued for 2 hours. A large quantity of insoluble, dark-brown precipitate was recovered. Again, the infrared spectrum indicated the presence of some phosphine, but bands in the Mo-Cl region resembled those of β-$MoCl_2$. The addition of hexane to the filtrate produced some crystals. When these

were redissolved in hexane, the visible spectrum was equivalent to the $Mo_4Cl_8[P(n\text{-}Bu)_3]_4$ spectrum.

The final reaction was done at a temperature below the boiling point of chlorobenzene. The temperature was increased gradually until all of the reactants had dissolved. After 15 minutes at that temperature, a small sample was withdrawn for a visible spectrum. Although the band at 430 nm had started to shift toward 420 nm, the absorption at 310 nm moved very little. After an additional 10 minutes, another sample was taken. This time the band at 310 nm had definitely broadened towards 300 nm. When the solution started to turn cloudy, about 15 minutes later, the reaction was stopped. The precipitate was filtered and the solvent vacuum distilled from the filtrate. The resultant tar was stirred with hexane. This treatment precipitated some material from the solution. Frequently, crystals can be obtained by extracting a powder with an appropriate solvent. This method was attempted using cyclohexane, but the solubility of the apparent octameric cluster was not sufficient to produce crystals. The octameric nature of the material was confirmed by the infrared spectrum which contained the three typical absorptions in the region between 200-400 cm^{-1}. A 38% yield was obtained.

The latter two reactions demonstrate that a material similar to β-$MoCl_2$ is formed in the synthesis of $Mo_8Cl_{16}[P(n\text{-}Bu)_3]_4$. If the reaction time is short, the proposed octanuclear cluster is formed. However, if the reaction time is too long, the tetrameric cluster is formed. These reactions suggest that although the proposed octameric cluster is formed, it is unstable with respect to disproportionation in refluxing

chlorobenzene. The stable compounds are the tetrameric cluster and material similar to β-$MoCl_2$, which is probably more highly linked than the octameric cluster. Two octameric clusters are perhaps linked (Eqn. 1) or possibly primarily β-$MoCl_2$ is formed (Eqn. 2). The instability of $Mo_8Cl_{16}[P(n\text{-}Bu)_3]_4$ decreases the chances of the growth of a single crystal suitable for an x-ray structure determination.

$$3\ Mo_8Cl_{16}[PR_3]_4 \longrightarrow 2\ Mo_4Cl_8[PE_3]_4 + Mo_{16}Cl_{32}[PR_3]_4 \qquad (1)$$

$$n\ Mo_8Cl_{16}[PR_3]_4 \longrightarrow n\ Mo_4Cl_8[PR_3]_4 + [Mo_4Cl_8]_n \qquad (2)$$

The apparent instability of $Mo_8Cl_{16}[P(n\text{-}Bu)_3]_4$ led to the synthesis of other octameric cluster compounds. The solubility of the proposed octanuclear cluster compounds can be varied by changing the length of the alkyl chain on the phosphine ligand. The tripropylphosphine derivative of the octameric cluster should have solubility properties between those of $Mo_8Cl_{16}[PEt_3]_4$ and $Mo_8Cl_{16}[P(n\text{-}Bu)_3]_4$. The reaction between $Mo[CO]_6$ and $Mo_4Cl_8[PPr_3]_4$ led to $Mo_8Cl_{16}[PPr_3]_4$ which was identified by the typical absorptions in the Mo-Cl stretching region of the infrared spectrum and visible absorptions at 420 and 300 nm of a dichloromethane solution. The chemical analysis of $Mo_8Cl_{16}[PPr_3]_4$ found significantly lower concentrations of molybdenum and chlorine than was calculated from the formula. However, a closer examination of the infrared spectrum indicated chlorobenzene was present, which would also account for the carbon analysis that is higher than calculated. The growth of single crystals was attempted by extracting the octamer with CH_2Cl_2, but only powder was obtained. If the formation of octamer proceeded more slowly, crystal

growth might be promoted. $Mo_4Cl_8[PPr_3]_4$ and $Mo[CO]_6$ were sealed in a tube with chlorobenzene and placed in a 70°C oil bath. Although larger crystals were formed, none were big enough for a structure determination. Very fibrous crystals were formed in dichloromethane by placing the material in a sealed tube. A temperature gradient along the tube was accomplished by placing the tube in a sand bath which was heated on the bottom. Again, a crystal of sufficient size was not obtained.

The dimethylphenylphosphine octameric cluster was also synthesized and found to have significantly better solubility in chlorobenzene or CH_2Cl_2 than $Mo_8Cl_{16}[PPr_3]_4$, yet it still precipitates from solution during the synthesis. The analyses are again significantly different from calculated values although the Cl/Mo and P/Mo ratios are correct. This is probably due to the inclusion of chlorobenzene in the crystals as was found for $Mo_8Cl_{16}[PPr_3]_4$. The analyses indicate that about 7% chlorobenzene is present. This would imply a PhCl:Mo_8 ratio of about 1.2:1.0. Apparently, the product that precipitates is not as pure as the product formed when other phosphine ligands are used. The infrared spectrum of the precipitated product did not have the distinctive absorptions in the Mo-Cl stretching region. After extracting the product with CH_2Cl_2, the infrared spectrum contained the expected absorptions. Although the solubility of the $PhMe_2P$ octamer in CH_2Cl_2 was greater than the other octameric cluster compounds, the solubility was still low enough that an extraction was possible without transporting a large amount of the desired compound through the frit. Guinier x-ray powder patterns of $Mo_4Cl_8[PMe_2Ph]_4$, $Mo_8Cl_{16}[PMe_2Ph]_4$ before CH_2Cl_2 extraction, and

$Mo_8Cl_{16}[PMe_2Ph]_4$ after the extraction were all different. The powder patterns indicated that the extraction removed a material less crystalline than the octameric cluster compound. The sealed tube-sand bath technique was used to grow crystals. Several crystals were ground up and a powder pattern was obtained to ensure that they were not crystals of the tetrameric compound.

A single crystal was found which, after considerable effort, was indexed (17) as monoclinic with the dimensions of a = 22.42 Å, b = 8.49 Å, c = 46.97 Å, and β = 102.7°. Even though about 9500 reflections were collected in two hemispheres, only 820 were observed. A reflection was considered to be observed if the intensity was greater than twice the standard deviation of the intensity (18). The Patterson map was very complicated due to many Mo-Mo vectors. A superposition was done using a vector corresponding to the Mo-Mo diagonal of the rectangular tetrameric cluster. This is a unique vector in the tetramer, but in a linear octamer, it would give three superimposed images. The superposition indicated only tetrameric clusters were present. The computer programs in MULTAN (19) also indicated tetrameric clusters. The positions did not refine well, probably due in part to the poor data set, and in part due to the high pseudosymmetry of the Mo atoms. The high symmetry of the Mo atoms originated from their lying on approximately y = 0 and y = 1/2 planes. Refinement was then attempted in two dimensions. The h00, h01, and 001 data were isolated and refined only in the x-z plane. The computer programs did not work properly when refinement was begun; however, the structure factors were calculated and an electron density map

was produced. This projected the cell contents into the x-z plane. The calculations were executed in the triclinic space group P1 to avoid generating any extra atoms. When positions for 4 Mo atoms were inserted in the program as one tetrameric unit, the electron density map showed density for 7 other tetrameric clusters in the unit cell. These additional tetrameric clusters had not been generated by symmetry. Presumably if the molecules were larger than tetrameric clusters, this procedure would have identified them. At this point, the structure was abandoned since it was not deemed of sufficient interest, particularly with the poor data set.

The solubility of $Mo_8Cl_{16}[PMe_2Ph]_4$ in CH_2Cl_2 was low, but the solution visible spectrum could be measured. Absorptions were found at 304, 420, 550, and 620 nm. Based on earlier reflectance data of $Mo_8Cl_{16}[PEt_3]_4$ and solution spectra of $Mo_8Cl_{16}[PPr_3]_4$ and $Mo_8Cl_{16}[P(n\text{-}Bu)_3]_4$, these absorptions are at the expected wavelengths (Table II-1).

Vapor phase osmometry was used to attempt the determination of the molecular weight of $Mo_8Cl_{16}[PMe_2Ph]_4$. Unfortunately, even saturated solutions were not concentrated enough to obtain reliable data. Samples were also submitted to the NSF Mass Spectrometry Center at Johns Hopkins University for analysis by the Fast Atom Bombardment method. Because of the low solubility of the octameric cluster, this method was not successful either.

Table II-1. Electronic absorption spectra of $Mo_4Cl_8L_4$ and $Mo_8Cl_{16}L_4$

$Mo_4Cl_8(PEt_3)_4$[a]		$Mo_4Cl_8(PEt_3)_4$	$Mo_8Cl_{16}(PEt_3)_4$
5.6×10^{-5} M THF		reflectance	reflectance
λ (nm)	ε ($M^{-1}cm^{-1}$)	λ (nm)	λ (nm)
245	2×10^4	270	275
308	1.7×10^4	305	400
430	2.2×10^3	420	520
		675	620

$Mo_4Cl_8[P(n\text{-}Bu)_3]_4$[a]		$Mo_8Cl_{16}[P(n\text{-}Bu)_3]_4$	$Mo_8Cl_{16}(PPr_3)_4$
6.3×10^{-5} M hexane		cyclohexane	CH_2Cl_2
λ(nm)	ε (M^{-1} cm^{-1})	λ (nm)	λ (nm)
248	2×10^4	282	300
312	2.8×10^4	288	350
435	3.5×10^3	360	420
685	100	420	

$Mo_4Cl_8(PMe_2\phi)_4$		$Mo_8Cl_{16}(PMe_2\phi)_4$	
4.9×10^{-4} M CH_2Cl_2		~ 5×10^{-5} M CH_2Cl_2	
λ (nm)	ε (M^{-1} cm^{-1})	λ (nm)	ε (M^{-1} cm^{-1})
310	2.2×10^4	304	3×10^4
430	2.4×10^3	420	5×10^3
680	50	550	7×10^2
		620	4×10^2

[a]Reference 11.

The structure of the octamers is in doubt since a crystal structure has not been done. However, based on the chemical and XPS evidence, the structures shown in Figure II-5 are proposed. Either structure contains tetrameric units which should be easy to abstract. Three types of chlorine atoms are also present as suggested by the XPS data. The molybdenum atoms could be arranged in either of two modes illustrated. The metal-metal distance between tetrameric units can be calculated if the positions of the bridging chlorines are assumed. If the intercluster chlorine atoms are separated from one another by 3.4 Å, the sum of the van der Waals radii (20), and the Mo-Cl distance is 2.41 Å, the molybdenum-bridging chlorine distance in $Mo_4Cl_8[PEt_3]_4$ (7), the molybdenum-molybdenum distance between linearly linked tetrameric units, Figure II-5a, is 3.21 Å. The pseudotetrahedron arrangement of molybdenum atoms found in the linkage between the tetrameric units in (b) is known to exist in $Mo_4F_4[O(i\text{-}Bu)]_8$ (21). This would allow the nonbonded metal atoms to be about 0.4 Å farther apart than in (a). Further work to determine the structure of the octanuclear compounds is being undertaken.

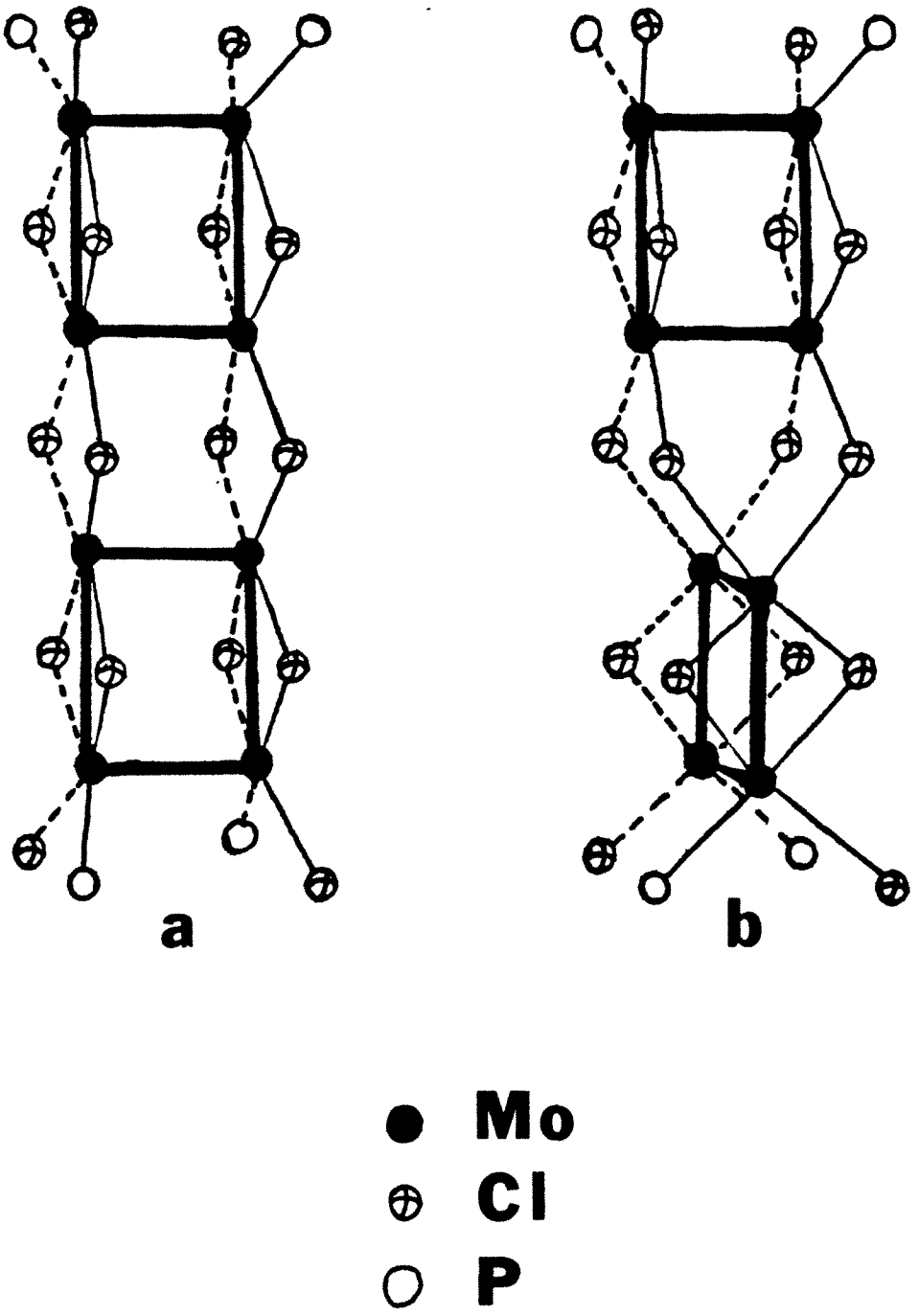

Figure II-5. Proposed structure for $Mo_8Cl_{16}[PEt_3]_4$

REFERENCES AND NOTES

1. Mutterties, E. L.; Rhodin, T. N.; Band, E.; Brucker, C. F.; Pretzer, W. R. Chem. Rev. 1979, 79, 91.

2. Longoni, G.; Chini, P. J. Amer. Chem. Soc. 1976, 98, 7225.

3. Schmid, G.; Pfeil, R.; Boese, R.; Bandermann, F.; Meyer, S.; Calis, G.H.M.; van der Velder, J.W.A. Chem. Ber. 1981, 114, 3634.

4. Chisholm, M. H.; Errington, R. J.; Folting, K.; Huffmann, J. C. J. Am. Chem. Soc. 1982, 104, 2025.

5. Farrugia, L. J.; Howard, J.A.K.; Mitrprachachon, P.; Stone, F.G.A.; Woodward, P. J. Chem. Soc., Dalton Trans. 1981, 155, 162.

6. McGinnis, R. N.; Ryan, T.R.; McCarley, R. E. J. Am. Chem. Soc. 1978, 100, 7900.

7. Beers, W. W. Ph.D. Dissertation, Iowa State University, Ames, Iowa, 1983; Section I.

8. McCarley, R. E.; Templeton, J. L.; Colburn, T. J.; Katovic, V.; Hoxmeier, R. J. Adv. Chem. Ser. 1976, 150, 319.

9. Colton, R.; Tomkins, J. B. Aust. J. Chem. 1966, 19, 1143.

10. Elwell, W. T.; Wood, D. F. "Analytical Chemistry of Molybdenum and Tungsten"; Pergamon Press: New York, 1971, pg. 41, 42.

11. Luly, M. H. (1979). "APES, A Fortran Program to Analyze Photoelectron Spectra", U.S.D.O.E. Report IS-4694.

12. Michel, J. B.; McCarley, R. E. Inorg. Chem. 1982, 21, 1864.

13. Ryan, T. R.; McCarley, R. E. Inorg. Chem. 1982, 21, 2072.

14. Beers, W. W. Ph.D. Dissertation, Iowa State University, Ames, Iowa, 1983; Section IV.

15. San Fillipo, Jr., J.; Sniadoch, H. J.; Grayson, R. L. Inorg. Chem. 1974, 13, 2121.

16. β-$MoCl_2$ used for this spectra was prepared as described in Glicksman, H. D.; Hamer, A. D.; Smith, T. J.; Walton, R. A. Inorg. Chem. 1976, 15, 2205.

17. Jacobson, R. A. J. Applied Crystallogr. 1976, 9, 115.

18. Calculations were carried out on a VAX 11/780 computer. Structure factor calculations and least squares refinements were done using the block matrix/full matrix program ALLS (R.L. Lapp and R. A. Jacobson), Fourier series calculations were done using the program FOUR (D. R. Powell and R. A. Jacobson), and superposition calculations were done using the program SUPERPOSITION (C. R. Hubbard, M. W. Babich, and R. A. Jacobson).

19. Main, P. "MULTAN 80, A System of Computer Programs for the Automatic Solution of Crystal Structures for X-ray Diffraction Data", University of York Printing Unit, York, United Kingdom, 1980.

20. Bondi, A. J. Phys. Chem. 1964, 68, 441.

21. Chisholm, M. H.; Huffman, J. C.; Kelley, R. L. J. Am. Chem. Soc. 1979, 101, 7100.

SECTION III. INSIGHT ON THE β-$MoCl_2$ STRUCTURE

INTRODUCTION

Although β-$MoCl_2$ was first synthesized nearly 20 years ago (1), its structure is still in doubt. There has been unanimous agreement that the compound is quite different from Mo_6Cl_{12} (α-$MoCl_2$) and is probably polymeric (1-4). The amorphous nature of β-$MoCl_2$ has made it difficult to determine the correct structure. The x-ray powder pattern, consisting of broad, diffuse lines, was said to resemble that of $CdCl_2$ (2), and therefore Allison, Anderson and Sheldon felt that β-$MoCl_2$ may have a similar close-packed layer structure. The measured magnetic moment of 0.49 BM suggested the presence of metal-metal bonding. The low chlorine/-molybdenum ratio implied that the majority of chlorine atoms were bridging between at least two molybdenum atoms. Later x-ray photoelectron spectroscopic work (4) also indicated the bridging nature of the chlorine atoms. The peaks in the Cl 2p XPS spectra of β-$MoCl_2$ and $CdCl_2$ were reported to have "very similar profiles", and again the structure of β-$MoCl_2$ was suggested to be similar to that of $CdCl_2$.

β-$MoCl_2$ is very insoluble in all common solvents and does not react as readily as Mo_6Cl_{12} (2). However, Glicksman et al. found that when β-$MoCl_2$ was refluxed in pyridine for 3 days, a 26% yield of the $Mo_2Cl_4Py_4$ was produced (5). The reaction between β-$MoCl_2$ and a ten-fold excess of trialkylphosphine in refluxing ethanol produced $Mo_2Cl_4[PR_3]_4$ in low yield, even though the reaction time was longer than 3 days. These products led to the conclusion that β-$MoCl_2$ should be thought of as $[Mo_2Cl_4]_n$, reflecting the presence of Mo_2 units with Mo-Mo bonds of multiple bond order.

Our interest in this problem was recently rekindled when similarities between $Mo_4Cl_8L_4$ tetranuclear clusters and β-$MoCl_2$ appeared. For example, Ryan observed that β-$MoCl_2$ was produced when $Mo_4Cl_8[C_4H_8O]_4$ lost THF upon vacuum drying at room temperature. The loss of methanol from $Mo_4Cl_8[MeOH]_4$ under similar conditions also led to β-$MoCl_2$ (6). In other work, it was found that tetranuclear clusters apparently may also be linked to produce octanuclear clusters, $Mo_8Cl_{16}[PR_3]_4$ (7). With certain trialkylphosphine ligands, linkage does not stop at the octanuclear compound but proceeds to a product similar to β-$MoCl_2$. The initial results of our probe into the structure and properties of β-$MoCl_2$ are presented here.

EXPERIMENTAL

Materials

Except where noted otherwise, samples were presumed to be air-sensitive and were handled accordingly. Chlorobenzene and acetonitrile were dried by refluxing with CaH_2. Chlorobenzene was then distilled and stored under nitrogen. The acetonitrile was vacuum distilled onto molecular sieves for storage. Triethylphosphine was used as received. $AlCl_3$ was purified by sublimation as previously described (8). Dry Et_4NCl was produced by dissolving it in acetone and precipitating with ether. The product was then dried under vacuum at room temperature for about 1 day (9). The preparations of $Mo_2[OAc]_4$ (10), $K_4Mo_2Cl_8$ (11), $Mo_4Cl_8[PEt_3]_4$ (8), and $Mo_8Cl_{16}[PEt_3]_4$ (7) have been described previously.

Analysis

Molybdenum analyses were accomplished by decomposition of the sample in a tared crucible using nitric acid. The resultant MoO_3 was fired at 550°C before weighing. Decomposition of the samples for chloride analysis was done in a $KOH-H_2O_2$ aqueous solution. The chloride content was obtained by potentiometric titration of the solution with standardized $AgNO_3$. Carbon, hydrogen, and nitrogen analyses were performed by the Ames Laboratory Analytical Services.

Physical Measurements

Routine infrared spectra were obtained in a Beckman IR4250 spectrometer. An IBM IR/90 spectrometer was used to measure the Fourier-transform infrared spectra. Instrumentation for the acquisition of reflectance and x-ray photoelectron spectra has been previously described (7).

Synthesis

Literature β-$MoCl_2$

Literature β-$MoCl_2$ was prepared from $Mo_2[OAc]_4$ and HCl(g) following the modified method of Glicksman et al. (5). The infrared spectrum of the product did not contain absorptions due to the acetate ligand; therefore, the reaction was assumed to be complete.

Reactive β-$MoCl_2$

If $Mo_2[OAc]_4$, $AlCl_3$, and PR_3 are refluxed in tetrahydrofuran, the crystalline $Mo_4Cl_8[PR_3]_4$ compounds are produced. However, if $Mo_2[OAc]_4$ and $AlCl_3$ are refluxed in chlorobenzene, a very amorphous form of β-$MoCl_2$ is produced. A typical preparation was performed using 2.00 g (4.67 mmol) $Mo_2[OAc]_4$ and 2.60 g (19.50 mmol) $AlCl_3$ in about 20 mL of refluxing chlorobenzene. Brown precipitate formed very quickly, but the reaction was usually continued for about 6 hours. The precipitate was then filtered and extracted with chlorobenzene until the yellow filtrate had cleared. An infrared spectrum indicated that some form of acetate was

still present in the precipitate. When the precipitate was extracted with acetonitrile, a dark green filtrate was observed, but the filtrate cleared after extracting for several hours. After vacuum drying at room temperature, a yield of about 90% was realized. The infrared spectrum of this product indicated that some acetonitrile and chlorobenzene were present, but there were no absorptions that could be attributed to an acetate ligand. Anal. Calcd. for $MoCl_2$: Mo, 57.50; Cl, 42.50. Found: Mo, 52.53; Cl, 38.22; C, 5.14; H, 0.56; N, 1.21 (Cl/Mo = 2.04, N/Mo = 0.16, C/N = 4.96). If the product was heated under vacuum at 85°C for 1.5 days, the infrared spectrum indicated that the acetonitrile was eliminated but that a very small amount of chlorobenzene remained. Anal. Found: Mo, 55.44; Cl, 41.82 (Cl/Mo = 2.04). If one assumes the balance of the material to be chlorobenzene, the chlorobenzene/molybdenum ratio is about 0.04.

Melt β-$MoCl_2$

Although this method for preparing β-$MoCl_2$ was originally found by others in this laboratory (12), the obscurity of the report led to its inclusion here. A 1:4 mol ratio of $K_4Mo_2Cl_8$ and $AlCl_3$ (2.82 g $K_4Mo_2Cl_8$ and 2.38 g $AlCl_3$) were added to a melt composed of 52 mol-% $AlCl_3$, 48 mol-% NaCl (6.93 g $AlCl_3$, 2.81 g NaCl). The reactants were sealed in a Pyrex tube and heated to 350°C for 4 days. The melt was cooled, pulverized in the air, and slowly added to 1M hydrochloric acid. The mixture was stirred for about 10 min., then the acid was decanted from the solid. Another extraction of the solid was done, followed by filtration

and washing the solid product with ethanol. The product was air dried. This form of β-$MoCl_2$, which seems to be fairly air stable, was obtained in about 70% yield. Anal. Found: Mo, 59.52; Cl, 42.77 (Cl/Mo = 1.94).

RESULTS AND DISCUSSION

A product very similar to β-$MoCl_2$ was frequently found during the characterization of $Mo_8Cl_{16}[PR_3]_4$ (7). Synthesis of $Mo_8Cl_{16}[PR_3]_4$ from $Mo_2[OAc]_4$ was a two step process. First a tetrameric cluster, $Mo_4Cl_8[PR_3]_4$, was formed. Abstraction of trialkylphosphine ligands from $Mo_4Cl_8[PR_3]_4$ by $Mo[CO]_6$ in chlorobenzene led to the apparent octanuclear cluster. If the synthesis of $Mo_8Cl_{16}[PR_3]_4$ from $Mo_2[OAc]_4$ was attempted in one step by reacting stoichiometric amounts of $Mo_2[OAc]_4$, $AlCl_3$, and PR_3 in chlorobenzene, β-$MoCl_2$ was obtained. This observation led to the synthesis of β-$MoCl_2$ using $AlCl_3$ to exhaustively chlorinate $Mo_2[OAc]_4$. Throughout the discussion, the origin of the β-$MoCl_2$ will be indicated as was done in the Experimental section.

The Fourier-transform infrared spectra of literature β-$MoCl_2$, $Mo_4Cl_8[PEt_3]_4$, and $Mo_8Cl_{16}[PEt_3]_4$ are presented in Figure III-1. Table III-1 contains the frequencies of the major bands. The band at 432 cm^{-1} common to both the $Mo_4Cl_8[PEt_3]_4$ and $Mo_8Cl_{16}[PEt_3]_4$ spectra probably arises from the phosphine ligand. This assignment is based upon the diminishing intensity of the band as the concentration of the phosphine in the three compounds decreases. The absorption at 374 cm^{-1} in the spectrum of the tetranuclear compound shifts slightly in the spectrum of the octanuclear compound and again in the β-$MoCl_2$ spectrum. The infrared spectrum of $Mo_8Cl_{16}[PEt_3]_4$ in the region of 330 cm^{-1} appears to be a composite of $Mo_4Cl_8[PEt_3]_4$ and β-$MoCl_2$. Although all three spectra have an absorption at 330 cm^{-1}, the band at 345 cm^{-1} appears only in the

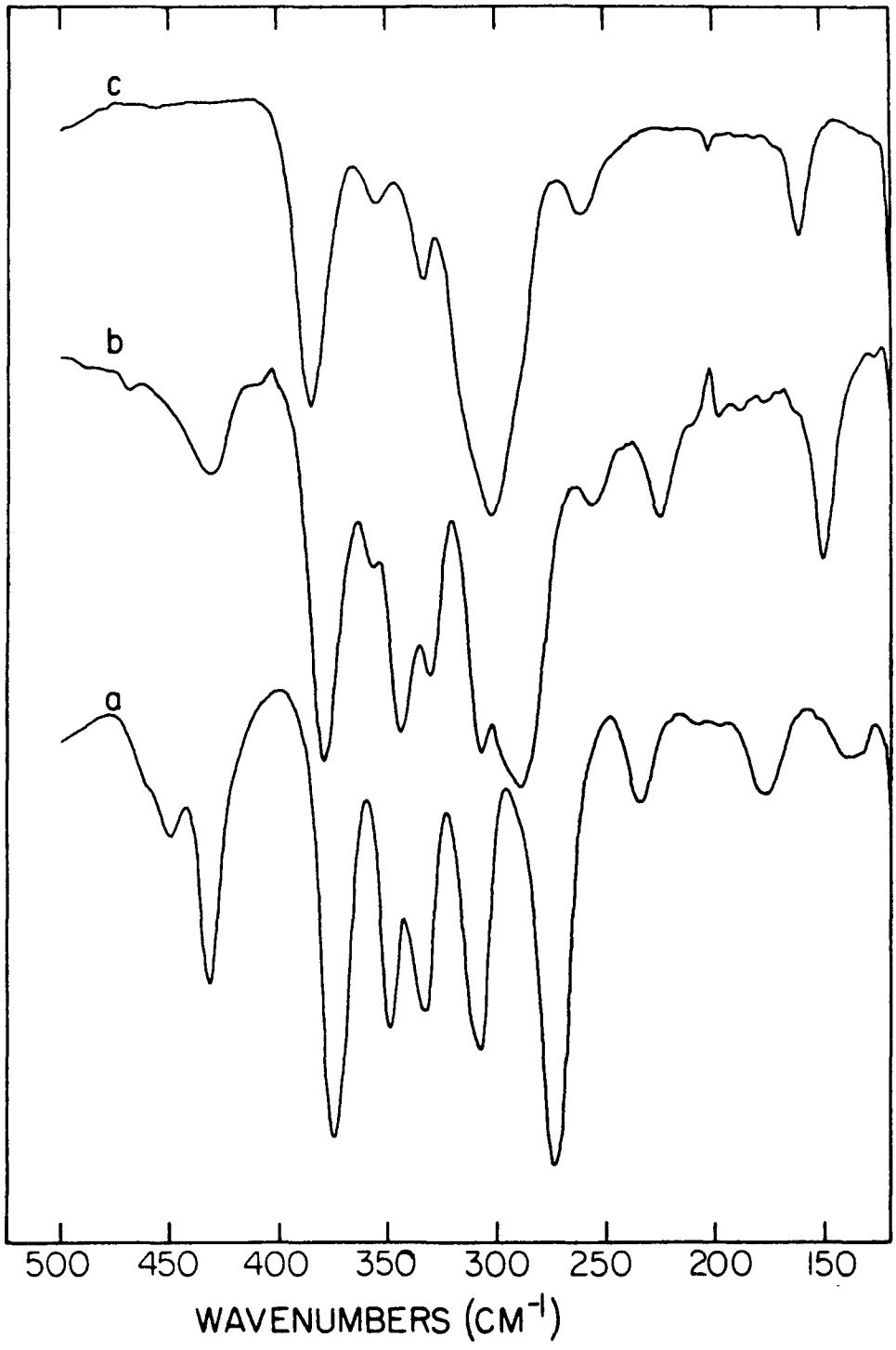

Figure III-1. Fourier-transform infrared spectra of: a) $Mo_4Cl_8[PEt_3]_4$, b) $Mo_8Cl_{16}[PEt_3]_4$, c) literature β-$MoCl_2$

Table III-1. Infrared absorption frequencies (cm^{-1}) below 450 cm^{-1} for $Mo_4Cl_8[PEt_3]_4$, $Mo_8Cl_{16}[PEt_3]_4$, and literature β-$MoCl_2$ (s = strong, m = medium, w = weak)

$Mo_4Cl_8[PEt_3]_4$	$Mo_8Cl_{16}[PEt_3]_4$	β-$MoCl_2$
449 w	432 m	385 s
432 m	380 s	354 w
374 s	357 w	331 w
348 m	345 m	301 s
331 m	330 m	260 w
306 m	308 s	161 m
273 s	289 s	
234 w	256 w	
177 w	225 w	
140 w	150 m	

spectra of the two compounds containing phosphine and the band at 357 cm^{-1} appears only in the spectra of $Mo_8Cl_{16}[PEt_3]_4$ and β-$MoCl_2$. The absorption at 289 cm^{-1} in the spectrum of the octanuclear compound is significantly broadened and shifted from the sharp absorption at 273 cm^{-1} in the spectrum of the tetranuclear compound. This trend seems to continue in

the β-$MoCl_2$ spectrum. The band at 300 cm^{-1} in the β-$MoCl_2$ spectrum is broad enough that it may overlap an absorption corresponding to the absorption that is found at about 308 cm^{-1} in the other two spectra. Few conclusions can be drawn from the infrared spectra. Since the three compounds contain various types of Mo-Cl bonds, the infrared spectra should be similar. One would expect that the Mo-Cl absorption at highest frequency would be due to a molybdenum-terminal chlorine stretch. The identity of the absorption at 385 cm^{-1} in the β-$MoCl_2$ spectrum is therefore puzzling. If β-$MoCl_2$ has a polymeric structure, the concentration of terminally bound chlorine atoms should be low. The x-ray photoelectron spectra indicate that all of the chlorine atoms are of the bridging type (vide infra). Therefore, assignment of the infrared absorptions of β-$MoCl_2$ must wait until a better understanding of the structure is obtained.

The three preparative methods led to products with significantly different stabilities to air and moisture. This feature suggested that the three products were not identical and that other methods of characterization should be pursued. The reflectance spectra of the three compounds are shown in Figure III-2. The major spectral features are the same; therefore, the reactivity differences are probably not due to major structural or compositional differences.

The reflectance spectrum of β-$MoCl_2$ lacks well-defined absorption bands; however, the shoulders observed in the spectrum are pronounced. These can be compared to the bands observed in the spectra of the tetranuclear and octanuclear clusters (Figure III-3). There are shoulders

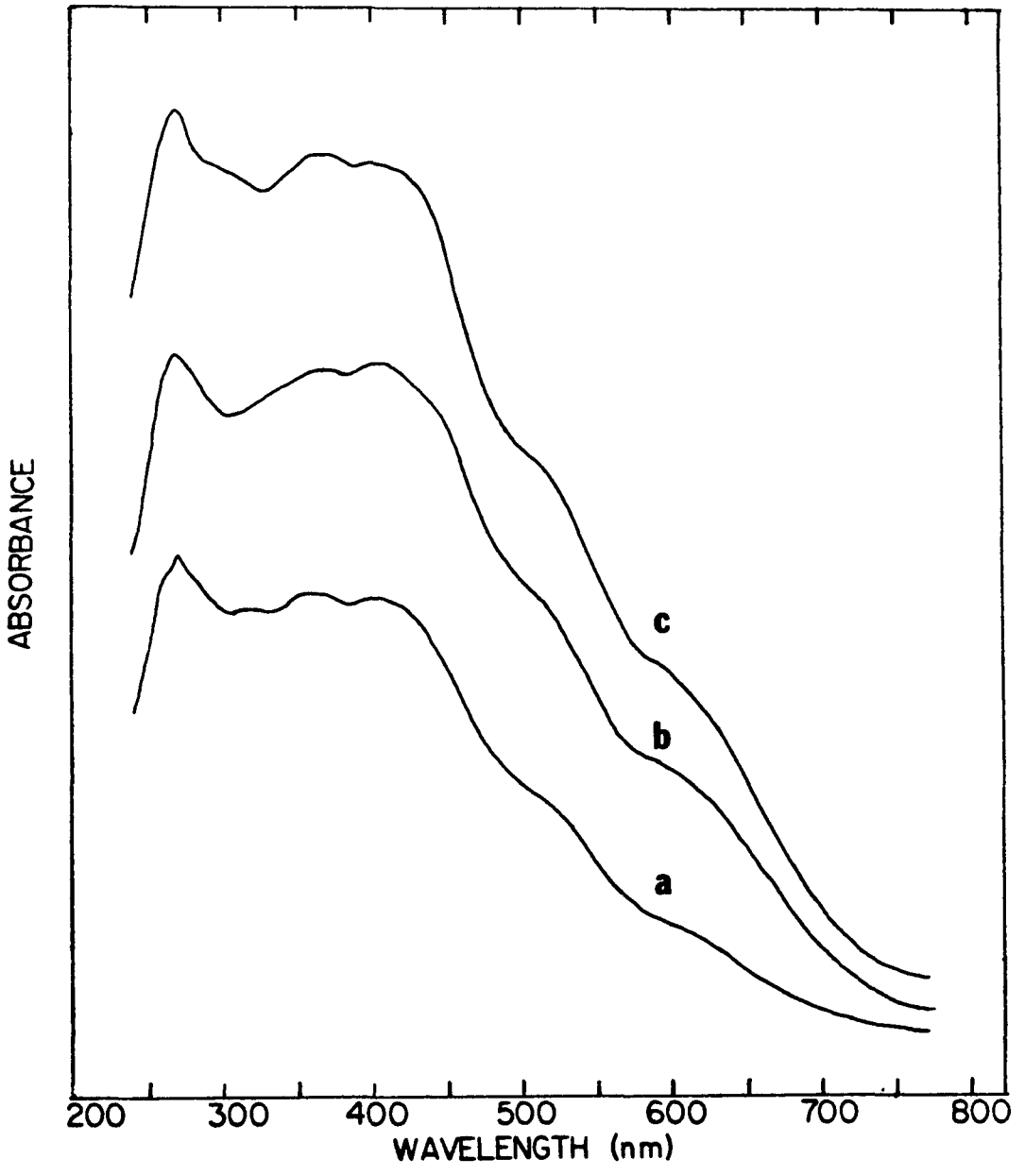

Figure III-2. Reflectance spectra of β-$MoCl_2$ prepared by different methods: a) literature, b) reactive, and c) melt

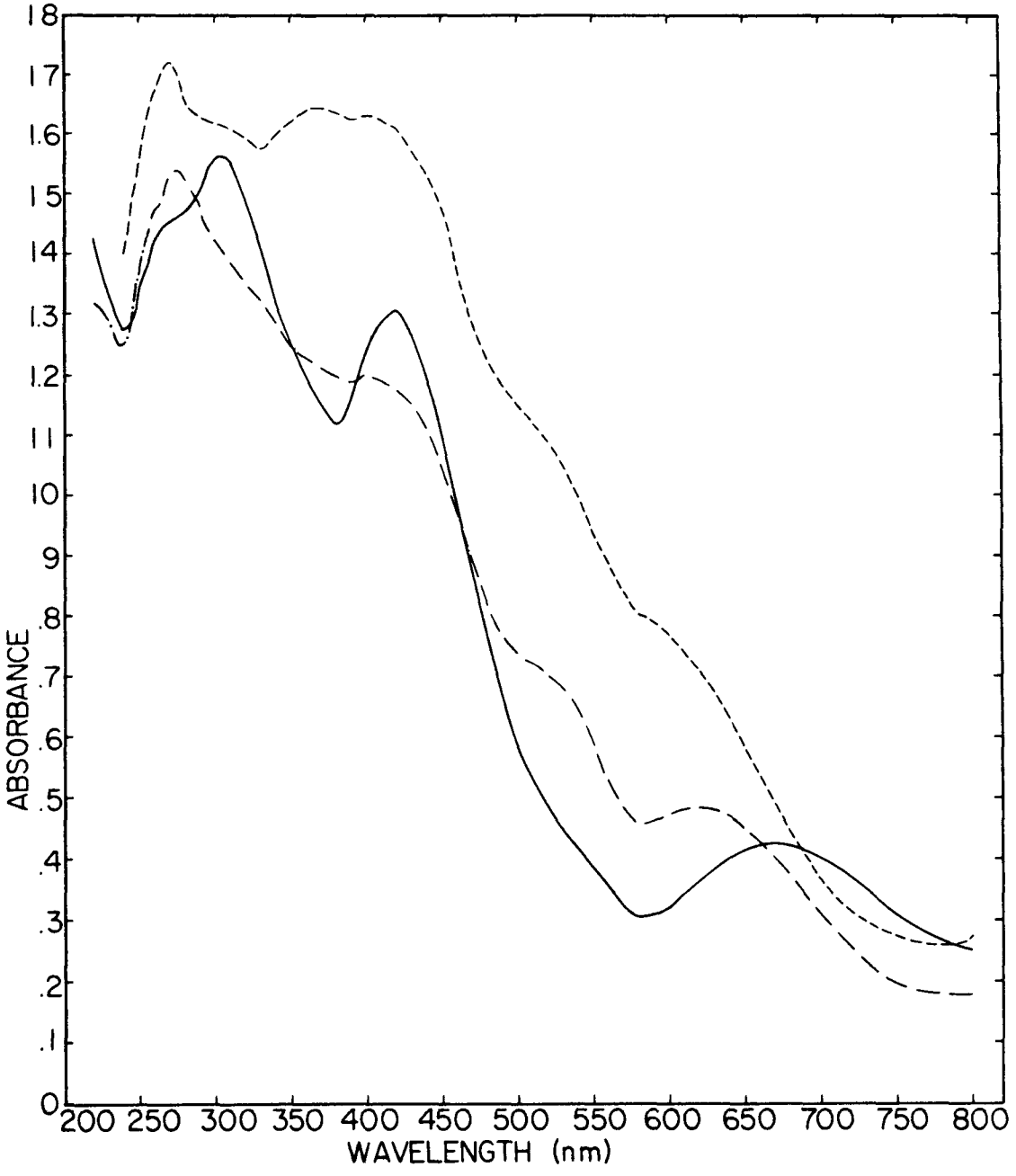

Figure III-3. Reflectance spectra of $Mo_4Cl_8[PEt_3]_4$ (——), $Mo_8Cl_{16}[PEt_3]_4$ (-•-), and β-$MoCl_2$ (---)

apparent in the spectrum of β-$MoCl_2$ at about 600, 520, and 400 nm. The frequencies of these absorptions show striking resemblance to the frequencies of the absorptions of the octanuclear cluster (Table III-2).

Table III-2. Reflectance absorptions (nm) for $Mo_4Cl_8[PEt_3]_4$, $Mo_8Cl_{16}[PEt_3]_4$, and β-$MoCl_2$

β-$MoCl_2$	600	520	400	370	270
$Mo_8Cl_{16}[PEt_3]_4$	620	520	400	275	
$Mo_4Cl_8[PEt_3]_4$	675	420	305	270	

The new absorption at 370 nm is unexplained, but the band at 270 nm compares favorably with the corresponding absorption in $Mo_8Cl_{16}[PEt_3]_4$. As the ligand field strength of L decreases in the $Mo_4Cl_8L_4$ compounds, a blue shift of bands in the visible spectra is observed (6). The earlier interpretation of the blue shift observed on comparing the spectrum of the tetranuclear cluster to that of the octanuclear cluster was based on the assumption that some of the trialkylphosphine ligands were replaced by bridging chlorine ligands which couple one cluster unit to another (7).

The additional blue shift observed between the spectrum of the octanuclear cluster and the β-$MoCl_2$ spectrum can be explained by the complete substitution of the trialkylphosphine ligands by bridging chlorine ligands. The evidence from the comparison of these spectra is by no means conclusive, but does provide further support for the possible structural similarity between $Mo_4Cl_8[PR_3]_4$, $Mo_8Cl_{16}[PR_3]_4$, and β-$MoCl_2$.

Guinier x-ray powder patterns were obtained on samples of β-$MoCl_2$ from each of the three preparative schemes. As might be expected, the crystallinity of the material is improved with increasing temperature of preparation. The powder pattern of the melt β-$MoCl_2$ has the same diffraction lines and relative intensities as literature β-$MoCl_2$, but the diffraction lines, although still broad and diffuse, are significantly sharper. On the other hand, the x-ray diffraction lines from reactive β-$MoCl_2$ are barely discernible.

The power of XPS to determine different environments for chlorine atoms is well-established (4). In light of our hypothesis that β-$MoCl_2$ contains tetrameric units, we believed that there might be more than the one type of chlorine previously suggested (4). The molybdenum $3d_{5/2}$ XPS data are listed in Table III-3. The binding energies and full-width at half-maximum height (FWHM) in this case were determined directly from a plot of the data and not by curve resolution. This method was reasonable because there was clearly only one type of molybdenum. The binding energy is comparable to that found in $Mo_4Cl_8[PR_3]_4$ and $Mo_8Cl_{16}[PR_3]_4$. The FWHM is fairly constant among the three samples and is slightly larger than that found in the octanuclear cluster. The chlorine $2p_{3/2}$ XPS data for

Table III-3. Molybdenum $3d_{5/2}$ binding energies (eV)

Compound	Binding Energy	FWHM (eV)
β-$MoCl_2$		
Literature	229.3	1.68
Reactive	229.4	1.62
Melt	229.4	1.62
$Mo_4Cl_8[P(n\text{-}Bu)_3]_4$[a]	229.0	---
$Mo_8Cl_{16}[PEt_3]_4$[b]	229.2	1.50

[a]Reference 13.

[b]Reference 14.

the products of all three preparative methods were collected. The computer program APES (15) was used to resolve the chlorine data. When parameters for only one type of chlorine were used to fit the data, the binding energies and FWHM given in Table III-4 were determined. Although these data were fit fairly well, our experience would indicate that, based on the large FWHM, additional types of chlorine atoms were probably needed.

Based on the FWHM and χ^2 values, these data are clearly fit better by parameters for at least two types of chlorine (Figure III-4 and Table III-4). For the compounds synthesized by both the reactive and melt preparations, the spectra were resolved with two major types of chlorine in a one-to-one ratio. This is what is expected for a compound that contains tetranuclear clusters linked by bridging chlorine atoms. The small fraction, about 6%, of a third type of chlorine found at the highest binding energy in the spectrum of melt β-$MoCl_2$ is not surprising. The preparation of Mo_6Cl_{12} from $K_4Mo_2Cl_8$ in an $AlCl_3$/KCl melt using longer reaction times has been reported (16). Possibly the initial steps in the conversion of β-$MoCl_2$ to Mo_6Cl_{12} are being observed in the XPS data. The FWHM for resolved bands in the spectrum of the reactive β-$MoCl_2$ sample is larger than normal; however, the generated curve provided a good match to the observed data. Therefore, the introduction of a third type of chlorine was determined to be unwarranted.

The parameters obtained from data for the most reasonable resolutions are listed in Table III-5 along with results from other compounds for comparison. The literature β-$MoCl_2$ contains chlorine atoms with binding energies similar to the intercluster doubly-bridging and intracluster doubly-bridging types of chlorine found in $Mo_8Cl_{16}[PEt_3]_4$ (7). The differences in chlorine binding energies between the samples from the three preparative methods could be due to the difficulty in resolving the data. Since the molybdenum binding energies are, within error, the same for all three samples, the data are probably referenced to carbon correctly.

Table III-4. XPS parameters derived in spectra resolution of β-$MoCl_2$[a]

One type of chlorine

Source of β-$MoCl_2$	Energy[b] (eV)	FWHM (eV)	χ^2
Literature	199.5	1.70	1.32×10^4
Reactive	199.8	1.77	1.46×10^4
Melt	199.8	1.74	2.60×10^5

Two types of chlorine

Source of β-$MoCl_2$	Energy[b] (eV)		Area Ratio	FWHM (eV)	χ^2
Literature	199.7	199.0	1.72/1.00	1.44	6.64×10^3
Reactive	200.1	199.4	1.02/1.00	1.55	1.04×10^4
Melt	200.5	199.7	1.00/5.35	1.58	1.50×10^4

Three types of chlorine

Source of β-$MoCl_2$	Energy[b] (eV)			Area Ratio	FWHM (eV)	χ^2
Reactive	200.3	199.7	198.8	2.08/5.00/1.00	1.35	8.21×10^3
Melt	201.2	200.0	199.4	1.00/7.13/7.34	1.38	9.63×10^3

[a]Spin orbit splitting was 1.60 eV.

[b]Values for $2p_{3/2}$ component.

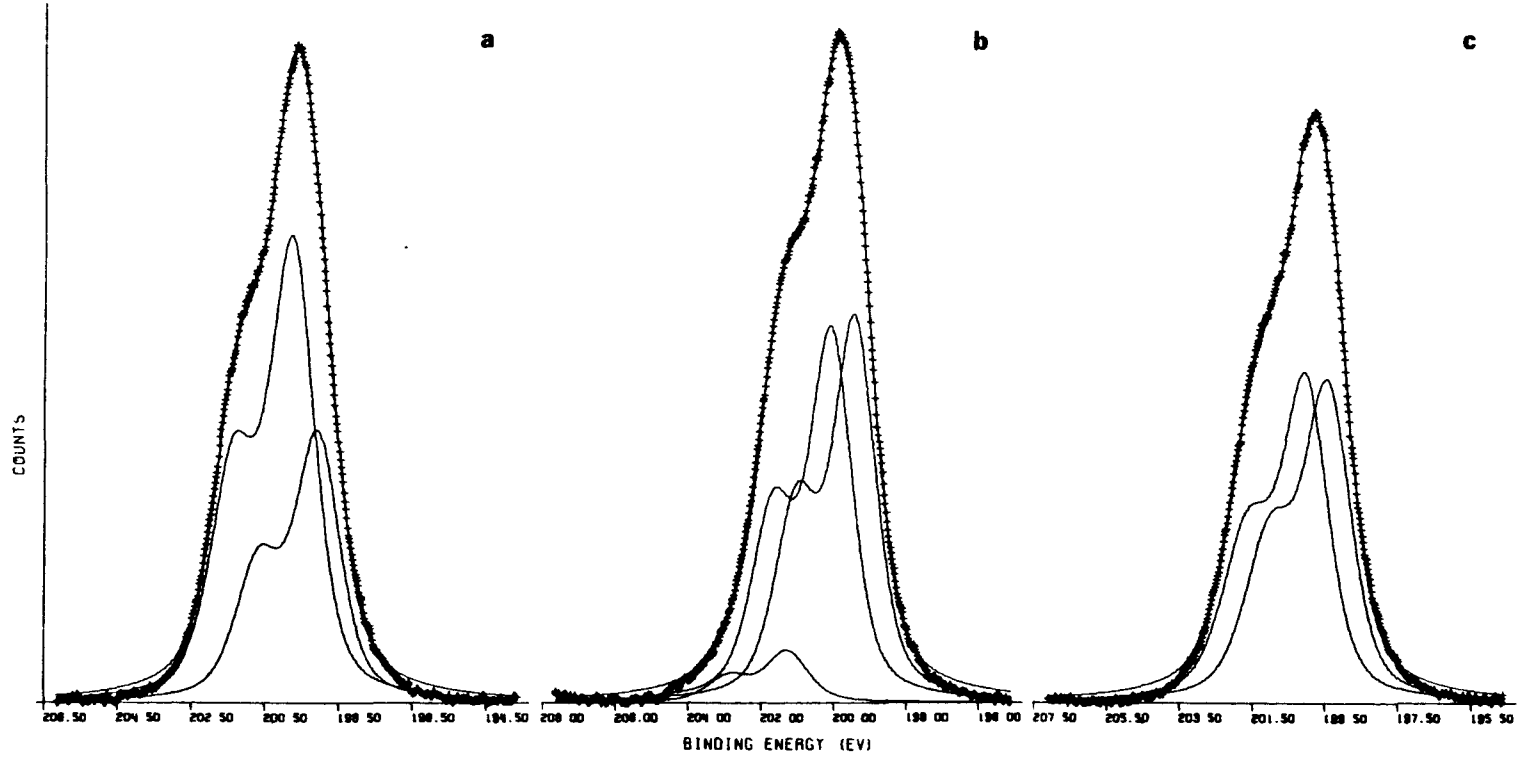

Figure III-4. Chlorine 2p XPS spectra of a) literature β-$MoCl_2$, b) melt β-$MoCl_2$, and c) reactive β-$MoCl_2$

Table III-5. Comparison of Cl $2p_{3/2}$ XPS data of β-$MoCo_2$ with other compounds[a]

	Intracluster triply-bridging	Intracluster doubly-bridging	Intercluster doubly-bridging	Terminal	FWHM (eV)	Area Ratio
Literature β-$MoCl_2$	---	199.7	199.0	---	1.44	1.72/1.00
Reactive β-$MoCl_2$	---	200.1	199.4	---	1.55	1.02/1.00
Melt β-$MoCl_2$	201.2	200.0	199.4	---	1.38	1.00/7.13/7.34
$Mo_8Cl_{16}[PEt_3]_4$[b]	---	199.6	198.9	198.1	1.30	2.72/1.51/1.00
$Mo_4Cl_8[P(n\text{-}Bu)_3]_4$[c]	---	199.6	---	198.3	1.2[d]	1.3/1.0
$(Bu_4N)_2Mo_5Cl_{13}$[e]	200.5	199.8	---	198.3	1.03[d]	1.00/1.00/1.33

[a]Reference is the C 1s binding energy (285.0 eV).

[b]From Reference 7.

[c]From Reference 6.

[d]Data was obtained using monochromatic radiation.

[e]From Reference 17.

The broad, featureless nature of the chlorine spectra admittedly makes the resolution difficult. The number of different types of chlorine atoms present was difficult to determine. The large FWHM was the major reason for fitting the data with multiple types of chlorine, but a contribution to the large FWHM may arise from the amorphous nature of these compounds. The molybdenum XPS data indicate that the FWHM is larger than for the crystalline $Mo_8Cl_{16}[PEt_3]_4$, and therefore the FWHM for the chlorine atoms should be expected to be somewhat larger than normal. These difficulties continue into the interpretation of the ratio of peak areas. Therefore, the XPS data can best be summarized by saying that there may be two major types of bridging chlorines in roughly equivalent concentrations.

The most useful information on the constitution of β-$MoCl_2$ came not from the physical measurements but from the results of several chemical reactions. The conversion of β-$MoCl_2$ to $Mo_2Cl_8L_4$ compounds (5) does not rule out the possibility of tetrameric units since $Mo_4Cl_8[PEt_3]_4$ reacts with excess trialkylphosphine to yield $Mo_2Cl_4[PR_3]_4$ (6). The direct conversion of β-$MoCl_2$ to $Mo_4Cl_8[PEt_3]_4$ would certainly substantiate the hypothesis that tetrameric units are contained in β-$MoCl_2$. The following reactions were all performed with reactive β-$MoCl_2$ which was vacuum dried at room temperature. When an equal molar quantity of PEt_3 and β-$MoCl_2$ were refluxed in chlorobenzene, a deep purple solution formed within an hour. The insolubility of β-$MoCl_2$, however, created an excess of triethylphosphine in the solution with respect to any products of the β-$MoCl_2$-triethylphosphine reaction. Therefore, if any $Mo_4Cl_8[PEt_3]_4$ was

formed, it subsequently reacted with more triethylphosphine to form the deep blue $Mo_2Cl_4[PEt_3]_4$ (Eqs. 1 and 2). It was thus concluded that if the

$$4\ \beta\text{-}MoCl_2 + 4\ PEt_3 \longrightarrow Mo_4Cl_8[PEt_3]_4 \qquad (1)$$

$$Mo_4Cl_8[PEt_3]_4 + 4\ PEt_3 \longrightarrow 2\ Mo_2Cl_4[PEt_3]_4 \qquad (2)$$

reaction conditions were less vigorous or the triethylphosphine concentration was decreased, tetranuclear clusters might be produced. Thus, when β-$MoCl_2$ was stirred at room temperature with about a 10% excess of PEt_3 in chlorobenzene for 3 days, a green filtrate was obtained. After the solvent was stripped from the filtrate, a cyclohexane extraction of the residue was used to remove the more soluble, blue $Mo_2Cl_4[PEt_3]_4$. The yellow, pure $Mo_4Cl_8[PEt_3]_4$ was recovered in a 32% yield. If one assumes that all of the observed $Mo_2Cl_4[PEt_3]_4$ resulted from the reaction of $Mo_4Cl_8[PEt_3]_4$ with excess PEt_3, the conversion of β-$MoCl_2$ to $Mo_4Cl_8[PEt_3]_4$ actually occurred in a 47% yield.

The reaction of β-$MoCl_2$ with trialkylphosphine was repeated using only a 5% excess of triethylphosphine and reacting for a shortened period of about 40 hours. Although the yield of pure tetranuclear cluster compound was decreased to about 27%, the concomitant $Mo_2Cl_4[PEt_3]_4$ formation was slashed by over one-half. In the reaction conducted with 10% excess of triethylphosphine, 31% of the total tetranuclear compound formed ended up as dinuclear compound, in the latter reaction only 13%.

Since dinuclear compound usually occurred as an unwanted side-product of the reactions performed at room temperature, the conversion of tetranuclear cluster compound to dinuclear compound at room temperature was investigated. Triethylphosphine and $Mo_4Cl_8[PEt_3]_4$, in a 4:1 mol ratio, were stirred for 45 hours in chlorobenzene. The solvent was stripped from the solution, and cyclohexane was again used to separate $Mo_2Cl_4[PEt_3]_4$ from $Mo_4Cl_8[PEt_3]_4$. About 15% of the tetrameric cluster was converted to dimer, fairly consistent with the formation of $Mo_2Cl_4[PEt_3]_4$ observed in the reactions of β-$MoCl_2$ with excess trialkylphosphine.

Convenient synthetic procedures for molybdenum tetrameric clusters of the type $Mo_4Cl_8L_4$ have been developed primarily with L = PR_3. If reactive β-$MoCl_2$ does indeed contain tetrameric units, it should be possible to abstract new tetrameric derivatives by reacting this form of β-$MoCl_2$ with the appropriate ligand. With this synthetic route, the isolation of highly reactive tetramers, that would be difficult to synthesize by other means, may be possible.

The propionitrile tetrameric cluster compound, $Mo_4Cl_8[NCC_2H_5]_4$, which is difficult to obtain, has already demonstrated synthetic usefulness (6). Synthesis of the corresponding acetonitrile tetrameric compound was attempted by refluxing reactive β-$MoCl_2$ in neat acetonitrile. A dark green solution was present after 6 hours. Because the solution color indicated that dinuclear compound was being formed, the reaction was stopped. A visible spectrum confirmed that the soluble green product was $Mo_2Cl_4[MeCN]_4$ (18). The infrared spectrum of the insoluble yellow-brown

material indicated that it was unreacted β-$MoCl_2$. Roughly one-third of the starting material had reacted in 6 hours.

None of the known $Mo_4Cl_8L_4$ clusters contain sulfur ligands. In an attempt to make this type of tetramer, a stoichiometric amount of tetrahydrothiophene (THT) was heated with β-$MoCl_2$ in chlorobenzene. After 2 hours no reaction was observed; therefore, the solution was brought to reflux. After 44 hours the reaction was stopped. The solvent had very little color, and the infrared spectrum of the residue matched that of β-$MoCl_2$. A higher concentration of THT may facilitate this reaction.

The reaction of $Mo_4Cl_8[MeOH]_4$ with excess Et_4NCl in refluxing CH_2Cl_2 produces a purple solid with the composition $[Et_4N]_4Mo_4Cl_{12}$ (19). Therefore, we speculated that if tetrameric units are in β-$MoCl_2$, it may also react with Et_4NCl. After refluxing excess Et_4NCl and β-$MoCl_2$ in CH_2Cl_2 for 2.5 days, the reaction was stopped and a purple solid was recovered. The removal of any excess Et_4Cl in the solid was then accomplished by extracting with solvent distilled from the filtrate. The Guinier x-ray powder pattern was identical to that of $[Et_4NCl]_4Mo_4Cl_{12}$. The carbon, hydrogen, and nitrogen analyses indicated a yield of approximately 75%; the rest of the solid is probably unreacted β-$MoCl_2$.

As β-$MoCl_2$ reacts with trialkylphosphine to yield $Mo_4Cl_8[PR_3]_4$, possibly methanol also would react with β-$MoCl_2$ to produce $Mo_4Cl_8[MeOH]_4$. This idea was tested by refluxing reactive β-$MoCl_2$ in 0.4 M MeOH/HCl for 40 hours. The solution turned emerald green, but very little β-$MoCl_2$ appeared to have reacted. When the methanol was removed by vacuum distillation, the product was purple. Both the purple solid and the

methanol insoluble residue had broad, featureless bands in their infrared spectra. Both spectra contained a band at 950 cm^{-1}, but the region between 200-400 cm^{-1} lacked the resolution needed to distinguish significant changes.

The reactivity of β-$MoCl_2$ is apparently promoted by maintaining a low temperature during its formation. The decrease in reactivity for material treated at high temperature is indicated by the following experiment. The sensitivity of reactive β-$MoCl_2$ to hydrogen was tested by passing hydrogen gas over β-$MoCl_2$ at 250°C for 7 hours. The infrared spectrum indicated that the chlorobenzene absorption was lost, but otherwise the spectrum was unchanged. However, when this product was refluxed for 2 days in acetonitrile, no reaction occurred. The solution contained very little material and the infrared spectrum of the unreacted material indicated little change. This behavior is similar to that observed for literature β-$MoCl_2$, which is prepared at 300°C.

The structure of β-$MoCl_2$ is still unknown; however, we presently believe that it is a polymer of $[Mo_4Cl_8]$ units. The tetrameric clusters may be connected in only two dimensions by bridging chlorines to form a layered structure. The chlorobenzene found in the reactive β-$MoCl_2$ may be trapped between adjacent sheets. This would explain the vigorous conditions needed to completely remove the solvent. When the molybdenum dichloride sheets are separated by occluded chlorobenzene, reactants are able to penetrate the structure and reach the reactive sites, which may be the Mo-Cl-Mo intercluster linkages. After the chlorobenzene is removed, the sheets may stack tightly, preventing facile penetration of the

structure by the ligands. This model would entail a layer structure, but the layers would not be close packed as in $CdCl_2$. Further structural information may be attainable using EXAFS. We are planning to participate in this study in the future.

REFERENCES AND NOTES

1. Stephenson, T. A.; Bannister, E.; Wilkinson, G. J. Chem. Soc. 1964, 2538.

2. Allison, G. B.; Anderson, I. R.; Sheldon, J. C. Aust. J. Chem. 1969, 22, 1091.

3. Holste, G.; Schafer, H. J. Less-Common Met. 1970, 20, 164.

4. Hamer, A. D.; Walton, R. A. Inorg. Chem. 1974, 13, 1446.

5. Glicksman, H. D.; Hamer, A. D.; Smith, T. J.; Walton, R. A. Inorg. Chem. 1976, 15, 2205.

6. Ryan, T. R.; McCarley, R. E. Inorg. Chem. 1982, 21, 2072.

7. Beers, W. W. Ph.D. Dissertation, Iowa State University, Ames, Iowa, 1983; Section II.

8. Beers, W. W. Ph.D. Dissertation, Iowa State University, Ames, Iowa, 1983; Section I.

9. Mann, C. K. In "Electroanalytical Chemistry"; Bard, A., Ed.; Marcel Dekker, Inc.: New York, 1969; Vol. 3, pg 57.

10. McCarley, R. E.; Templeton, J. L.; Colburn, T. J.; Katovic, V.; Hoxmeier, R. J. Adv. Chem. Ser. 1976, 150, 319.

11. Brencic, J. V.; Cotton, F. A. Inorg. Chem. 1970, 9, 351.

12. McGinnis, R. N. Department of Chemistry, Iowa State University; unpublished research, 1976.

13. Ryan, T. R. Department of Chemistry, Iowa State University; unpublished research, 1979.

14. Beers, W. W. Department of Chemistry, Iowa State University; unpublished research, 1981.

15. Luly, M. H. (1979). "APES, A Fortran Program to Analyze Photoelectron Spectra", U.S.D.O.E. Report IS-4694.

16. Jödden, K.; Schäfer, H. Z. anorg. allg. Chem. 1977, 430, 5.

17. Beers, W. W. Ph.D. Dissertation, Iowa State University, Ames,Iowa, 1983; Section IV.

18. San Fillipo, Jr., J.; Sniadoch, H. J.; Grayson, R. L. Inorg. Chem. 1974, 13, 2121.

19. Aufdembrink, B. A. Department of Chemistry, Iowa State University; work revealed through private communication, 1982.

SECTION IV. REDOX CHEMISTRY AND PHYSICAL CHARACTERIZATION OF THE PENTANUCLEAR ANIONS $[(Mo_5Cl_8)Cl_5]^{n-}$ WITH n = 1, 2, AND 3

INTRODUCTION

In our continuing studies of the synthesis, reactions and properties of molybdenum clusters, we became interested in the pentanuclear cluster unit found in $[Bu_4N]_2Mo_5Cl_{13}$. Although this cluster was first prepared in 1975 (1), very little is known about its properties and reactions (2). The tetragonal pyramidal cluster in $[Mo_5Cl_{13}]^{2-}$ can be viewed as a fragment of the well-known octahedral cluster anion $[Mo_6Cl_{14}]^{2-}$. Since the $[Mo_5Cl_{13}]^{2-}$ cluster has 19 metal-centered valence electrons and only 16 electrons are required for forming 8 bonds corresponding to the 8 edges of the square pyramid, the question arises as to the disposition of the electrons and the metal-metal bond order. A rough molecular orbital analysis of the metal-metal bonding in $[Mo_5Cl_{13}]^{2-}$ with C_{4v} symmetry suggested that 14 electrons should reside in strongly bonding orbitals $(3a_1+b_1+b_2+e)$, and that the 5 remaining electrons should occupy closely spaced, weakly bonding or nonbonding orbital doublets in the configuration $e^4 + e^1$. Experimental evidence concerning the electronic structure was thus sought in this work, along with other physical measurements needed for better characterization of the cluster.

EXPERIMENTAL SECTION

Materials

Spectro-grade acetonitrile was dried with CaH_2 and vacuum distilled as needed for electrochemical work. Reagent acetonitrile, which was used for syntheses, and toluene were also dried with CaH_2, distilled, and then stored over molecular sieves. Other solvents were used as received. The tetraalkylammonium chlorides that were used in experiments where the Mo_5 cluster was reduced were recrystallized from acetone by adding ether, vacuum dried for one day, and stored in a drybox (3). The infrared spectrum indicated the product was free from water. The support electrolyte, Bu_4NBF_4, was prepared from Bu_4NBr and HBF_4 (4), recrystallized from acetone and ether, and vacuum dried. The magnetic susceptibility standard, $[NH_4]_2[Ni(H_2O)_6][SO_4]_2$, was prepared by crystallization from an aqueous solution containing equimolar amounts of $[NH_4]_2SO_4$ and $NiSO_4$ (5). Carbon, hydrogen and nitrogen analyses were performed by the Ames Laboratory Analytical Services.

Synthesis

$[Mo_5Cl_{13}]^{2-}$

The $[Mo_5Cl_{13}]^{2-}$ anion was prepared from "monomeric" $MoCl_2$ in an $AlCl_3/KCl/BiCl_3/Bi$ melt according to literature procedure (1). After heating the mixture at 310°C for 5 hours, the mixture was cooled, powdered, and stirred with 6 M HCl. The cluster species dissolved readily

in the acid. Several tetraalkylammonium cations were used to precipitate the cluster from solution. In addition to the tetrabutylammonium salt (1), precipitation of the benzyltrimethylammonium (BTMA) and tetraethylammonium salts occurred readily. The pyridinium salt of the cluster could also be isolated, but it was more soluble. The precipitated material was recrystallized in the air from a mixture of CH_2Cl_2 and ether or acetonitrile and ethyl acetate. Identification of the products formed with cations other than the tetrabutylammonium cation was based on the visible spectra. Typical yields were 15-20%. Attempts to produce the cluster using K_3MoCl_6 (2) as the starting material resulted in lower yields.

$[Mo_5Cl_{13}]^{3-}$

The $[R_4N]_2Mo_5Cl_{13}$ and a three-fold excess of the alkylammonium chloride of the cation were dissolved in acetonitrile. Excess zinc metal (30 mesh) was added and the solution was stirred for several hours during which time the solution turned color from brown to peach. The reduced compound was significantly less soluble in acetonitrile. For dilute solutions, toluene was added to precipitate the cluster. The solution was filtered to remove the excess tetraalkylammonium chloride leaving a mixture of zinc metal and the desired product. The product was separated from the zinc by an extraction with acetonitrile. Several cations were used successfully including $[Bu_4N]^+$, $[BTMA]^+$, and $[Et_4N]^+$. The pyridinium cation could not be used because zinc reduces pyridinium. Several attempts were made to grow crystals of the reduced cluster. When the

$[Bu_4N]^+$ cation was used, the compound was very soluble, but the $[BTMA]^+$ and $[Et_4N]^+$ cations yielded a compound whose solubility was too low for easy crystal growth. Analysis indicated that $[Bu_4N]_3Mo_5Cl_{13}$ crystallizes as the double salt $[Bu_4N]_3Mo_5Cl_{13}\cdot Bu_4NCl$. Anal. Calcd. for $[Bu_4N]_3Mo_5Cl_{13}\cdot Bu_4NCl$: Mo, 24.65; Cl, 25.50; C, 39.50; H, 7.47; N, 2.88. Found: C, 39.64; H, 7.50; N. 2.78; (C/N = 16.0).

Electrochemistry

Electrochemistry was performed with a PAR 173/139 Potentiostat/Coulometer and PAR 175 Programmer. Cyclic voltammograms (CV) were recorded on a Houston Instruments Model 2200 x-y recorder. A platinum disc electrode was used to measure cyclic voltammograms and a coil of platinum wire was used for electrolysis. Potentials are referenced to SCE and are uncorrected for junction potential effects. Acetonitrile solutions, 0.1 M Bu_4NBF_4, were prepared by vacuum distilling acetonitrile into a flask containing the support electrolyte. The solutions were purged and blanketed with argon from which oxygen and water were carefully removed prior to use (Chemalog catalyst R3-11 and molecular sieves). No compensation was used for the residual potential drop of the cell.

X-ray Photoelectron Spectra

The instrumentation and data processing procedures have been described in an earlier section of this dissertation (6); however, data were collected using monochromatic radiation.

Magnetic Susceptibility

Magnetic susceptibility data were collected on an automated Faraday balance constructed and maintained in this laboratory. A Cahn RH Electrobalance was used to measure weight changes. The temperature was determined with a platinum resistance thermometer. Both platinum metal and $[NH_4]_2Ni[H_2O]_6[SO_4]_2$ were used to calibrate the balance. Control of the balance and recording of data were performed by MITS Altair 8800. Further details of the system will be discussed in a future paper (7).

The sample container was machined from a Teflon rod to form a thin-walled cylindrical bucket with a threaded cap. Lowering the bucket into the balance accumulated a static charge on the bucket causing it to cling to the side of the chamber. This problem was eliminated by lightly wiping the bucket with ethanol before inserting it in the balance.

The magnetic susceptibility was measured between 100°K and room temperature utilizing a field gradient of 2.2×10^7 $Gauss^2/cm$. The measured susceptibility was corrected for diamagnetic contributions assuming atomic diamagnetic correction factors for C, H, N, and Cl (8). Since the electrons on the metal atoms were delocalized over the cluster, a cluster diamagnetic factor was calculated (5) based on the core diamagnetism of Mo[VI] (9). This term was 67×10^{-6} emu/mol greater than the sum of the atomic constants for the atoms in their appropriate oxidation state. Data processing was accomplished on a VAX 11/780 with a linear least squares program (10). The linear correlation coefficient, R,

was 0.9943 for the calculation of μ and 0.9933 for the calculation of θ for the $[Bu_4N]_2Mo_5Cl_{13}$ data.

NMR Measurements

NMR data were obtained on a Bruker WM-300 operating at 300 MHz. Measurements were made at ten degree increments between 245°K and 295°K and the observed shifts were corrected for variation of the solvent density with temperature changes (11). Samples were prepared in an air tight system by vacuum distilling acetonitrile and a little toluene into the system, dissolving all of the $[Bu_4N]_2Mo_5Cl_{13}$ and the supporting electroyte, Bu_4NCl, then filling a capillary constructed from a melting point tube. This tube was sealed and the remainder of the solution was filtered into a second compartment containing zinc dust. After maintaining the reducing conditions for two hours, the solution containing the $[Mo_5Cl_{13}]^{3-}$ cluster was filtered into another capillary which was then sealed. This method provided solutions of the 2^- and 3^- clusters having the same cluster concentration. The capillary was then centered with a Teflon sleeve in an NMR tube containing CD_3CN and several drops of toluene. The data for the 3^- species were collected within 3 hours after reduction.

Visible Spectra

All spectra were measured on a Cary 14 Spectrophotometer. Molar absorption coefficients were calculated by ratios of absorbances using $\varepsilon = 2.0 \times 10^3$ for the 455 nm absorption of $[Bu_4N]_2Mo_5Cl_{13}$ (2) as the

standard. For securing the spectrum of $[Mo_5Cl_{13}]^{3-}$, acetonitrile was vacuum distilled into an air tight cell containing $[Bu_4N]_2Mo_5Cl_{13}$ and Bu_4NCl. Zinc dust was then added to the solution to reduce the cluster, the solution was filtered back into the cell and the spectrum was obtained. To obtain the spectrum of the oxidized species $[Mo_5Cl_{13}]^{1-}$, a spectroelectrochemical cell was used so that the spectrum of the 2^- cluster could first be obtained, electrolysis to the 1^- cluster accomplished, and its spectrum recorded without transfer of the solution. The oxidation potential, +1.00 V, was maintained while the spectrum was being recorded.

X-ray Structure Determination

Crystals of $[BTMA]_2Mo_5Cl_{13}$ were grown by slow evaporation in the air of a solution of acetonitrile and ether. Subsequent work revealed that a mixed solvent system of acetonitrile and ethyl acetate also works very well. A crystal was indexed on the Ames Laboratory diffractometer (12) using the automatic indexing program ALICE (13). The unit cell was indicated to be primitive orthorhombic. Standard reflections were checked every 75 reflections and found not to vary significantly. The entire hkl octant and a portion of the -h,-k,l octant of data were collected to 50 deg in 2θ, which provided a total of 11,025 reflections. After data reduction and averaging, 3467 reflections remained. These data were corrected for Lorentz and polarization effects, and an empirical absorption correction was carried out using diffractometer ϕ-scan data and

the program ABSN (14). Other important crystallographic data are given in Table IV-1.

Table VI-1. Crystal data for $[C_6H_5CH_2N(CH_3)_3]_2Mo_5Cl_{13}$

mol. wt.	1241 g/mol
color	dark brown
cryst. dimens. mm	0.20X0.20X0.02
space group	Pcnb
cell dimens.[a]	
a Å	17.863(2)
b Å	35.714(4)
c Å	11.849(1)
cell volume, $Å^3$	7559(1)
molecules/cell	8
wavelength Å	0.71034
linear abs. coeff. cm^{-1}	25.6
2θ limit, deg	42
obs. data [Fo>3σ(Fo)]	2691
final residuals	
R_F	0.052
R_w	0.064
max. residual e^- density	1.1 $e^-/Å^3$

[a]At 25°C, least-squares fit of 24 reflections with 2θ>23°.

Structure Solution and Refinement

Determination of the proper space group was very difficult. In each class of possible systematic extinctions there were several minor violations. The Patterson map (15) was also difficult to interpret because of the many nearly coincident Mo-Mo vectors. Several superposition maps were created, but no additional information was obtained.

The MULTAN (16) package of programs requires the knowledge of the space group. Since the space group was not known, the programs were run in each of the most probable standard setting space groups. Although Mo_5 groups were identified, the positional parameters did not refine properly. At this point, all usual methods of determination of initial atom positions had seemed to fail. Fortunately, a new method of Patterson map analysis was under development in Ames Laboratory. Portions of the computer program package now known as ALCAMPS (17) were used to determine the position of 5 molybdenum and 1 chlorine atoms. ALCAMPS interprets Harker vectors in Patterson and superposition maps to find a possible origin, then determines if the rest of the peaks in the map are consistent with the origin chosen. Information is also provided which aids in the determination of the space group. The correct space group, Pcnb, is a nonstandard setting of the Pbcn space group. Positional parameter refinement of the first 6 atoms led to an electron density map in which other atom positions could be identified (18). Hydrogen atom positions were calculated for methylene and phenyl hydrogens. The data were inspected and observed to have a poor fit at high 2θ angle. After eliminating the data with $\sin \theta/\lambda > 0.50$, 2691 reflections remained. Tables IV-2 and IV-3 list final atom positional and thermal parameters for nonhydrogen atoms. Positional parameters for hydrogen atoms are listed in Table IV-4. Table IV-5 contains important bonding distances and angles. Figure IV-1 is an ORTEP drawing of the molecule, and Figure IV-2 is a basal view which illustrates the distortion in the base of the cluster.

Table IV-2. Positional parameters [x10^4] for $[BTMA]_2Mo_5Cl_{13}$[a]

Atom	x	y	z	U(ave)[b]
Mo(1)	9176.8(9)	3673.4(4)	9162(1)	33
Mo(2)	10309.6(9)	4105.6(5)	9474(1)	35
Mo(3)	10684.2(9)	3951.4(4)	7432(1)	34
Mo(4)	9585.8(9)	3493.6(5)	7156(1)	36
Mo(5)	10509.4(9)	3406.9(4)	8850(1)	31
Cl(1)	10060(3)	3572(1)	10756(4)	45
Cl(2)	9030(3)	4322(1)	9738(4)	49
Cl(3)	9388(3)	3006(1)	8600(4)	43
Cl(4)	8352(3)	3743(1)	7552(4)	43
Cl(5)	11563(3)	3849(1)	9051(4)	42
Cl(6)	10482(3)	4589(1)	8063(4)	51
Cl(7)	10891(3)	3282(1)	6882(4)	43
Cl(8)	9811(3)	4021(1)	5887(4)	44
Cl(9)	8175(3)	3469(1)	10386(1)	48
Cl(10)	10795(3)	4509(2)	10947(4)	62
Cl(11)	11736(3)	4131(1)	6245(4)	49
Cl(12)	9098(3)	3078(2)	5704(4)	61
Cl(13)	11234(3)	2887(1)	9566(5)	56
N(1)	1765(8)	4944(4)	3728(12)	45
C(1)	1738(12)	5272(5)	2891(17)	56
C(2)	976(11)	4804(6)	3971(18)	58
C(3)	2216(12)	4627(6)	3195(17)	64
C(4)	2199(10)	5049(5)	4779(15)	44
C(5)	1822(11)	5352(6)	5504(15)	48
C(6)	2017(10)	5729(5)	5353(16)	45
C(7)	1646(12)	6004(5)	6043(21)	60
C(8)	1211(14)	5887(6)	6881(19)	65
C(9)	1026(12)	5515(7)	7079(18)	67
C(10)	1353(12)	5254(6)	6399(17)	60
N(2)	8131(8)	2638(4)	2722(13)	44

[a]Estimated standard deviations are given in parentheses for the last significant digits.

[b]U(ave) [x 10^3, $Å^2$] is the average of U_{11}, U_{22} and U_{33}.

Table IV-2. (Continued)

Atom	x	y	z	U(ave)[b]
C(11)	7650(13)	2527(6)	1769(17)	67
C(12)	8923(10)	2705(6)	2302(19)	61
C(13)	7808(13)	3001(5)	3219(18)	68
C(14)	8111(11)	2364(6)	3705(17)	60
C(15)	8475(12)	1988(5)	3478(16)	49
C(16)	9202(11)	1905(6)	3859(15)	46
C(17)	9510(13)	1560(7)	3703(17)	61
C(18)	9104(13)	1290(6)	3150(15)	49
C(19)	8412(14)	1365(5)	2759(19)	62
C(20)	8072(11)	1703(6)	2929(18)	56

Table IV-3. Thermal parameters [x10^3] for $[BTMA]_2Mo_5Cl_{13}$[a]

Atom	U_{11}	U_{22}	U_{33}	U_{12}	U_{13}	U_{23}
Mo(1)	37(1)	35(1)	27.7(9)	-2.2(8)	-0.8(8)	0.7(8)
Mo(2)	43(1)	34(1)	28.3(9)	-5.1(8)	1.9(8)	-1.8(8)
Mo(3)	37(1)	35(1)	29(1)	-2.3(8)	-2.8(8)	-1.7(8)
Mo(4)	33(1)	45(1)	29.0(9)	-5.0(8)	-2.6(8)	0.7(8)
Mo(5)	33.1(9)	31.6(9)	29.4(9)	-2.3(8)	-2.7(8)	0.4(8)
Cl(1)	54(3)	50(3)	31(3)	-2(3)	-6(2)	3(2)
Cl(2)	49(3)	41(3)	57(3)	-2(3)	-1(3)	0(3)
Cl(3)	46(3)	34(3)	49(3)	-3(2)	3(2)	3(2)
Cl(4)	43(3)	47(3)	38(3)	1(2)	-3(2)	6(2)
Cl(5)	40(3)	47(3)	39(3)	-8(2)	-2(2)	0(2)
Cl(6)	67(4)	40(3)	45(3)	1(3)	11(3)	9(3)
Cl(7)	42(3)	49(3)	39(3)	0(2)	2(2)	-9(2)
Cl(8)	44(3)	47(3)	42(3)	0(2)	-5(2)	3(2)
Cl(9)	46(3)	57(3)	42(3)	-3(3)	9(2)	6(3)
Cl(10)	80(4)	62(4)	44(3)	-10(3)	-9(3)	-19(3)
Cl(11)	45(3)	56(3)	45(3)	-11(3)	4(2)	9(3)
Cl(12)	60(4)	72(4)	51(3)	-20(3)	-13(3)	-17(3)
Cl(13)	51(3)	50(3)	68(4)	12(3)	-13(3)	8(3)
N(1)	57(11)	51(10)	26(9)	4(9)	-17(8)	5(8)
C(1)	73(16)	49(13)	47(14)	10(11)	0(12)	11(11)
C(2)	37(13)	68(15)	69(16)	2(11)	-8(11)	-3(13)
C(3)	83(17)	58(14)	50(14)	36(12)	16(13)	-20(12)
C(4)	61(13)	49(13)	24(11)	3(10)	-1(10)	-14(10)
C(5)	55(14)	57(15)	32(13)	-12(11)	-21(11)	-19(11)
C(6)	34(11)	47(13)	55(14)	-11(11)	12(10)	-16(11)
C(7)	49(14)	41(13)	89(19)	-5(12)	-24(14)	6(14)
C(8)	99(19)	35(14)	60(16)	-20(13)	6(15)	-17(12)
C(9)	59(15)	98(20)	44(14)	-15(14)	10(12)	-48(15)
C(10)	78(17)	70(16)	32(13)	-23(13)	11(12)	9(12)
N(2)	58(11)	36(10)	39(10)	17(8)	-4(9)	0(8)
C(11)	91(18)	63(14)	47(14)	-2(13)	-49(13)	-11(13)
C(12)	18(12)	66(15)	99(18)	-9(10)	15(12)	27(14)
C(13)	107(20)	39(13)	57(15)	38(12)	-7(14)	-16(11)
C(14)	53(15)	86(17)	41(13)	-19(12)	13(11)	-12(13)

[a]Estimated standard deviations are given in parentheses for the last significant digits. The anisotropic thermal parameter expression used is $\exp[-2\pi^2(U_{11}h^2a^{*2} + U_{22}k^2b^{*2} + U_{33}l^2c^{*2} + 2U_{12}hka^*b^* + 2U_{13}hla^*c^* + 2U_{23}klb^*c^*)]$ with U's in $Å^2$.

Table IV-3. (Continued)

Atom	U_{11}	U_{22}	U_{33}	U_{12}	U_{13}	U_{23}
C(15)	61(15)	40(13)	45(14)	-6(12)	26(12)	-10(11)
C(16)	46(13)	66(15)	25(11)	3(12)	-8(10)	-10(11)
C(17)	80(17)	71(17)	32(13)	11(15)	-2(12)	3(13)
C(18)	84(17)	51(14)	12(10)	10(13)	6(11)	22(10)
C(19)	97(19)	13(12)	76(17)	-1(12)	0(15)	11(11)
C(20)	42(13)	62(16)	63(15)	-6(12)	-3(12)	15(13)

Table IV-4. Hydrogen positional parameters [$x10^4$][a]

Atom	x	y	z
H(6)	2377	5810	4696
H(7)	1773	6288	5911
H(8)	961	6089	7403
H(9)	665	5433	7736
H(10)	1227	4969	6531
H(16)	9507	2114	4278
H(17)	10052	1501	3994
H(18)	9347	1024	3022
H(19)	8105	1155	2336
H(20)	7529	1760	2634
H(4A)	2728	5147	4532
H(4B)	2263	4807	5277
H(14A)	7549	2315	3920
H(14B)	8390	2487	4390

[a]All hydrogen atoms were assigned isotropic U values of 50.7×10^{-3} $Å^2$.

Table IV-5. Distances (Å) and angles (deg) for $[BTMA]_2Mo_5Cl_{13}$

Bond distances within cluster

Mo(1)-Mo(2)	2.572(2)	Mo(2)-Mo(5)	2.627(2)
Mo(1)-Mo(4)	2.569(2)	Mo(3)-Mo(4)	2.575(2)
Mo(1)-Mo(5)	2.590(2)	Mo(3)-Mo(5)	2.588(2)
Mo(2)-Mo(3)	2.569(2)	Mo(4)-Mo(5)	2.617(2)
Cl(1)-Mo(1)	2.487(5)	Cl(5)-Mo(2)	2.471(5)
Cl(1)-Mo(2)	2.477(5)	Cl(5)-Mo(3)	2.505(5)
Cl(1)-Mo(5)	2.470(5)	Cl(5)-Mo(5)	2.467(5)
Cl(3)-Mo(1)	2.505(5)	Cl(7)-Mo(3)	2.505(5)
Cl(3)-Mo(4)	2.468(5)	Cl(7)-Mo(4)	2.473(5)
Cl(3)-Mo(5)	2.480(5)	Cl(7)-Mo(5)	2.470(5)
Cl(2)-Mo(1)	2.428(5)	Cl(6)-Mo(2)	2.424(5)
Cl(2)-Mo(2)	2.433(5)	Cl(6)-Mo(3)	2.425(5)
Cl(4)-Mo(1)	2.423(5)	Cl(8)-Mo(3)	2.428(5)
Cl(4)-Mo(4)	2.423(5)	Cl(8)-Mo(4)	2.443(5)
Mo(1)-Cl(9)	2.416(5)	Mo(4)-Cl(12)	2.433(6)
Mo(2)-Cl(10)	2.423(6)	Mo(5)-Cl(13)	2.418(5)
Mo(3)-Cl(11)	2.434(5)		

Bond angles within cluster

Mo(2)-Mo(1)-Mo(4)	93.39(7)	Mo(1)-Mo(4)-Mo(3)	86.97(7)
Mo(2)-Mo(1)-Mo(5)	61.18(6)	Mo(1)-Mo(4)-Mo(5)	59.93(6)
Mo(4)-Mo(1)-Mo(5)	60.95(6)	Mo(3)-Mo(4)-Mo(5)	59.80(6)
Mo(1)-Mo(2)-Mo(3)	86.63(7)	Mo(1)-Mo(5)-Mo(2)	59.06(6)
Mo(1)-Mo(2)-Mo(5)	59.76(6)	Mo(1)-Mo(5)-Mo(3)	85.85(7)
Mo(3)-Mo(2)-Mo(5)	59.73(6)	Mo(1)-Mo(5)-Mo(4)	59.12(6)
Mo(2)-Mo(3)-Mo(4)	93.30(7)	Mo(2)-Mo(5)-Mo(3)	59.03(6)
Mo(2)-Mo(3)-Mo(5)	61.24(6)	Mo(2)-Mo(5)-Mo(4)	91.03(7)
Mo(4)-Mo(3)-Mo(5)	60.90(6)	Mo(3)-Mo(5)-Mo(4)	59.30(6)
Mo(2)-Mo(1)-Cl(1)	58.6(1)	Mo(5)-Mo(3)-Cl(5)	57.9(1)
Mo(2)-Mo(1)-Cl(2)	58.2(1)	Mo(5)-Mo(3)-Cl(6)	119.2(1)
Mo(2)-Mo(1)-Cl(3)	119.4(1)	Mo(5)-Mo(3)-Cl(7)	58.0(1)
Mo(2)-Mo(1)-Cl(4)	122.0(1)	Mo(5)-Mo(3)-Cl(8)	119.4(1)
Mo(2)-Mo(1)-Cl(9)	132.7(1)	Mo(5)-Mo(3)-Cl(11)	131.8(1)
Mo(4)-Mo(1)-Cl(1)	119.1(1)	Mo(1)-Mo(4)-Cl(3)	59.6(1)
Mo(4)-Mo(1)-Cl(2)	122.0(1)	Mo(1)-Mo(4)-Cl(4)	58.0(1)
Mo(4)-Mo(1)-Cl(3)	58.2(1)	Mo(1)-Mo(4)-Cl(7)	117.8(1)
Mo(4)-Mo(1)-Cl(4)	58.0(1)	Mo(1)-Mo(4)-Cl(8)	115.1(1)
Mo(4)-Mo(1)-Cl(9)	133.7(1)	Mo(1)-Mo(4)-Cl(12)	134.8(1)

Table IV-5. (Continued)

Mo(5)-Mo(1)-Cl(1)	58.2(1)	Mo(3)-Mo(4)-Cl(3)	118.0(1)
Mo(5)-Mo(1)-Cl(2)	119.4(1)	Mo(3)-Mo(4)-Cl(4)	115.8(1)
Mo(5)-Mo(1)-Cl(3)	58.2(1)	Mo(3)-Mo(4)-Cl(7)	59.5(1)
Mo(5)-Mo(1)-Cl(4)	118.9(1)	Mo(3)-Mo(4)-Cl(8)	57.5(1)
Mo(5)-Mo(1)-Cl(9)	131.0(1)	Mo(3)-Mo(4)-Cl(12)	138.6(1)
Mo(1)-Mo(2)-Cl(1)	59.0(1)	Mo(5)-Mo(4)-Cl(3)	58.3(1)
Mo(1)-Mo(2)-Cl(2)	58.0(1)	Mo(5)-Mo(4)-Cl(4)	117.9(1)
Mo(1)-Mo(2)-Cl(5)	117.4(1)	Mo(5)-Mo(4)-Cl(7)	57.9(1)
Mo(1)-Mo(2)-Cl(6)	115.4(1)	Mo(5)-Mo(4)-Cl(8)	117.3(1)
Mo(1)-Mo(2)-Cl(10)	137.9(1)	Mo(5)-Mo(4)-Mo(12)	134.1(1)
Mo(3)-Mo(2)-Cl(1)	117.4(1)	Mo(1)-Mo(5)-Cl(1)	58.8(1)
Mo(3)-Mo(2)-Cl(2)	115.7(1)	Mo(1)-Mo(5)-Cl(3)	59.2(1)
Mo(3)-Mo(2)-Cl(5)	59.6(1)	Mo(1)-Mo(5)-Cl(5)	116.9(1)
Mo(3)-Mo(2)-Cl(6)	58.0(1)	Mo(1)-Mo(5)-Cl(7)	117.1(1)
Mo(3)-Mo(2)-Cl(10)	135.4(1)	Mo(1)-Mo(5)-Cl(13)	136.4(1)
Mo(5)-Mo(2)-Cl(1)	57.8(1)	Mo(2)-Mo(5)-Cl(1)	58.1(1)
Mo(5)-Mo(2)-Cl(2)	117.7(1)	Mo(2)-Mo(5)-Cl(3)	118.2(1)
Mo(5)-Mo(2)-Cl(5)	57.8(1)	Mo(2)-Mo(5)-Cl(5)	57.9(1)
Mo(5)-Mo(2)-Cl(6)	117.7(1)	Mo(2)-Mo(5)-Cl(7)	118.4(1)
Mo(5)-Mo(2)-Cl(10)	135.9(1)	Mo(2)-Mo(5)-Cl(13)	134.7(1)
Mo(2)-Mo(3)-Cl(5)	58.3(1)	Mo(3)-Mo(5)-Cl(1)	116.9(1)
Mo(2)-Mo(3)-Cl(6)	58.0(1)	Mo(3)-Mo(5)-Cl(3)	117.0(1)
Mo(2)-Mo(3)-Cl(7)	119.2(1)	Mo(3)-Mo(5)-Cl(5)	59.4(1)
Mo(2)-Mo(3)-Cl(8)	121.5(1)	Mo(3)-Mo(5)-Cl(7)	59.3(1)
Mo(2)-Mo(3)-Cl(11)	133.5(1)	Mo(3)-Mo(5)-Cl(13)	137.8(1)
Mo(4)-Mo(3)-Cl(5)	118.8(1)	Mo(4)-Mo(5)-Cl(1)	117.9(1)
Mo(4)-Mo(3)-Cl(6)	121.5(1)	Mo(4)-Mo(5)-Cl(3)	57.8(1)
Mo(4)-Mo(3)-Cl(7)	58.2(1)	Mo(4)-Mo(5)-Cl(5)	118.7(1)
Mo(4)-Mo(3)-Cl(8)	58.5(1)	Mo(4)-Mo(5)-Cl(7)	58.1(1)
Mo(4)-Mo(3)-Cl(11)	133.0(1)	Mo(4)-Mo(5)-Cl(13)	134.3(1)
Cl(1)-Mo(1)-Cl(2)	89.6(2)	Cl(6)-Mo(3)-Cl(8)	92.3(2)
Cl(1)-Mo(1)-Cl(3)	88.2(2)	Cl(6)-Mo(3)-Cl(11)	92.6(2)
Cl(1)-Mo(1)-Cl(4)	176.7(2)	Cl(7)-Mo(3)-Cl(8)	89.8(2)
Cl(1)-Mo(1)-Cl(9)	88.3(2)	Cl(7)-Mo(3)-Cl(11)	89.3(2)
Cl(2)-Mo(1)-Cl(3)	177.4(2)	Cl(8)-Mo(3)-Cl(11)	91.9(2)
Cl(2)-Mo(1)-Cl(4)	93.3(2)	Cl(3)-Mo(4)-Cl(4)	89.7(2)
Cl(2)-Mo(1)-Cl(9)	92.2(2)	Cl(3)-Mo(4)-Cl(7)	90.6(2)
Cl(3)-Mo(1)-Cl(4)	88.9(2)	Cl(3)-Mo(4)-Cl(8)	174.1(2)
Cl(3)-Mo(1)-Cl(9)	89.1(2)	Cl(3)-Mo(4)-Cl(12)	90.5(2)
Cl(4)-Mo(1)-Cl(9)	93.1(2)	Cl(4)-Mo(4)-Cl(7)	174.6(2)
Cl(1)-Mo(2)-Cl(2)	89.7(2)	Cl(4)-Mo(4)-Cl(8)	89.2(2)
Cl(1)-Mo(2)-Cl(5)	90.1(2)	Cl(4)-Mo(4)-Cl(12)	92.1(2)
Cl(1)-Mo(2)-Cl(6)	173.8(2)	Cl(7)-Mo(4)-Cl(8)	90.0(2)
Cl(1)-Mo(2)-Cl(10)	94.5(2)	Cl(7)-Mo(4)-Cl(12)	93.4(2)
Cl(2)-Mo(2)-Cl(5)	174.4(2)	Cl(8)-Mo(4)-Cl(12)	95.4(2)

Table IV-5. (Continued)

Cl(2)-Mo(2)-Cl(6)	89.0(2)	Cl(1)-Mo(5)-Cl(3)	89.1(2)
Cl(2)-Mo(2)-Cl(10)	93.2(2)	Cl(1)-Mo(5)-Cl(5)	90.4(2)
Cl(5)-Mo(2)-Cl(6)	90.6(2)	Cl(1)-Mo(5)-Cl(7)	175.3(2)
Cl(5)-Mo(2)-Cl(10)	92.3(2)	Cl(1)-Mo(5)-Cl(13)	91.7(2)
Cl(6)-Mo(2)-Cl(10)	91.6(2)	Cl(3)-Mo(5)-Cl(5)	175.5(2)
Cl(5)-Mo(3)-Cl(6)	89.7(2)	Cl(3)-Mo(5)-Cl(7)	90.4(2)
Cl(5)-Mo(3)-Cl(7)	88.1(2)	Cl(3)-Mo(5)-Cl(13)	89.8(2)
Cl(5)-Mo(3)-Cl(8)	177.2(2)	Cl(5)-Mo(5)-Cl(7)	89.8(2)
Cl(5)-Mo(3)-Cl(11)	89.9(2)	Cl(5)-Mo(5)-Cl(13)	92.8(2)
Cl(6)-Mo(3)-Cl(7)	177.1(2)	Cl(7)-Mo(5)-Cl(13)	92.6(2)
Mo(1)-Cl(1)-Mo(2)	62.4(1)	Mo(2)-Cl(5)-Mo(3)	62.2(1)
Mo(1)-Cl(1)-Mo(5)	63.0(1)	Mo(2)-Cl(5)-Mo(5)	64.3(1)
Mo(2)-Cl(1)-Mo(5)	64.2(1)	Mo(3)-Cl(5)-Mo(5)	62.7(1)
Mo(1)-Cl(2)-Mo(2)	63.9(1)	Mo(2)-Cl(6)-Mo(3)	64.0(1)
Mo(1)-Cl(3)-Mo(4)	62.2(1)	Mo(3)-Cl(7)-Mo(4)	62.3(1)
Mo(1)-Cl(3)-Mo(5)	62.6(1)	Mo(3)-Cl(7)-Mo(5)	62.7(1)
Mo(4)-Cl(3)-Mo(5)	63.9(1)	Mo(4)-Cl(7)-Mo(5)	63.9(1)
Mo(1)-Cl(4)-Mo(4)	64.0(1)	Mo(3)-Cl(8)-Mo(4)	64.0(1)

Bond distances in cations

N(1)-C(1)	1.54(2)	N(2)-C(11)	1.47(3)
N(1)-C(2)	1.52(2)	N(2)-C(12)	1.52(2)
N(1)-C(3)	1.53(3)	N(2)-C(13)	1.54(2)
N(1)-C(4)	1.52(2)	N(2)-C(14)	1.52(3)
C(4)-C(5)	1.54(3)	C(14)-C(15)	1.52(2)
C(5)-C(6)	1.40(3)	C(15)-C(16)	1.41(3)
C(5)-C(10)	1.40(3)	C(15)-C(20)	1.41(3)
C(6)-C(7)	1.44(3)	C(16)-C(17)	1.36(3)
C(7)-C(8)	1.33(3)	C(17)-C 18)	1.37(3)
C(8)-C(9)	1.39(3)	C(18)-C(19)	1.35(3)
C(9)-C(10)	1.36(3)	C(19)-C(20)	1.37(3)

Hydrogen-chlorine distances less than 3.00 A

Atom	Distance (A)	C-H-Cl Angle (deg)
C(10)-H(10)-Cl(6)	2.628	135
C(6)-H(6)-Cl(9)	2.943	124
C(19)-H(19)-Cl(11)	2.950	152
C(4)-H(4B)-Cl(11)	2.835	153
C(14)-H(14B)-Cl(12)	2.909	158
C(17)-H(17)-Cl(12)	2.943	127
C(14)-H(14A)-Cl(13)	2.575	172

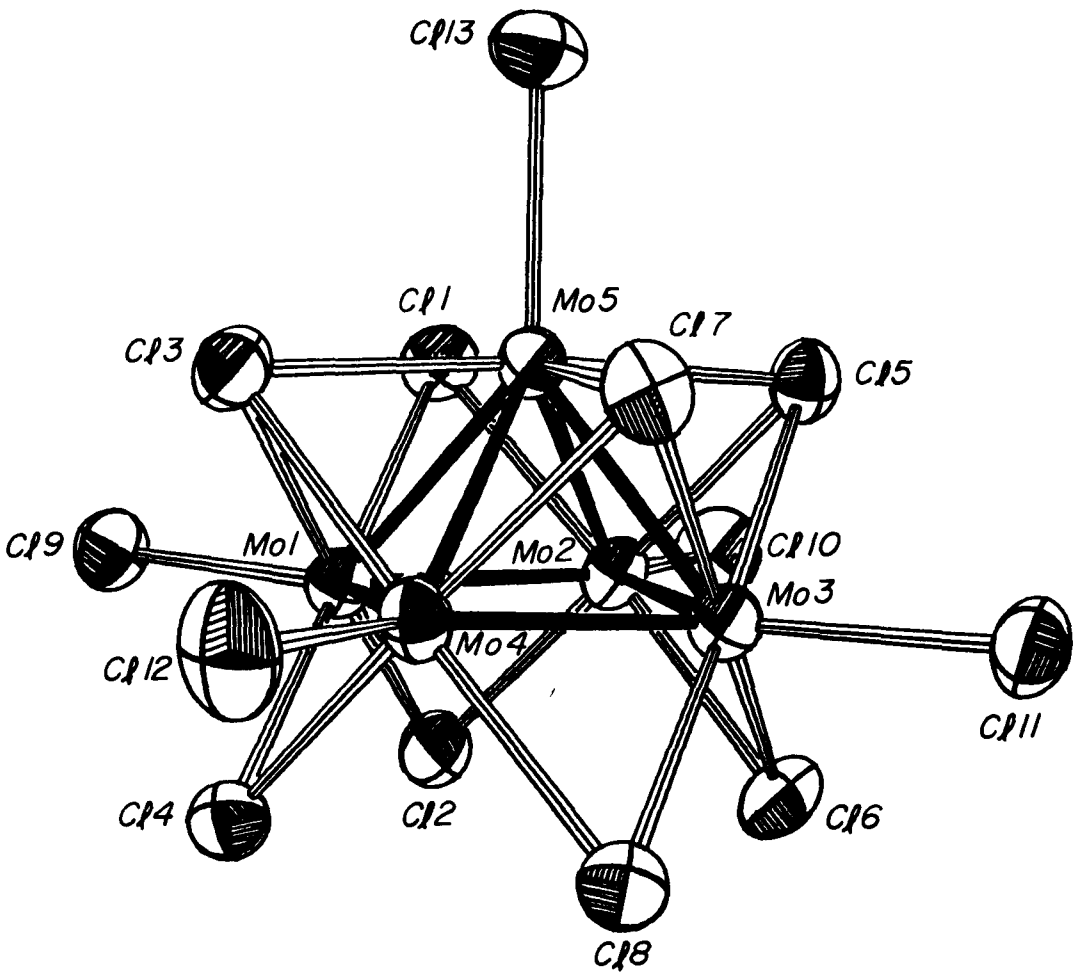

Figure IV-1. Structure of $[Mo_5Cl_{13}]^{2-}$ unit found in $[BTMA]_2Mo_5Cl_{13}$. Thermal ellipsoids are scaled to enclose 50% of the electron density

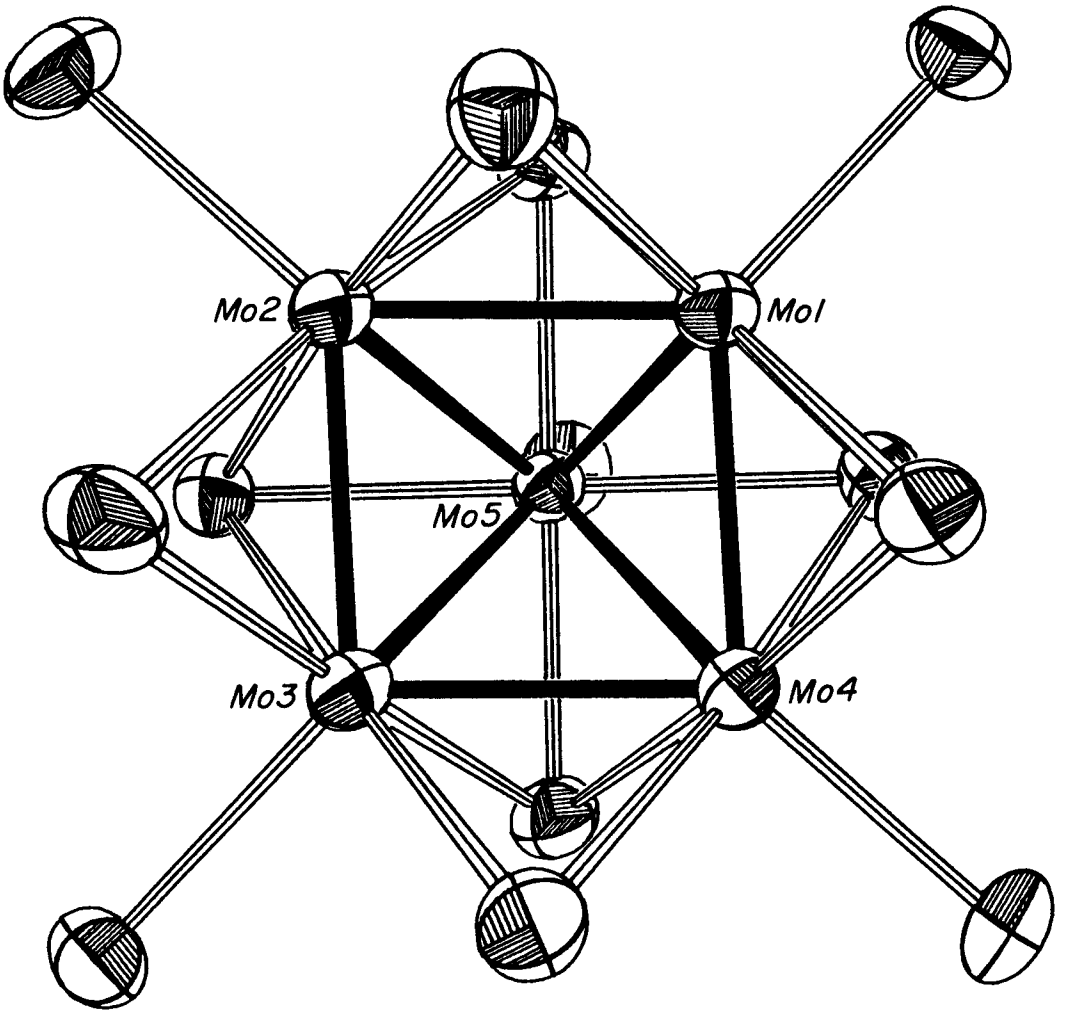

Figure IV-2. Basal view of $Mo_5Cl_{13}^{2-}$ unit found in $[BTMA]_2Mo_5Cl_{13}$

Electron Spin Resonance

Electron spin resonance measurements were executed with a Bruker ER 200D-SRC instrument equipped with an Oxford ESR-900 flow-through cryostat and DTC-2 digital temperature controller. A Hewlett-Packard 5342A microwave frequency counter was used to accurately measure the spectrometer frequency. Calibration of the instrument with DPPH was accomplished before g values were measured.

A frozen-glass spectrum of $[Bu_4N]_2Mo_5Cl_{13}$ was obtained by adding the compound to toluene and adding a minimum of acetonitrile until dissolution occurred. The solution was then filtered into a 3 mm o.d. quartz tube and sealed.

Extended Hückel Calculations

The program used for extended Hückel calculations and the method of calculating input parameters has been described previously (19). Calculations were done on the $[Mo_5Cl_{13}]^{2-}$ cluster as it is found in $[Bu_4N]_2Mo_5Cl_{13}$ (C_{4v} symmetry), $[BTMA]_2Mo_5Cl_{13}$ (C_{2v} symmetry), and hypothetical rectangular based pyramid of $[Mo_5Cl_{13}]^{2-}$. The Mo_5 unit in $[BTMA]_2Mo_5Cl_{13}$ does not have any crystallographic symmetry, although it is very close to C_{2v} symmetry. Therefore, appropriate bond distances were averaged and an idealized C_{2v} cluster constructed.

The molecular orbital diagram for $[Mo_6Cl_{14}]^{2-}$ was also calculated. An octahedron of metal atoms was used for one calculation. Another calculation was done with one axial Mo and its terminal Cl tetragonally

extended by 0.2 Å. This series of calculations allowed a correlation diagram to be drawn between the Mo_6 and Mo_5 clusters yielding further information on which orbitals were involved in the addition of a metal atom to complete the Mo_5 cluster.

Data from Table 6 of Cusachs and Corrington's work (20) were also used in one calculation for $[Mo_6Cl_{14}]^{2-}$. These zeta exponents grouped the three highest occupied t levels extremely close together so that they were essentially equivalent. Since zeta exponents from Table 4 of reference (20) gave better agreement to previous molecular orbital calculations on the $[Mo_6X_{14}]^{2-}$ cluster, they were used for the $[Mo_5Cl_{13}]^{2-}$ calculations. Atomic coordinates and final atomic charges for all calculations are given in Table IV-6.

Table IV-6. Parameters used in extended Hückel calculation[a]

$[Bu_4N]_2Mo_5Cl_{13}$

Atom	x	y	z	final charge
Mo(b)	1.282	1.282	0.000	0.22
Mo(a)	0.000	0.000	1.861	0.22
Cl(t)	3.005	3.005	0.011	-0.37
Cl(t)	0.000	0.000	4.274	-0.37
Cl(db)	2.422	0.000	-1.714	-0.21
Cl(db)	0.000	2.422	-1.714	-0.19
Cl(tb)	2.459	0.000	1.771	-0.11
Cl(tb)	0.000	2.459	1.771	-0.12

[a]Atom types are designated as follows: b, basal; a, apical; t, terminal; db, doubly bridging; tb, triply bridging.

Table IV-6. (Continued)

$[BTMA]_2Mo_5Cl_{13}$

Atom	x	y	z	final charge
Mo(b)	0.000	1.763	0.000	0.23
Mo(b)	1.870	0.000	0.000	0.21
Mo(a)	0.000	0.000	1.867	0.22
Cl(t)	4.297	0.000	0.043	-0.38
Cl(t)	0.000	4.190	0.043	-0.37
Cl(t)	0.000	0.000	4.284	-0.38
Cl(db)	1.756	1.705	-1.700	-0.20
Cl(tb)	1.739	1.753	1.767	-0.11

Rectangular pyramid of $[Mo_5Cl_{13}]^{2-}$

Atom	x	y	z	final charge
Mo(b)	1.302	1.282	0.000	0.22
Mo(a)	0.000	0.000	1.861	0.22
Cl(t)	3.005	3.005	0.011	-0.38
Cl(t)	0.000	0.000	4.274	-0.38
Cl(db)	2.422	0.000	-1.714	-0.19
Cl(db)	0.000	2.422	-1.714	-0.19
Cl(tb)	2.459	0.000	1.771	-0.10
Cl(tb)	0.000	2.459	1.771	-0.11

$[Mo_6Cl_{14}]^{2-}$

Atom	x	y	z	final charge
Mo	1.305	1.305	0.000	0.21
Mo	0.000	0.000	1.846	0.20
Mo[b]	0.000	0.000	-1.846	0.20
Cl(t)	3.042	3.042	0.000	-0.39
Cl(t)	0.000	0.000	4.302	-0.39
Cl(t)[b]	0.000	0.000	-4.302	-0.39
Cl(tb)	2.472	0.000	1.748	-0.11
Cl(tb)	0.000	-2.472	1.748	-0.11
Cl(tb)	2.472	0.000	-1.748	-0.11
Cl(tb)	0.000	-2.471	-1.748	-0.10

[b]For the distorted $[Mo_6Cl_{14}]^{2-}$ cluster, these parameters were:
Mo: x 0.000; y 0.000; z -2.046; charge 0.19
Cl: x 0.000; y 0.000; z -4.502; charge -0.39;
all other parameters were the same.

RESULTS AND DISCUSSION

Cyclic Voltammetry

Cyclic voltammetry is a powerful tool for the investigation of multiple oxidation states. Since the highest occupied molecular orbital (HOMO) appears to be approximately nonbonding, we felt this cluster should have other accessible oxidation states. The cyclic voltammogram (Figure IV-3) clearly indicates both a reduction and an oxidation of the cluster can occur. A steady-state cyclic voltammogram was achieved for both processes within 3 cycles. The lack of an oxidation potential corresponding to that for Cl^- indicates that there is little dissociation of chlorine. The cyclic voltammogram of $[Mo_6Cl_{14}]^{2-}$ also indicated no chlorine dissociation (21).

The reduction of the cluster occurred at $E_{1/2}$ = -0.15 V. The ratio of the current peak for the forward and reverse sweeps was 1.00 and did not vary with scan rate. Peak separation was also investigated as a function of scan rate and found to vary from 70 mV at 20 mV/sec to 170 mV at 200 mV/sec. Because of rapid attainment of the steady-state shape and no other indications of irreversibility, the peak separation dependence on sweep rate is probably a result of uncompensated resistance usually found when working in organic solvents (22). We thus believe the reduction is a one electron reversible process.

The oxidation process, which has $E_{1/2}$ = +0.77 V, may not be as reversible as the reduction process. Although the steady-state shape of the CV is reached quickly, the peak current ratio is no longer unity and

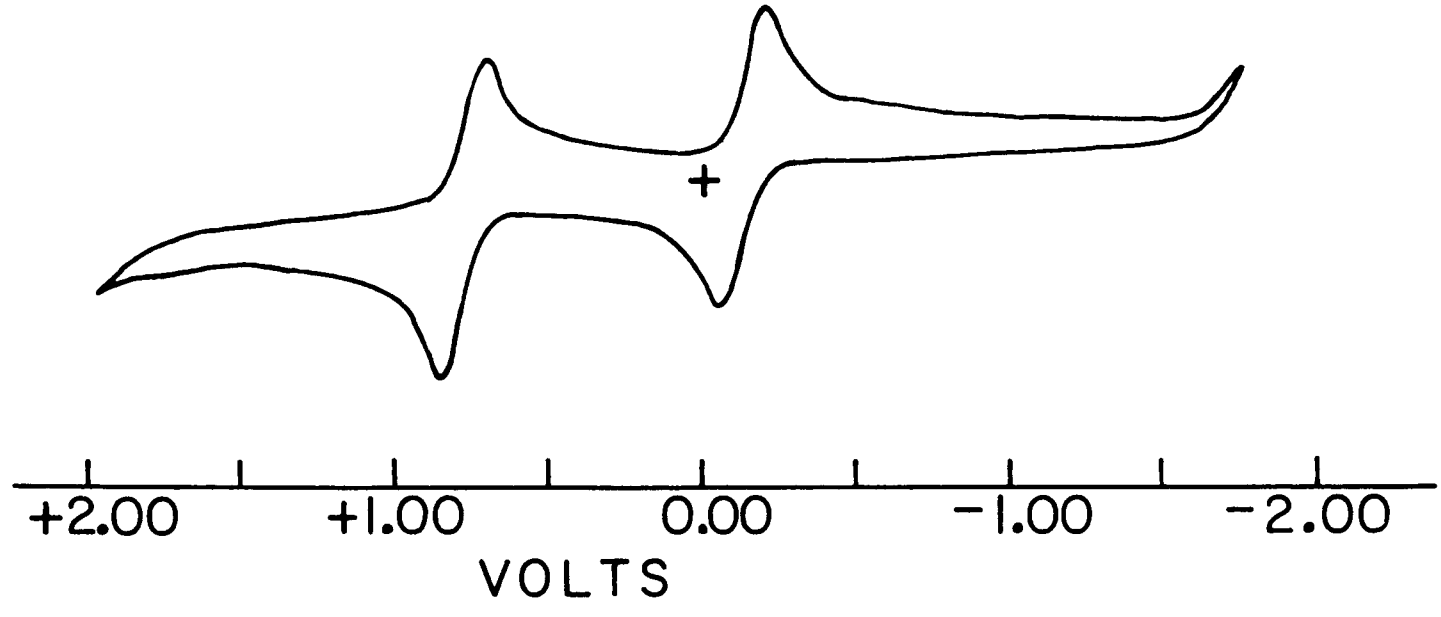

Figure IV-3. Cyclic voltammogram of $[Bu_4N]_2Mo_5Cl_{13}$ in acetonitrile

varies slightly with scan rate. At a slow scan rate, peak to peak time of 66 seconds, the I_{pf}/I_{pr} ratio is 0.87. When the peak to peak time separation is decreased to 7 seconds, the I_{pf}/I_{pr} ratio increases to 0.93. Peak separation was found to vary from 100 mV at 20 mV/sec to 225 mV at 200 mV/sec. Oxidation of the cluster appears to involve one electron and should be considered to be quasi-reversible.

Electrolysis of an acetonitrile solution at -0.50 V resulted in a noticeable color change from brown to orange-brown. The solution color was also much less intense. The cyclic voltammogram of the resulting solution contained a wave for the oxidation back to the 2^- cluster. The further oxidation step was not clean. Another reaction appears to be occurring at a potential slightly more positive than the cluster oxidation potential.

It is also possible to produce $[Mo_5Cl_{13}]^{3-}$ by reduction with zinc powder. The CV of a solution containing the cluster reduced with zinc was considerably more complex than the solution of the reduced cluster formed by electrolytic reduction. Reversible, one-electron oxidations were observed at -0.15 and +0.08 V (Figure IV-4a). Two additional oxidations at about +0.7 to +0.9 V were also apparent. Resolution of this region into its components was not possible. The oxidation that occurred at +0.08 V suggested that a chemical reaction may have occurred, possibly changing the cluster slightly. We thought that it was likely that Zn^{2+} was abstracting chlorine from the cluster. This hypothesis was tested by conducting the zinc reduction in the presence of excess dry Bu_4NCl. The CV of this solution indicated only one oxidation at the potential expected

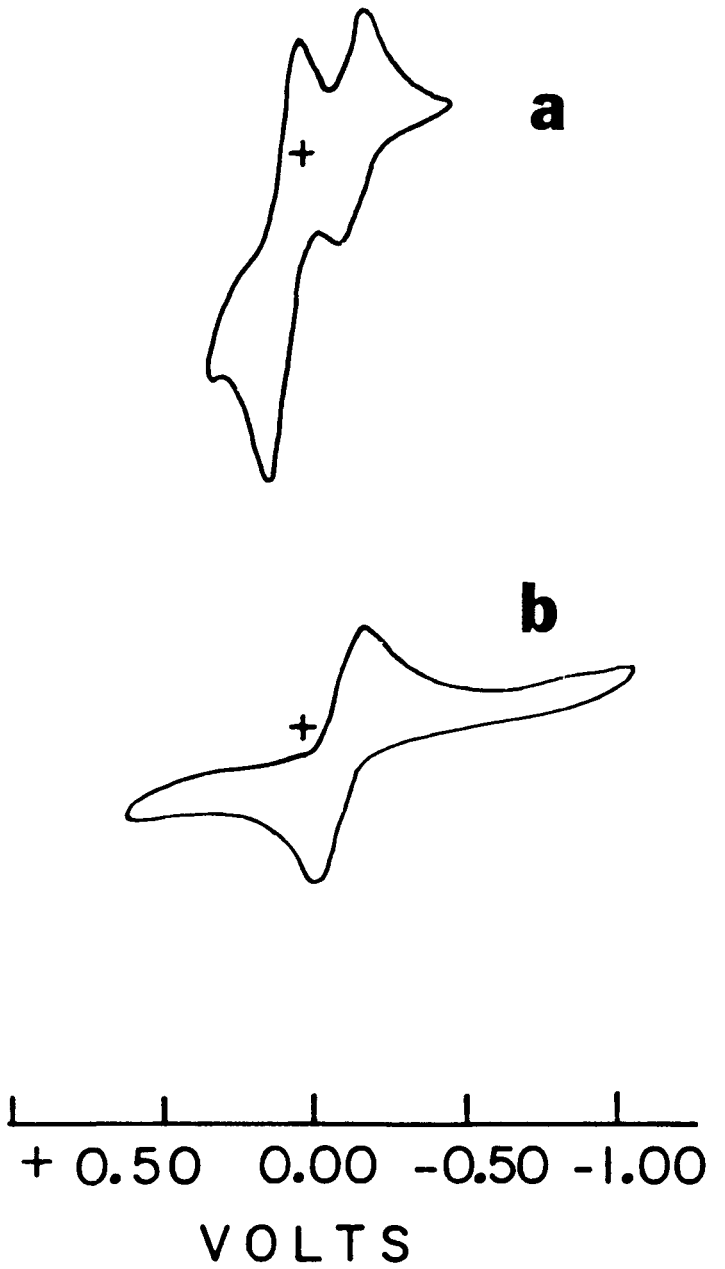

Figure IV-4. Cyclic voltammogram of cluster after zinc reduction a) without excess Cl^-, b) with excess Cl^-

for an oxidation of the 3^- cluster to the 2^- cluster (Figure IV-4b). Further oxidation to the 1^- cluster was obscured by oxidation of the excess chloride anion.

Electrolysis at +1.00 V changed the color of the solution to a deep purple. The CV of the purple solution contained the reductions back to the 2^- and 3^- clusters. Another irreversible reduction was visible at about -0.9 V and was probably due to decomposition products. After about 15 minutes, the color of the electrolyzed solution was obviously returning to the brown color of the 2^- cluster.

Visible Spectra

The visible spectrum of $[Mo_5Cl_{13}]^{2-}$ (Figure IV-5) revealed that in addition to the two absorptions previously reported (2), there is also an absorption in the near infrared region which extends to 1100 nm. No other cluster absorptions were observed in the region 700 to 1500 nm.

Reduction of the 2^- cluster with zinc occurs readily. The solution changes color slightly, but most notable is the decrease in intensity of the color. This is demonstrated in the molar absorptivity coefficients of the new species (Table IV-7). If the solution was carefully prepared and protected from air and moisture, the reduced compound was stable. A spectrum run one day after the preparation showed no change.

The reversibility of the reduction was demonstrated by exposing a carefully prepared, filtered acetonitrile solution of $[Mo_5Cl_{13}]^{3-}$ to the air overnight. A spectrum of $[Mo_5Cl_{13}]^{2-}$ had been recorded before reduction. After the solution containing the 3^- cluster was exposed to

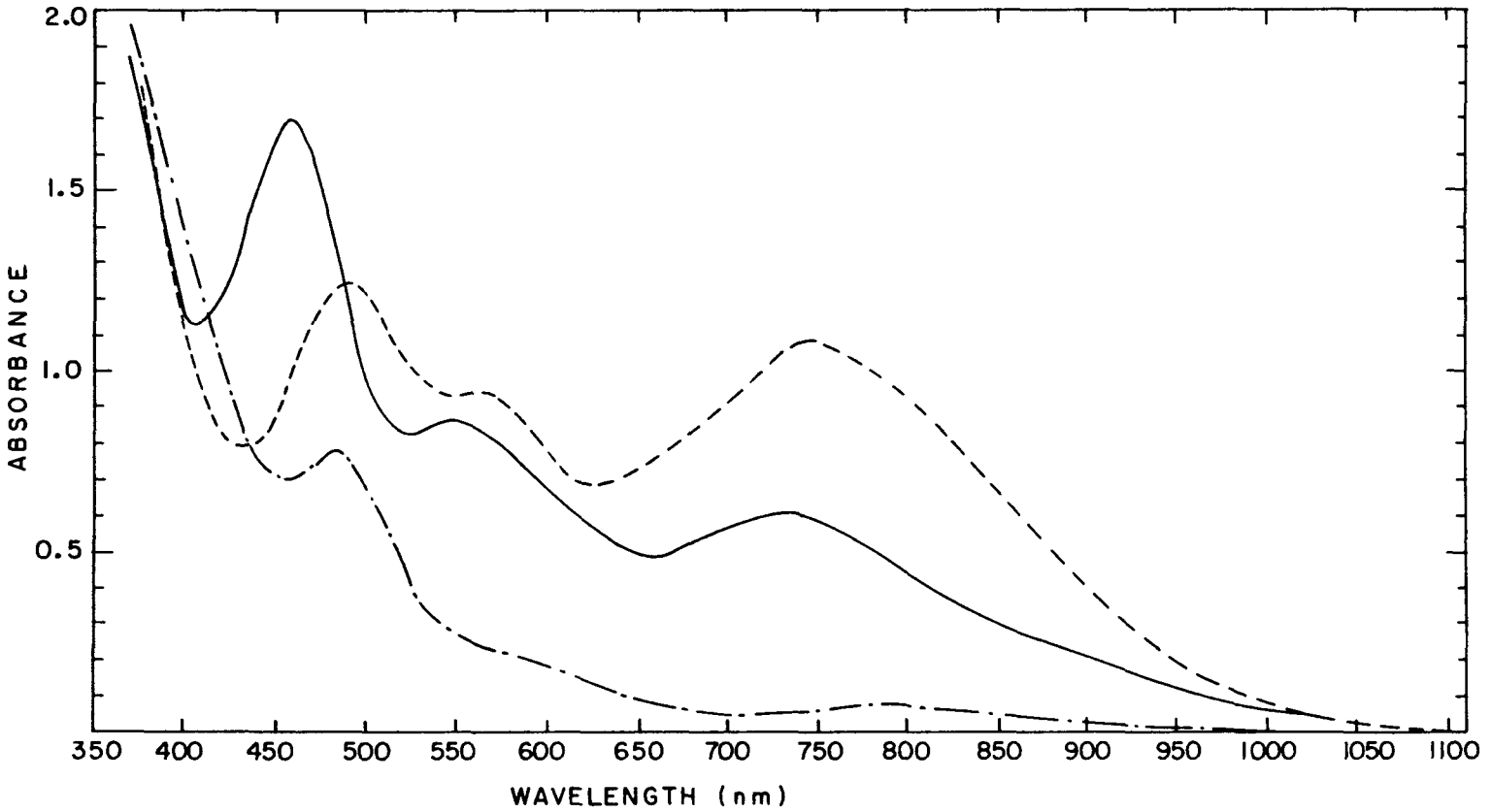

Figure IV-5. Visible spectra of $[Mo_5Cl_{13}]^{n-}$; n = 1 (---), n = 2 (——), n = 3 (-•-)

Table IV-7. Electronic absorption data for $[Mo_5Cl_{13}]^{n-}$

1^-		2^-		3^-	
λ(nm)	ε(ℓ/mole-cm)	λ(nm)	ε(ℓ/mole-cm)	λ(nm)	ε(ℓ/mole-cm)
745	1.3×10^3	725	7.2×10^2	790	1.0×10^2
560	1.1×10^3	550	1.0×10^3	580	2.8×10^2
490	1.5×10^3	455	2.0×10^3	485	9.3×10^2

air, the absorption occurred at the proper wavelengths for the 2^- cluster and with at least 90% of their original absorbance.

The dark brown solution of $[Mo_5Cl_{13}]^{2-}$ changed to a dark purple upon electrolytic oxidation. If the potential was removed after the oxidation was complete, the solution began to turn brown very quickly. Therefore, the spectrum was recorded with the potential applied.

The method used to determine absorption coefficients assumes that the concentrations of the old and new species are identical. Although we are confident that this is true for the reduced species, there is some doubt in the case of the oxidized species. Since decomposition occurs quickly, there may have been decomposition during the electrolysis. This would lead to actual absorptivities greater than those reported in Table IV-7.

Not all of the decomposition products have been identified, but after 2 1/2 hours, the solution color is stable and the spectrum is that of $[Mo_5Cl_{13}]^{2-}$. The absorbance is about 3/4 of the initial value. This

leads us to believe that a disproportionation of the 1^- species is occurring.

The spectra show little change in band positions as the oxidation state varies. If one of the absorptions observed in the spectra of the 2^- and 3^- species was not present in the spectrum of the 1^- species, one could assume that transition would be from the HOMO. Since this is not observed, the transitions must be from lower lying orbitals.

Magnetic Properties

A plot of χ_M^C *vs* 1/T for $[Bu_4N]_2Mo_5Cl_{13}$ (Figure IV-6) reveals that the susceptibility follows typical Curie-Weiss behavior. These data corresponded very well with a line whose equation was: χ_M^C = [0.347(3)][1/T] + 2.12(2) x 10^{-4} cm^3/mol. The magnetic moment was found to be 1.67(1), and the Weiss constant was -14(2)°K. The temperature independent paramagnetism was 208(23) x 10^{-6} cm^3/mol.

The simple MO calculation indicated that the two doubly degenerate, highest occupied molecular orbitals are both essentially nonbonding and may have about the same energy. The spin-orbit coupling for these orbitals could be different, thereby leading to different susceptibilities for the different orbitals. The observed susceptibility would be the sum of the ground state susceptibility and the susceptibility of the thermally excited state, weighted by a Boltzmann distribution. If the susceptibility of the energy levels is sufficiently different and thermal population of the higher energy level occurs, an exponential temperature

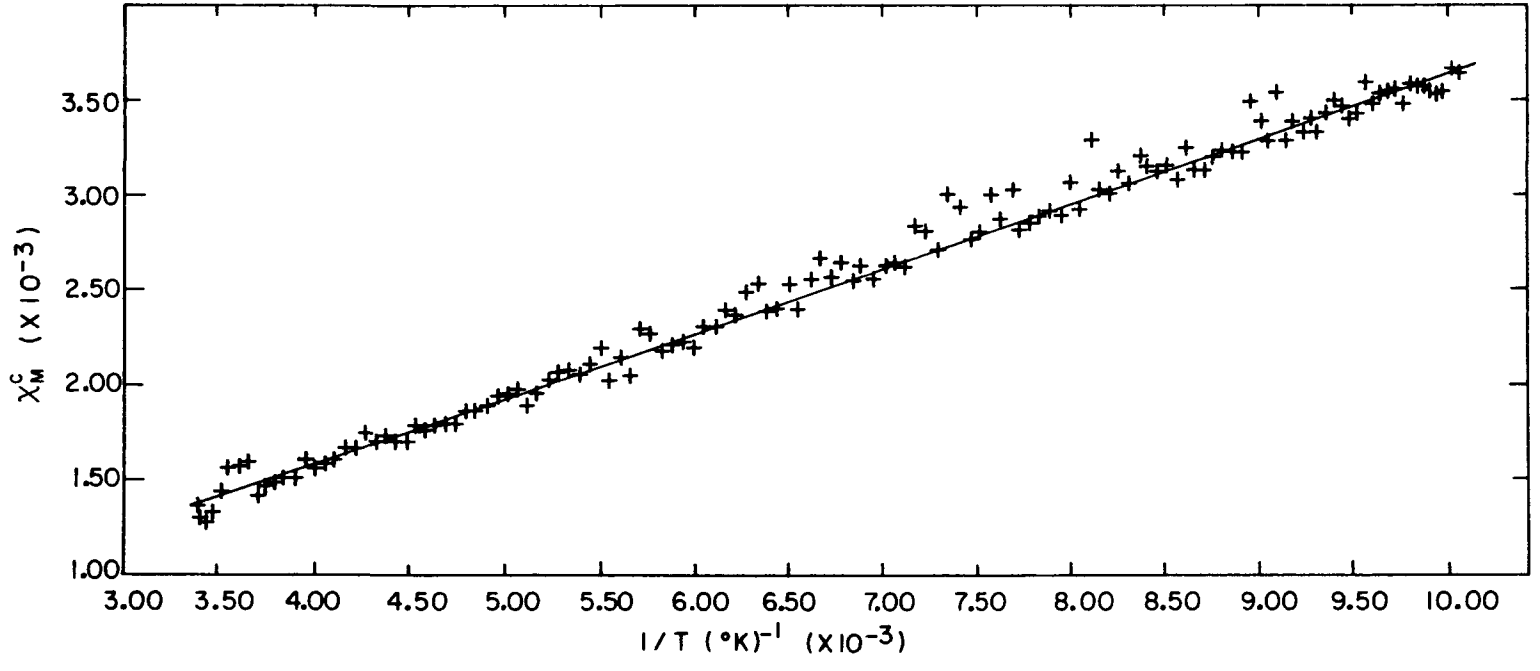

Figure IV-6. Magnetic susceptibility of $[Bu_4N]_2Mo_5Cl_{13}$. Line of best fit is given by line through data points

dependence of the susceptibility would be observed. Within the temperature range investigated, this is not observed.

The electron spin resonance measurements of $[Bu_4N]_2Mo_5Cl_{13}$ were at first very perplexing. At room temperature no signal was initially observed. As the sample temperature was decreased, a signal which increased in strength was observed. At 5°K an anisotropic ground state signal was observed in the spectrum of powdered $[Bu_4N]_2Mo_5Cl_{13}$ (Figure IV-7). As the temperature was increased, the signal became nearly isotropic due to motional narrowing, a process which continues to affect the signal to about 140°K. The motional narrowing phenomenon at low temperatures is indicative of a dynamic Jahn-Teller process (23,24). Above 140°K, the isotropic signal begins to broaden and decrease in intensity until at room temperature the signal was over 850 G wide. This signal broadening is probably due to a short relaxation time caused by spin-lattice relaxation (25,26).

The solution spectrum of $[Bu_4N]_2Mo_5Cl_{13}$ was broad and weak at room temperature. A very small amount of impurity with g = 1.948 was observed, but no hyperfine signals were evident. The narrow signal width and g value suggest that the impurity might be $[MoOCl_5]^{2-}$ (27). The glass spectrum was obtained at 50°K (Figure IV-8) and g values of $g_{\parallel} = 2.003$ and $g_{\perp} = 1.954$ were obtained. Several additive accumulations of the spectrum enhanced the hyperfine signals. The signal strength of $[MoOCl_5]^{2-}$ does not vary appreciably with temperature (28); therefore, the observed hyperfine signal probably arises from the $[Mo_5Cl_{13}]^{2-}$ cluster. The interpretation of the hyperfine data would be very complex.

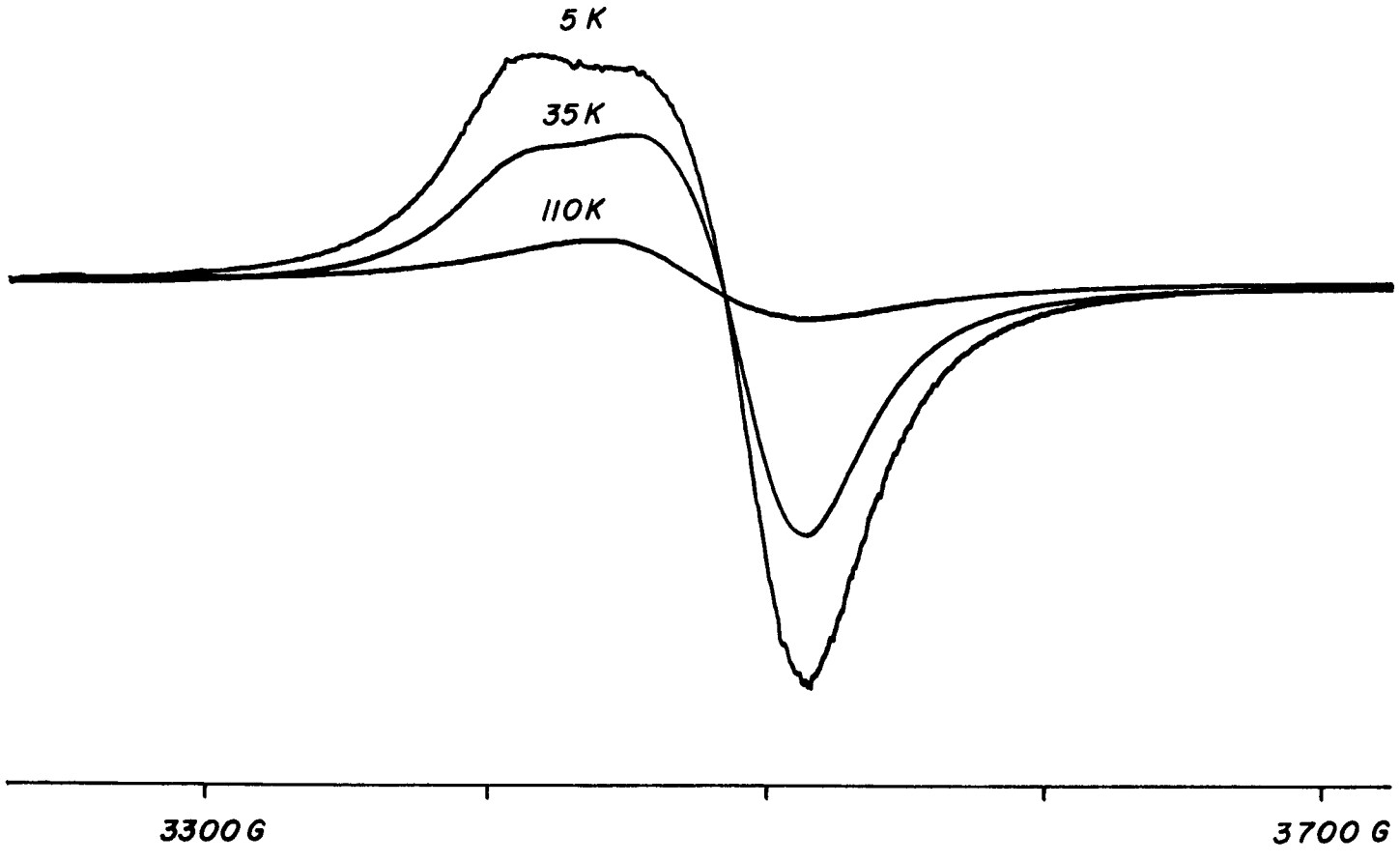

Figure IV-7. ESR powder spectrum of $[Bu_4N]_2Mo_5Cl_{13}$

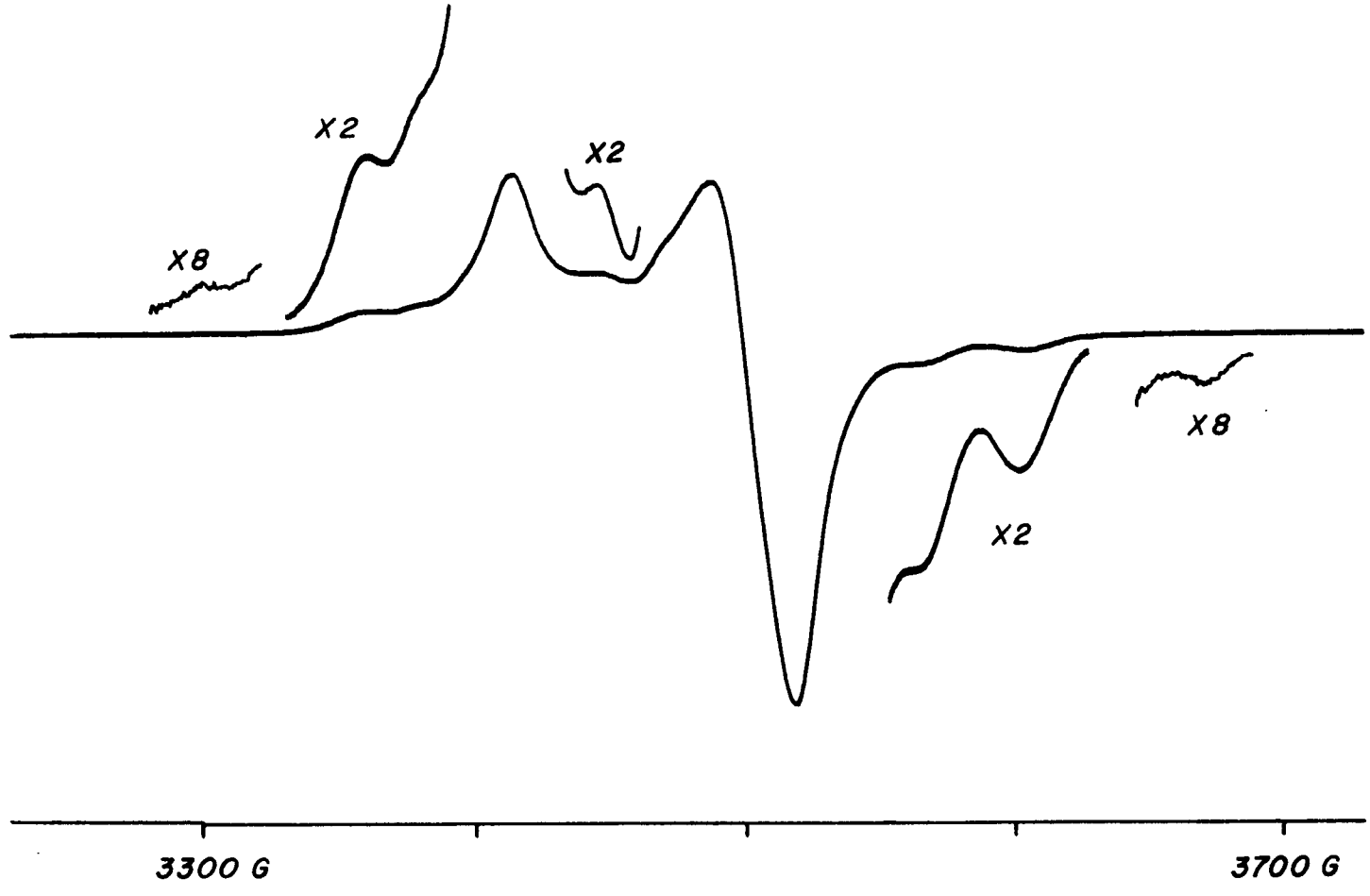

Figure IV-8. ESR glass spectrum of $[Bu_4N]_2Mo_5Cl_{13}$ in toluene/acetonitrile

Table IV-8 contains the calculated abundance of clusters containing from zero to five molybdenum nuclei of spin 5/2. The ^{95}Mo and ^{97}Mo were considered to be indistinguishable and all five molybdenums were considered to be equivalent for ease of calculations of abundance. Apparently, a significant portion of the cluster will have a total spin of 5. Due to the noncubic symmetry of the molecule, there will also be parallel and perpendicular components of the hyperfine transitions. This would probably generate overlapping lines making it more difficult to assign absorptions in the spectrum. The separation between hyperfine lines varies between 24 G and 70 G. Very little work has been reported on polynuclear molybdenum compounds; however, hyperfine separations in dinuclear molybdenum compounds have been reported to be between about 20 and 50 G (29). Therefore, the separations observed for $[Mo_5Cl_{13}]^{2-}$ appear to be of the correct magnitude.

Table IV-8. Abundance of clusters containing $Mo_{5/2}$ nuclei

Number spin 5/2 nuclei	Number spin 0 nuclei	total spin	% abundance
0	5	0	23.4
1	4	5/2	39.5
2	3	5	26.6
3	2	15/2	8.9
4	1	10	1.5
5	0	25/2	0.1

Below 20°K, the ESR signals in the spectrum of the glass began to broaden. As the ESR studies were being concluded, the cause for the signal broadening was determined to be power saturation of the sample. Above 20°K, a power level of 20 milliwatts was utilized. Between 10 and 15°K, the instrument would not tune properly and the signal began to broaden. If the power was reduced, the signal would sharpen. This indicates power saturation is possible at low temperature. At 5°K, the power had to be reduced to 2×10^{-5} milliwatts to avoid saturation.

Structure and ESR of $[BTMA]_2Mo_5Cl_{13}$

If the $[Mo_5Cl_{13}]^{2-}$ cluster is undergoing Jahn-Teller distortion, we wondered why there was no sign of the distortion in the crystal structure of $[Bu_4N]_2Mo_5Cl_{13}$. The cluster was crystallized with the BTMA cation to see if the cluster consistently contained a square pyramid of Mo atoms. All of the metal and chlorine atoms were crystallographically independent in this new compound. The metal-metal distances within the base were equal, within error; however, the metal-metal-metal angles in the base were no longer 90 degrees. Two of the angles average 93.3 deg, and the other two average 86.8 degrees. The rhombic distortion could be due to either the electronic structure of the cluster, or crystal packing. Inspection of distances between the cation and the cluster revealed that several of the calculated hydrogen positions were very close to chlorine atoms of the cluster (Table IV-5). The sum of the van der Waals radii for hydrogen and chlorine is 3.00 Å; therefore, any hydrogen-chlorine distance less than 3.00 Å with a carbon-hydrogen-chlorine angle greater than 90

degrees suggests that hydrogen bonding may be occurring (30). At this point, crystal packing appeared to be causing the distortion of the metal framework. The angles involving basal terminal chlorine atoms might be expected to deviate further from 90 degrees than the basal metal angles if crystal packing is the dominate force. Actually, the Cl(9)-Cl(10)-Cl(11) and Cl(11)-Cl(12)-Cl(9) angles average 88.5 deg, and the Cl(12)-Cl(9)-Cl(10) and Cl(10)-Cl(11)-Cl(12) angles average 91.5 deg, a smaller distortion than is observed within the metal framework.

The ESR spectrum of this compound also has a pronounced temperature dependence. At room temperature, however, the peak width is only 400 G. This nearly isotropic signal sharpens much more quickly than observed for $[Bu_4N]_2Mo_5Cl_{13}$. The anisotropic signal is also observed at a higher temperature. An accurate $g_{||}$ value is difficult to obtain from the powder spectrum due to its closeness to the $g_{\perp}$ value; however, the $g_{||}$ is about 1.98 and $g_{\perp}$ is about 1.96. Although the powder spectra are different from the spectra of $[Bu_4N]_2Mo_5Cl_{13}$, the glass spectrum is identical to that obtained for $[Bu_4N]_2Mo_5Cl_{13}$.

Magnetic Properties of $[Mo_5Cl_{13}]^{3-}$

Information concerning the magnetic properties of the 3^- cluster would clarify the molecular orbital picture considerably. If the HOMO is doubly degenerate, the 3^- species should have two unpaired electrons. The Evans method (31) of determining magnetic susceptibility in solutions was well suited to the small amount of the cluster available. The shift of the acetonitrile, toluene methyl, and toluene aromatic protons were

measured. The shift was larger for acetonitrile than toluene, but the temperature dependence was the same. In both the solutions of 2^- and 3^- clusters, the observed shift was about three times that expected for a shift due solely to the solution susceptibility change. The temperature dependence of the shift was linear for the 2^- cluster; however, the shift decreased with decreasing temperature rather than increasing. The shift of the solution containing the 3^- cluster also decreased with decreasing temperature but does not appear to be linear. Since the shift of the reduced cluster solution is larger than that for the 2^- solution and since the temperature dependence is different, we believed that the shift was due to the reduced species. The magnitude of the shift indicated that an interaction such as contact shift or dipolar shift may be occurring (32). These shifts can exist only for a paramagnetic compound. Therefore, the NMR measurements indicated that the reduced cluster should have two unpaired electrons.

After the synthesis of $[Bu_4N]_3Mo_5Cl_{13}$ was perfected so that a solid product could be isolated, the magnetic susceptibility was measured on a Faraday balance. The compound was diamagnetic over the temperature range of 100°K to room temperature. The magnetic moment of 0.4(2) was calculated from the slope of a line of best fit through the data. The temperature independent paramagnetism was 370(56) x 10^{-6} cm^3/mol.

Extended Hückel Results

The diamagnetic nature of $[Bu_4N]_3Mo_5Cl_{13}$ made us ask if the simplistic molecular orbital diagram determination of a doubly degenerate

HOMO was correct, although the ESR results certainly supported this interpretation. The extended Hückel calculation of $[Mo_6Cl_{14}]^{2-}$ was done first to provide results that could be compared with previous work. In general, the resultant molecular orbital diagram, a portion of which is shown in Figure IV-9a, agrees with work done by Guggenberger and Sleight (33). The calculation presented here orders the three highest occupied triply degenerate orbitals differently and has them more closely spaced. This may be due to the larger 4d orbital exponent that was used. The energy level separation has been shown to decrease with increasing orbital exponent, and the energy level ordering also changes (33). The calculated molecular orbital diagrams for the Mo_5 clusters may also have the energy levels too closely spaced. The diagram in Figure IV-9b illustrates the movement of the energy levels in the transformation of an $[Mo_6Cl_{14}]^{2-}$ cluster to the $[Mo_5Cl_{13}]^{2-}$ cluster (Figure IV-9c). As expected, the HOMO and lowest unoccupied molecular orbital (LUMO), which are composed mainly of atomic orbitals from the basal atoms of the Mo_5 pyramid, are strongly involved in the bonding to the sixth position of the octahedron in $[Mo_6Cl_{14}]^{2-}$.

There are two vibrational modes that will break the degeneracy of an e level in C_{4v} symmetry (34). One mode corresponds to an elongation of the square base of the pyramid so that the base becomes a rectangle. The other mode is a rhombic distortion, as is observed in the crystal structure of $[BTMA]_2Mo_5Cl_{13}$. The effect on the energy levels of creating a rectangular based pyramid is shown in Figure IV-10. The width of the base was not changed, but the length of the base in the x direction was

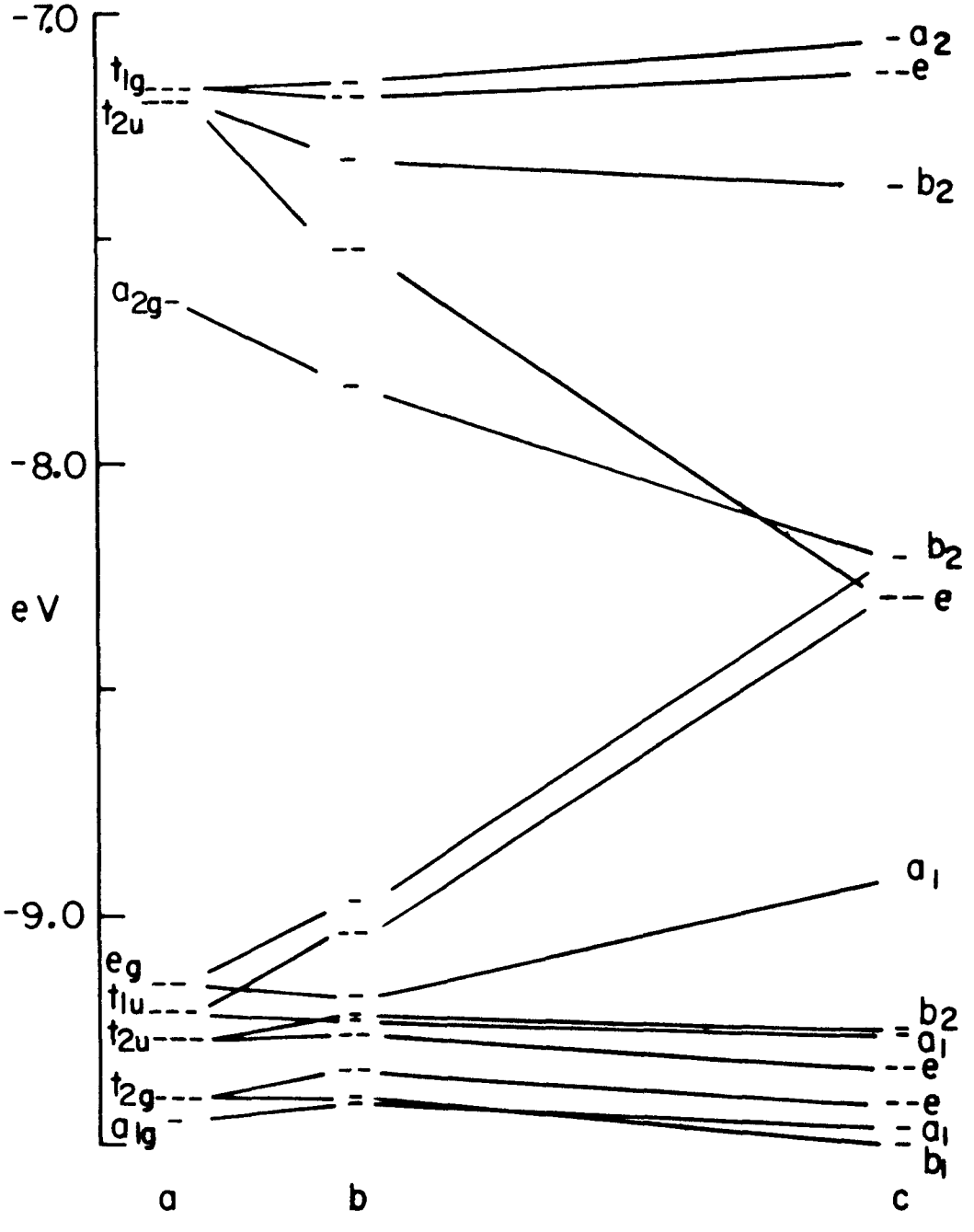

Figure IV-9. Molecular orbital diagram for a) $[Mo_6Cl_{14}]^{2-}$; b) distorted $[Mo_6Cl_{14}]^{2-}$; c) undistorted $[Mo_5Cl_{13}]^{2-}$

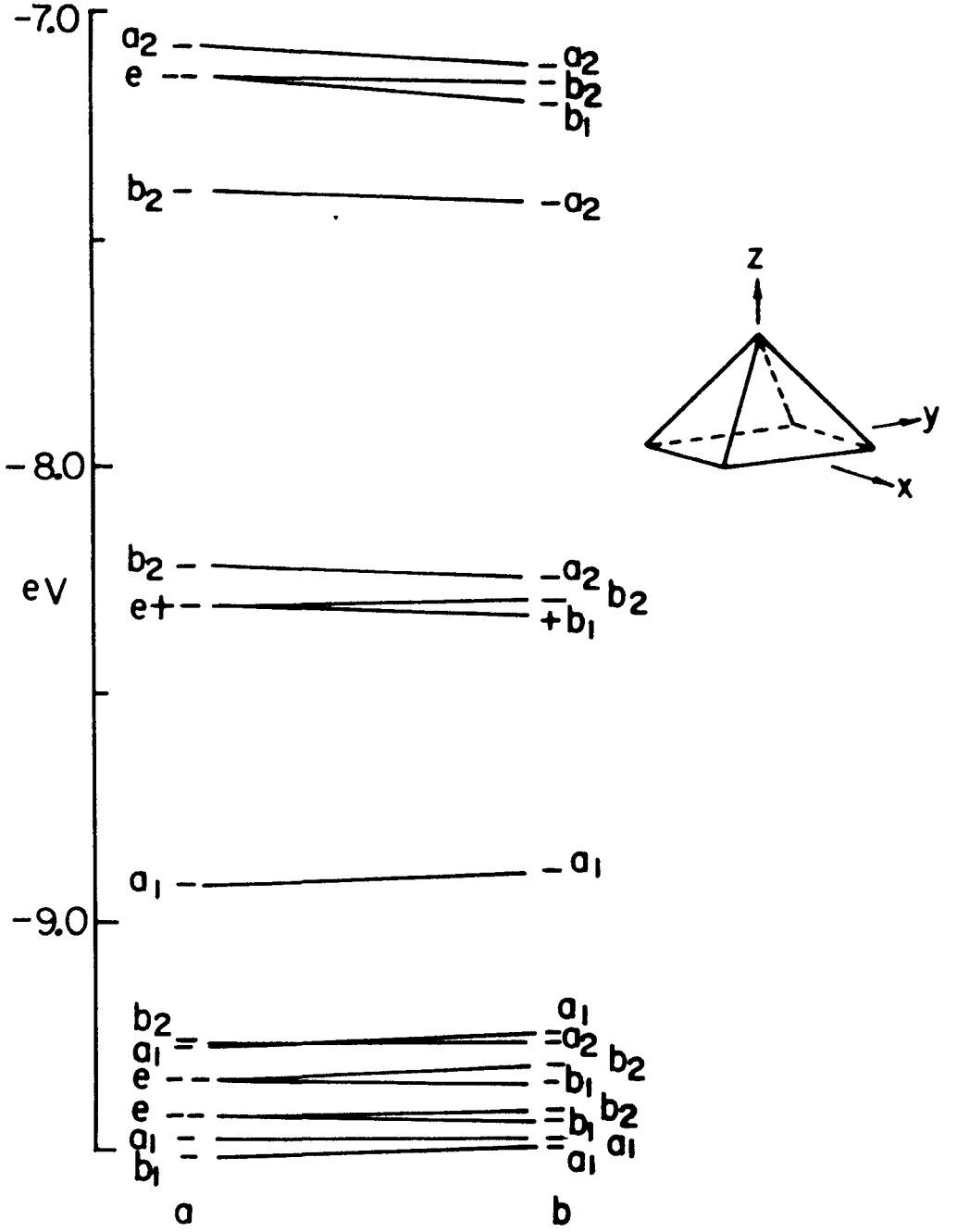

Figure IV-10. Molecular orbital diagram for $[Mo_5Cl_{13}]^{2-}$ with a) square base; b) rectangular base

increased by 0.04 Å. The standard deviation of the basal Mo-Mo distance in $[Bu_4N]_2Mo_5Cl_{13}$ is 0.003 Å; so an increase of 0.04 Å in a metal-metal bond seemed rather significant. This distortion does remove the degeneracy from the HOMO, but the energy gap between the resultant orbitals is very small. A rhombic distortion of the base so that the angles within the base are 93 deg and 87 deg leads to a molecular orbital diagram as shown in Figure IV-11b. Although this distortion has a larger effect on the molecular orbital diagram, the energy separation between the resultant HOMO and LUMO was calculated to be less than 0.1 eV.

Explanation of the magnetic properties of $[Mo_5Cl_{13}]^{3-}$ is still difficult. The ESR spectra of the $[Mo_5Cl_{13}]^{2-}$ cluster support the calculated doubly degenerate HOMO for the undistorted cluster. The calculations also suggest that the energy gained from a distortion of the molecule would be fairly small. It is difficult to determine if the energy gained from distortion is larger than that needed to pair electrons. Since the magnetic susceptibility indicated the cluster is diamagnetic, one would predict that a cluster distortion must have occurred. A crystal structure of the $[Mo_5Cl_{13}]^{3-}$ cluster is needed to resolve the problem. The metal-metal bond lengths in the reduced cluster might also shed light on the amount of bonding character of the HOMO.

Chlorine 2p Photoelectron Spectrum

Terminal chlorines can be discerned from triply bridging chlorines in the XPS data of derivatives of $[Mo_6Cl_{14}]^{2-}$ (35). Doubly bridging chlorines can also be distinguished from terminal chlorine (36). The

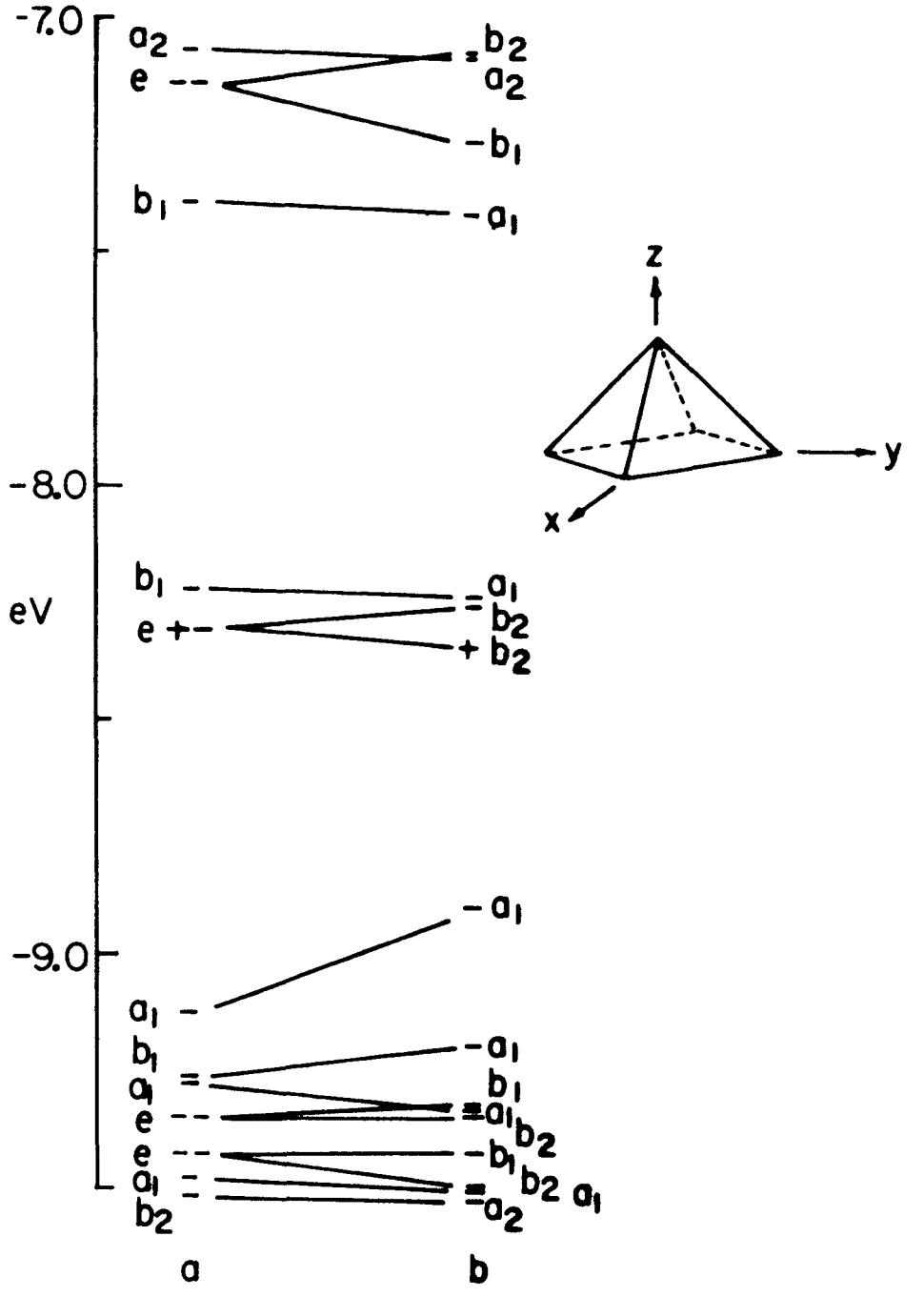

Figure IV-11. Molecular orbital diagram for $[Mo_5Cl_{13}]^{2-}$ with a) square base; b) rhombic base

$[Mo_5Cl_{13}]^{2-}$ cluster provides a unique example of a compound containing terminal, doubly bridging, and triply bridging chlorine atoms. The first attempt to resolve the Cl 2p XPS data was done using just two types of chlorine atoms. This led to a full-width at half-maximum (FWHM) for the bands arising from the bridging chlorine atoms that was larger than was acceptable. Further resolution was done with parameters for three types of chlorine atoms. The position and height of each peak was varied, and the FWHM was also varied, but was the same for all chlorine atom types. The parameters for the best resolution (see Figure IV-12) are in Table IV-9, along with the resolution data of other comparable compounds. The area

Table IV-9. Chlorine 2p XPS data

	Cl $2p_{3/2}$ binding energies (eV)[a]				
Compound	Triple	Double	Terminal	FWHM (eV)	Reference
$(Bu_4N)_2Mo_5Cl_{13}$	200.5	199.8	198.3	1.03	This work
$(Bu_4N)_2Mo_6Cl_{14}$	200.4	---	198.2	1.14	35
$Mo_4Cl_8(PBu_3)_4$	---	199.6	198.3	1.2	36

[a]Reference is the Cls binding energy (285.0 eV).

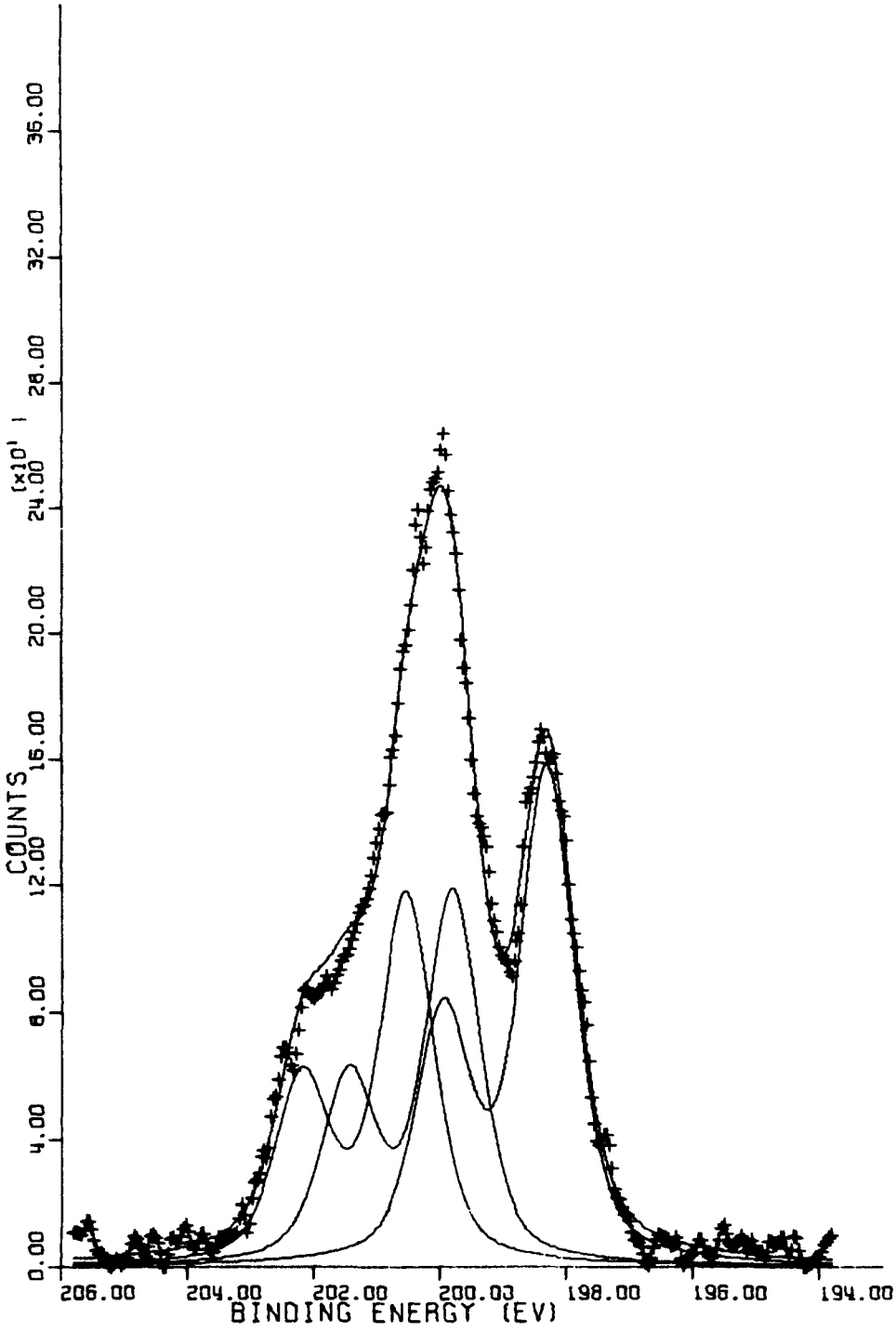

Figure IV-12. Chlorine 2p x-ray photoelectron spectrum of $[Bu_4N]_2Mo_5Cl_{13}$. Sum of resolved components is given by the solid line through the data points

ratio of triply bridging/doubly bridging/terminal chlorine atoms is 1.00/1.00/1.33. This is in good agreement with the anticipated ratio of 1.00/1.00/1.25. A calculated spectrum using the correct ratios of chlorine types also provided a good match to the data.

The binding energies agree very well, for both the triply bridging and terminal chlorines, with previous work on other compounds. The doubly bridging binding energy also agrees, within the error limits, to previous work. This experiment indicates that triply and doubly bridging chlorines are resolvable in XPS data even though they are separated by only 0.7 eV.

REFERENCES AND NOTES

1. Jödden, K.; von Schnering, H.; Schäfer, H. Angew. Chem. Int. Ed. 1975, 14, 570.

2. Jödden, K.; Schäfer, H. Z. Anorg. Allg. Chem. 1977, 430, 5.

3. Mann, C. K. In "Electroanalytical Chemistry"; Bard, A., Ed.; Marcel Dekker, Inc.: New York, 1969; Vol. 3, p. 132.

4. Sawyer, D.; Roberts, Jr., J. "Experimental Electrochemistry for Chemists"; Wiley: New York, 1974; p. 212.

5. Converse, J. G.; McCarley, R. E. Inorg. Chem. 1970, 9, 1361.

6. Beers, W. W. Ph.D. Dissertation, Iowa State University, Ames, Iowa, 1983; Section II.

7. Steirman, R. J.; Gschneider, K. A. Department of Materials Science and Engineering, Iowa State University; to be published.

8. Figgis, B. N.; Lewis, J. In "Modern Coordination Chemistry"; Lewis, J.; Wilkins, R. G., Eds.; Interscience: New York, 1960; p. 403.

9. Selwood, P. W. "Magnetochemistry", 2nd ed.; Interscience: New York, 1956; p. 78.

10. Bevington, P. R. "Data Reduction and Error Analysis for the Physical Sciences"; McGraw-Hill: New York, 1969; p. 104.

11. Ostfeld, D.; Cohen, I. A. J. Chem. Ed. 1972, 49, 829.

12. Rohrbaugh, W. J.; Jacobson, R. A. Inorg. Chem. 1974, 13, 2535.

13. Jacobson, R. A. J. Applied Crystallogr. 1969, 9, 115.

14. Karcher, B. A. Ph.D. Dissertation, Iowa State University, Ames, Iowa, 1981.

15. Structure factor calculations and least squares refinements were done using the block matrix/full matrix program ALLS (R. L. Lapp and R. A. Jacobson), Fourier series calculations were done using the program FOUR (D. R. Powell and R. A. Jacobson), and for molecular drawings the program ORTEP (C. K. Johnson) was used. Superposition calculations were done using the program SUPERPOSITION (C. R. Hubbard, M. W. Babich, and R. A. Jacobson).

16. Main, P. "MULTAN 80, A System of Computer Programs for the Automatic Solution of Crystal Structures for X-ray Diffraction Data", University of York Printing Unit, York, United Kingdom, 1980.

17. Richardson, Jr., J. W.; Jacobson, R. A. Department of Chemistry, Iowa State University; to be published.

18. The determination of atom positions and the correct space group was done by Jim Richardson.

19. Beers, W. W. Ph.D. Dissertation, Iowa State University, Ames, Iowa, 1983; Section I.

20. Cusachs, L. C.; Corrington, J. H. In "Sigma Molecular Orbital Theory"; Sinanoglu, O.; Wiberg, K. B., Eds.; Yale University Press: New Haven, Conn., 1970; Chapter IV-4.

21. Maverick, A. W.; Gray, H. B. J. Am. Chem. Soc. 1981, 103, 1298.

22. Bard, A. J.; Faulkner, L. "Electrochemical Methods Fundamentals and Applications"; John Wiley & Sons: New York, 1980; p. 230.

23. Ham, F. S. In "Electron Paramagnetic Resonance"; Geschwind, S., Ed.; Plenum: New York, 1972; Chapter 1.

24. Abragam, A.; Bleaney, B. "Electron Paramagnetic Resonance of Transition Ions"; Clarendon: Oxford, 1970; Chapter 21.

25. Orbach, R.; Stapleton, H. J. In "Electron Paramagnetic Resonance"; Geschwind, S., Ed.; Plenum: New York, 1972; Chapter 2.

26. Abragam, A.; Bleaney, B. "Electron Paramagnetic Resonance of Transition Ions"; Clarendon: Oxford, 1970; Chapter 10.

27. Kon, H.; Sharpless,N.E. J. Phys. Chem. 1966, 70, 105.

28. DeArmond, K.; Garrett, B. B.; Gutowsky, H. S. J. Chem. Phys. 1965, 42, 1019.

29. Cotton, F. A.; Pedersen, E. Inorg. Chem. 1975, 14, 391, 399.

30. Taylor, R.; Kennard, O. J. Am. Chem. Soc. 1982, 104, 5063.

31. Evans, D. F. J. Chem. Soc. 1959, 230.

32. Horrocks, W. D. In "ESR and NMR of Paramagnetic Species in Biological and Related Systems" NATO Advanced Study Institute Series: Series C, Mathematical and Physical Sciences; Bertini, I.; Drago, R. S., Eds.; D. Reidel: Boston, 1980; p. 55.

33. Guggenberger, L. J.; Sleight, A. W. Inorg. Chem. 1969, 8, 2041.

34. Hougen, J. T. J. Mol. Spectry. 1964, 13, 149.

35. Michel, J. B.; McCarley, R. E. Inorg. Chem. 1982, 21, 1864.

36. Ryan, T. R.; McCarley, R. E. Inorg. Chem. 1982, 21, 2072.

SUMMARY

The crystal structure and molecular orbital calculation of the $Mo_4Cl_8[PR_3]_4$ cluster demonstrate the presence of multiple metal-metal bonds in the cluster. This electron density reservoir should provide the capability of addition reactions. Future attempts to add metal atoms to the cluster should be attempted with molecules that will not scavenge phosphine from the cluster.

With careful synthetic procedures, the isolation of $Mo_8Cl_{16}[PBu_3]_4$ may be possible. This compound may have sufficient solubility for FAB mass spectrometry data to be obtained. Crystal growth may also be possible. If a crystalline derivative of $Mo_8Cl_{16}[PR_3]_4$ cannot be obtained, confirmation of the proposed structure may be attainable with EXAFS. This technique would also yield enlightening information on the β-$MoCl_2$ structure.

The doubly degenerate highest occupied molecular orbital in $[Mo_5Cl_{13}]^{2-}$ leads to either dynamic Jahn-Teller distortion as observed in $[Bu_4N]_2Mo_5Cl_{13}$ or a static distortion as found in $[BTMA]_2Mo_5Cl_{13}$. Future work on the $[Mo_5Cl_{13}]^{n-}$ system must include the crystal structure determination for a salt of $[Mo_5Cl_{13}]^{3-}$. A more detailed investigation of the temperature dependence of the $[Mo_5Cl_{13}]^{2-}$ ESR signal would produce additional information on energy level separation. Power saturation ESR studies would also provide information on relaxation times.

ADDITIONAL LITERATURE CITED

1. Cotton, F. A. Quart. Rev. 1966, 20, 389.

2. Chapin, W. H. J. Am. Chem. Soc. 1910, 32, 323.

3. Vaughn, P. A.; Sturtivant, J. H.; Pauling, L. J. Am. Chem. Soc. 1950, 72, 5477.

4. Brosset, C. Nature 1935, 135, 874.

5. Brosset, C. Arkiv. Kemi. Mineral. Geol. 1946, 22A, No. 11.

6. Bertrand, J. A.; Cotton, F. A.; Dollase, W. A. Inorg. Chem. 1963, 2, 1166.

7. Chisholm, M. H., Ed. "Reactivity of Metal-Metal Bonds"; American Chemical Society: Washington, D.C., 1981; ACS Symp. Ser. No. 155.

8. Cotton, F. A.; Walton, R. A. "Multiple Bonds Between Metal Atoms"; John Wiley and Sons: New York, 1982.

9. Chisholm, M. H.; Rothwell, I. P. Prog. Inorg. Chem. 1982, 29, 1.

10. Muetterties, E. L. Science 1977, 196, 839.

11. Lauher, J. W. J. Am. Chem. Soc. 1979, 101, 2604.

12. Moskovits, M. Accts. Chem. Res. 1979, 12, 229.

13. Baetzold, R. Adv. Catal. 1976, 25, 1.

14. Day, V. W.; Day, R. O.; Kristoff, J. S.; Hirsekorn, F. J.; Muetterties, E. L. J. Am. Chem. Soc. 1975, 97, 2571.

15. Thomas, M. G.; Pretzer, W. R.; Beier, B. F.; Hirsekorn, F. J.; Muetterties, E. L. J. Am. Chem. Soc. 1977, 99, 743.

16. Hemminger, J. C.; Muetterties, E. L.; Somorjai, G. A. J. Am. Chem. Soc. 1979, 101, 62.

17. Muetterties, E. L.; Rhodin, T. N.; Band, E.; Bucker, C. F.; Pretzer, W. R. Chem. Rev. 1979, 79, 91.

18. Taylor, N. J.; Chieh, P. C.; Carty, A. J. J. Chem. Soc., Chem. Commun. 1975, 448.

19. McGinnis, R. N.; Ryan, T. R.; McCarley, R. E. J. Am. Chem. Soc. 1978, 100, 7900.

20. Chetcuti, M. J.; Green, M.; Jeffrey, J. C.; Stone, F.G.A.; Wilson, A. J. Chem. Soc., Chem. Commun. 1980, 948.

21. Chetcuti, M. J.; Green, M.; Howard, J.A.K.; Jeffrey, J. C.; Mills, R. M.; Pain, G. N.; Porter, S. J.; Stone, F.G.A.; Wilson, A. A.; Woodward, P. J. Chem. Soc., Chem. Commun. 1980, 1057.

22. Chisholm, M. H.; Folting, K.; Huffman, J. C.; Kirkpatrick, C. C. J. Am. Chem. Soc. 1981, 103, 5967.

23. Curtis, M. D.; Messerle, L.; Fotinos, N. A.; Gerlach, R. F. In "Reactivity of Metal-Metal Bonds"; Chisholm, M. H., Ed.; American Chemical Society: Washington, D.C., 1981; ACS Symp. Ser. No. 155; Chapter 12.

24. Farrugia, L. J.; Howard, J.A.K.; Mitrprachachon, P.; Stone, F.G.A.; Woodward, P. J. Chem. Soc., Dalton Trans. 1981, 155, 162.

25. Chisholm, M. H.; Errington, R. J.; Folting, K.; Huffman, J. C. J. Am. Chem. Soc. 1982, 104, 2025.

26. Stensvad, S.; Helland, B. J.; Babich, M. W.; Jacobson, R. A.; McCarley, R. E. J. Am. Chem. Soc. 1978, 100, 6257.

27. Glicksman, H. D.; Walton, R. A. Inorg. Chem. 1978, 17, 3197.

28. Chisholm, M. H.; Leonelli, J.; Huffman, J. C. J. Chem. Soc., Chem. Commun. 1981, 270.

29. Glicksman, H. D.; Hamer, A. D.; Smith, T. J.; Walton, R. A. Inorg. Chem. 1976, 15, 2205.

30. Glicksman, H. D.; Walton, R. A. Inorg. Chem. 1978, 17, 200.

31. Jödden, K.; von Schnering, H.; Schäfer, H. Angew. Chem. Int. Ed. 1975, 14, 570.

32. Jödden, K.; Schäfer, H. Z. Anorg. Alleg. Chem. 1977, 430, 5.

33. Lauher, J. W. J. Am. Chem. Soc. 1978, 100, 5305.

34. Jemmis, E. D.; Pinkas, A. R.; Hoffmann, R. J. Am. Chem. Soc. 1980, 102, 2576.

ACKNOWLEDGMENTS

There are many people who have assisted me during my graduate studies. I am indebted to Dr. Robert E. McCarley for his guidance in the research conducted for this dissertation. Discussions with other members of the group were also valuable. The members of Dr. R. A. Jacobson's group were very helpful during crystal structure determinations. A special note of gratitude is due Jim Richardson for without his work on the $[BTMA]_2Mo_5Cl_{13}$ crystal structure, the structure would not have been solved. The assistance of Dr. Stephen Elbert during the extended Hückel molecular orbital calculations was also appreciated.

My parents also played an important part in my obtaining this degree. Their love of education and encouragement to pursue new horizons have carried me far. Last, but certainly not least, the love, support, and patience of my wife, Carolyn, has been invaluable.